USAAMRDL-TR-77-18

HELICOPTER FREEWHEEL UNIT DESIGN GUIDE

Sikorsky Aircraft
Division of United Technologies Corporation
North Main Street
Stratford, Conn. 06602

October 1977

Final Report

Approved for public release;
distribution unlimited.

Prepared for
APPLIED TECHNOLOGY LABORATORY
RESEARCH AND TECHNOLOGY LABORATORIES (AVRADCOM)
Fort Eustis, Va. 23604

DISCLAIMER NOTICE

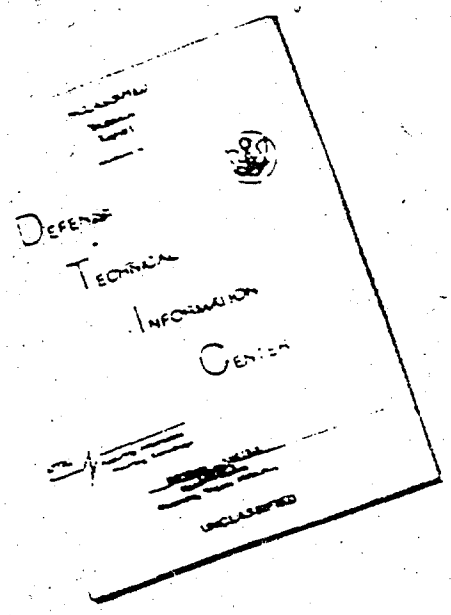

THIS DOCUMENT IS BEST QUALITY AVAILABLE. THE COPY FURNISHED TO DTIC CONTAINED A SIGNIFICANT NUMBER OF PAGES WHICH DO NOT REPRODUCE LEGIBLY.

APPLIED TECHNOLOGY LABORATORY POSITION STATEMENT

This report contains detailed information for the design of spring, sprag, and ramp roller helicopter freewheel units, which were tested delivering 1500 horsepower at a speed of 20,000 RPM. The information is considered to be accurate and, when used as a design guide, will result in a reliable helicopter freewheel unit design.

Michael Dobrolet, Propulsion Technical Area, Technology Applications Division, served as Project Engineer for this effort.

On 1 September 1977, *after this report had been prepared,* the name of this organization was changed from Eustis Directorate, U.S. Army Air Mobility Research and Development Laboratories to Applied Technology Laboratory, U.S. Army Research and Technology Laboratories (AVRADCOM).

Unclassified
SECURITY CLASSIFICATION OF THIS PAGE (When Data Entered)

REPORT DOCUMENTATION PAGE

READ INSTRUCTIONS BEFORE COMPLETING FORM

1. REPORT NUMBER: USAAMRDL TR-77-18	2. GOVT ACCESSION NO.
3. RECIPIENT'S CATALOG NUMBER	
4. TITLE (and Subtitle): HELICOPTER FREEWHEEL UNIT DESIGN GUIDE	5. TYPE OF REPORT & PERIOD COVERED: Final Report, 1974 to March 77,
6. PERFORMING ORG. REPORT NUMBER	
7. AUTHOR(s): J. Kish	8. CONTRACT OR GRANT NUMBER(s): DAAJ02-74-C-0028
9. PERFORMING ORGANIZATION NAME AND ADDRESS: Sikorsky Aircraft, North Main Street, Stratford, Conn. 06602	10. PROGRAM ELEMENT, PROJECT, TASK AREA & WORK UNIT NUMBERS: 62209A 1F262208AH76 006 EK
11. CONTROLLING OFFICE NAME AND ADDRESS: Applied Technology Laboratory, U.S. Army Research & Technology Laboratories (AVRADCOM) Fort Eustis, Va. 23604.	12. REPORT DATE: October 1977
	13. NUMBER OF PAGES: 239
14. MONITORING AGENCY NAME & ADDRESS (if different from Controlling Office)	15. SECURITY CLASS. (of this report): Unclassified
	15a. DECLASSIFICATION/DOWNGRADING SCHEDULE

16. DISTRIBUTION STATEMENT (of this Report)

Approved for public release; distribution unlimited.

17. DISTRIBUTION STATEMENT (of the abstract entered in Block 20, if different from Report)

DDC
DEC 14 1977
E

18. SUPPLEMENTARY NOTES

19. KEY WORDS (Continue on reverse side if necessary and identify by block number)

Freewheel Unit
Clutch
Overrunning
One Way Clutch
Spring Clutch
Sprag Clutch
Ramp Roller Clutch

20. ABSTRACT (Continue on reverse side if necessary and identify by block number)

This report is intended to aid the transmission designer in selecting an overrunning clutch for use in a helicopter transmission. Preliminary sizing as well as detailed stress analysis procedures are presented for all aspects of spring, sprag, and ramp roller clutch designs. An example of the procedure for each clutch is included. Operation up to 20,000 rpm is feasible if the design procedures presented herein are followed.

DD FORM 1 JAN 73 1473 EDITION OF 1 NOV 65 IS OBSOLETE

Unclassified
SECURITY CLASSIFICATION OF THIS PAGE (When Data Entered)

328 3.0

PREFACE

Technical assistance, data, and procedures used in the preparation of this design guide have been provided by the Borg-Warner Corp, Bellwood, Illinois (sprag clutch design), by Curtiss-Wright Corp, Caldwell, New Jersey (spring clutch design), and by Avco Lycoming Division, Stratford, Connecticut (test data).

Appreciation is extended to Mr. M. Dobrolet of USAAMRDL, Messrs. P. Lynwander, A. Meyer, and S. Chachakis of Avco Lycoming Division, Messrs. W. Steinberg, S. Avena, J. Nevill, and G. Brewer of Curtiss-Wright Corp., and Messrs. J. Tippett and J. Havranek of Borg-Warner Corp. Test data found in this design guide were generated during the course of contract DAAJ02-74-C-0028. The final report generated during this contract is USAAMRDL-TR-77-16 "Advanced Overrunning Clutch Technology."

TABLE OF CONTENTS

TABLE OF CONTENTS (Cont'd)

TABLE OF CONTENTS (Cont'd)

LIST OF ILLUSTRATIONS

LIST OF ILLUSTRATIONS (Continued)

LIST OF ILLUSTRATIONS (Continued)

LIST OF ILLUSTRATIONS (Continued)

LIST OF ILLUSTRATIONS (Continued)

LIST OF TABLES

INTRODUCTION

PRINCIPLES OF OVERRUNNING CLUTCH OPERATION

Spring Clutch

The spring clutch is the most recently developed of the three types reported here. Operation of the spring overrunning clutch depends on the radial expansion and contraction of a helical spring of rectangular cross section for driving and overrunning, respectively. Such a clutch is illustrated in Figure 1.

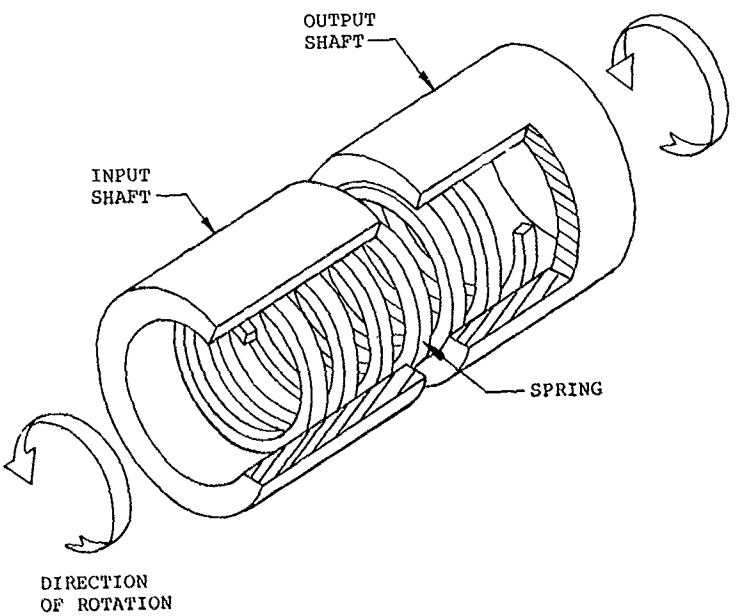

Figure 1. Spring Overrunning Clutch.

Looking at the input end of the clutch, the helical spring is wound in the same direction as that of rotation. When the direction of rotation of the input is the same as the direction of rotation of the output and the input member attempts to rotate faster than the output, the tangential force on the spring due to friction causes the spring to expand radially outward against both input and output members. This action locks the input to the output, and the clutch is in the driving mode. When the direction of rotation of the input relative to the output is opposite to the direction of rotation (i.e., the output member rotates faster than the input member), the tangential force on the spring due to friction causes the spring to contract radially inward. In this position, the spring normal load on the housing is reduced so that friction cannot carry the load and the spring slips; thus, the clutch is in the overrunning mode.

The design of the spring itself is the most critical aspect in the proper operation of the spring clutch. While this topic is covered extensively in the body of the design guide, it will be instructive to mention briefly some of the design features incorporated to assure proper clutch operation. First, it is necessary that the spring coil element that bridges the gap between the input and the output be sufficiently large to transmit the entire torque load within the allowable stress of the material. Second, it is necessary that the spring be compliant enough so that the frictional forces generated between the spring and the shafts can force the spring to expand and contract readily. These two requirements make it impractical to design a spring clutch with a constant coil cross section. A spring compliant enough for deflection with a constant cross section large enough to carry the entire torque load would be prohibitively long. In practice, the spring is designed with an exponentially varying coil width, wider in the middle and narrower at the ends. This design meets both compliance and strength requirements in a compact envelope. Theoretically, if the application of torque from the housing to the spring varies exponentially, a spring with exponentially varying width coils will have a constant stress distribution.

Figure 2 shows a typical spring clutch arrangement in cross section. The ends of the spring are interference fitted into both the input and output shafts. This permits instantaneous engagement whenever the input attempts to rotate faster than the output. The central coils of the spring are relieved on the outside diameter to minimize the length of spring that is subjected to wear and to reduce the overrunning torque. A spring guide arbor through the center of the coils provides positive alignment of the spring with the input and output members during overrunning.

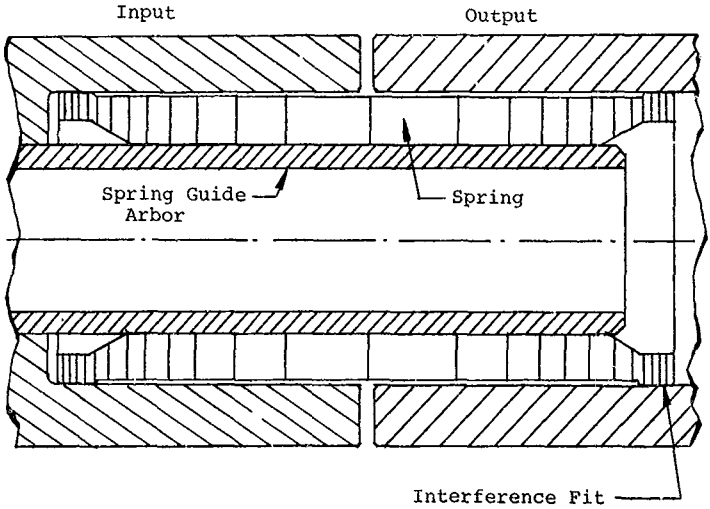

Figure 2. Cross Section of Active Spring Clutch Components.

The spring is designed so that at rest an interference fit exists between spring and arbor. When the input speed reaches the design output speed and just prior to clutch engagement, the spring should remain on the arbor and should not lift off because of centrifugal force. During overrunning, slippage is forced to occur at the end of the spring opposite to the member to which the arbor is attached.

Another requirement in the design of the spring clutch is the proper lubrication of the spring end that slips during overrunning. The slipping will take place on the output end of the spring. Lubricant is fed through the center of the spring whereupon it is forced to the inner bore of the rotating output housing under the influence of centrifugal force. The spring teaser coils are lubricated as the oil passes through slots on the teaser coil outside diameter. Holes in the output housing allow the oil to drain.

Sprag Clutch

The sprag clutch is the type most commonly used today in helicopter transmissions. Its operation depends on a complement of friction elements called sprags, which wedge between the races to transmit torque. The basic sprag clutch package consists of a circular shaft outer race, usually the driving member; a circular shaft inner race, usually the driven member; one or two rows of sprags; one or more retainers; energizing springs; and appropriate bearings to provide support and concentric positioning of the two races. A section of a sprag clutch is illustrated in Figure 3.

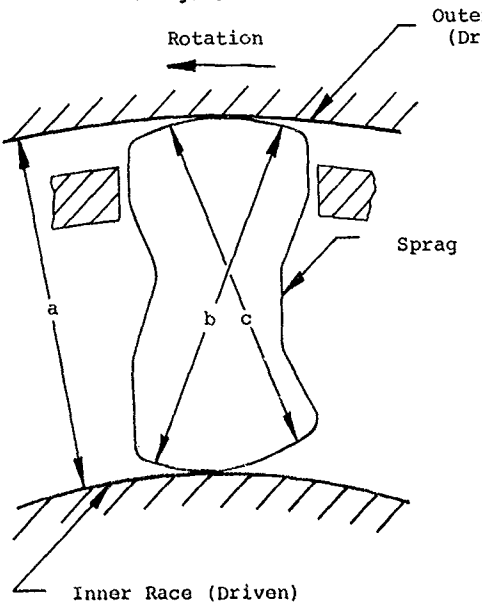

Figure 3. Sprag Cross Section.

If the outer race attempts to rotate faster than the inner race, the frictional force and the expansive force of the energizing spring tend to rotate the sprags in a counterclockwise direction about their centers. Because the "b" dimension of the sprags exceeds the radial distance between races, "a", the sprags become wedged (as illustrated) between

the inner and outer races, thereby locking the races together and transmitting torque. If the inner race attempts to rotate faster than the outer race, the frictional force between the sprags and the race tend to rotate the sprags in a clockwise direction about their centers against the expansive force of the spring. Because the "c" dimension of the sprags is less than the radial distance between races, the sprags do not wedge, and the two races are allowed to rotate independently of one another. During overrunning, the energizing spring forces the sprags to remain in contact with both races.

The key to the proper operation of the sprag clutch is the proper choice of the initial contact or gripping angle. For economical reasons, companies that manufacture sprags usually have a standardized selection of cross sections from which to choose. These standard sprag cross sections have been selected to satisfy a large range of torques and race diameter sizes, which cover the entire usage of helicopter transmissions.

Unlike the ramp roller clutch, two unequal gripping angles are formed in the sprag clutch, one at the inner race contact or tangency point and the other at the outer race contact point. These angles are defined in Figure 4. By drawing two radial lines, O-A and O-B, from the center of rotation, through the centers of the radii of curvature of the sprag surfaces, points A and B, the angle, ψ, is formed. Point Q is the inner race contact point, while point T is the outer race contact point. A line that connects points Q and T together with the previously constructed lines, O-A and O-B, form the outer and inner race gripping angles, W and V, respectively.

For proper clutch operation, the gripping angles must be such that the radial force produced at the start of engagement combines with the coefficient of friction at the inner race contact point to resist the tangential force due to torque. In other words, the tangent of the inner contact angle, V, must be less than the coefficient of friction or the clutch will not engage.

Sprag clutches, because of their wide usage, have attained a high degree of refinement. The sprag cams generally consist of precision-machined compound curves that provide optimum contact angles for overrunning and driving. The sprags are also designed to give an increase in contact angle with an increase in applied torque. The higher contact angle reduces the radial loads transmitted by the sprags, thus permitting higher transmitted torques for given values of Hertz and hoop stresses.

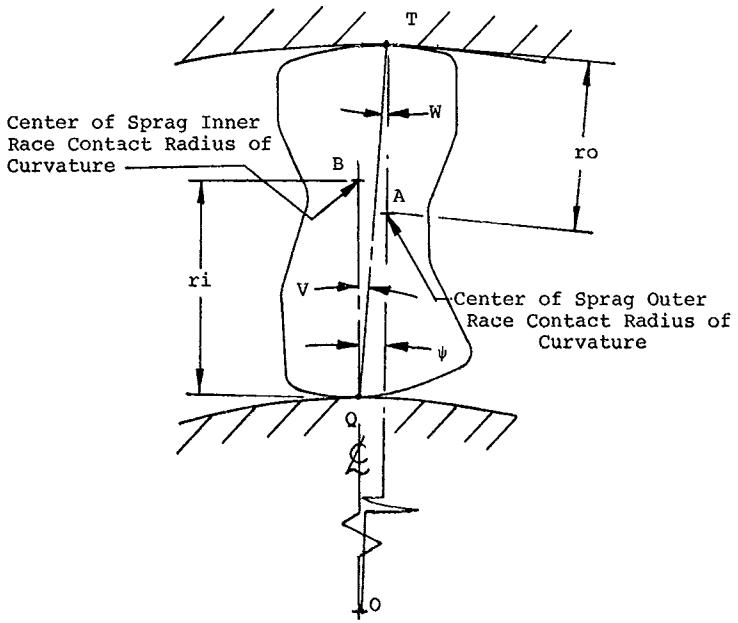

Figure 4. Sprag Contact Angle.

There are two different types of sprag clutches currently in use today: the full-phasing type and the positive-continuous-engagement (PCE) type. These two basic types are depicted in Figure 5. The full-phasing type of clutch generally employs a double cage, a ribbon spring, and frictional devices attached to the cages that insure that all sprags assume the same relative angular position at all times. These frictional devices overcome the inertial forces of the cages and the sprags during accelerations and decelerations. The PCE type generally employs a single cage and garter-type spring that allows each sprag to move independently of its neighbor. This type of clutch has the added feature that, under overload conditions, the sprags abut one another, thereby forming a "solid" unit that cannot "roll over." With the full-phasing type of clutch, "roll over" of the sprags is a possible mode of failure if the clutch ultimate capacity is exceeded. The PCE type of clutch will slip when overloaded, and due to the very high pressures at the contact points, scoring of the races is a possible mode of failure.

The lubrication and the surface finishes of the sprags and races are very important for the proper operation of a sprag clutch.

Ramp Roller Clutch

Like the sprag clutch, the ramp roller clutch depends on wedging action to transmit torque. However, instead of sprags, cylindrical rollers are used to transmit torque from the input to the output member. The basic ramp roller clutch consists of an inner cam shaft, a complement of rollers, a retainer or cage, an energizing spring or springs, and a circular outer housing. The basic configuration is illustrated by Figure 6. The cam shaft is an equilateral polygon with the number of sides equal to the number of rollers. The rollers are positioned on the cam by the roller retainer, which is positioned by a spring/pin mechanism so that the rollers touch both the outer housing and the cam. When torque is applied to the cam so as to force the rollers up the ramp, the rollers become wedged between the cam and the outer housing, thereby locking these members together and the clutch is in the driving mode. When the outer housing attempts to rotate faster than the cam (i.e., torque is applied in the clockwise direction), the rollers roll out from the wedged position and slide on the cam, thereby decoupling the cam from the outer housing. The clutch is then in the overrunning mode. A ramp roller clutch in which the outer member is an internal cam is also used but not in aircraft because of the difficulty in manufacturing the flats with accuracy. There is also a loss of sensitivity to accelerations when the cam is in the outer race. Energizing springs must be designed with centrifugal effects of the rollers in mind.

FULL PHASING

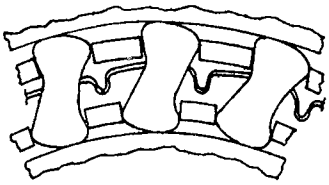

Overrunning

POSITIVE CONTINUOUS ENGAGEMENT (PCE)

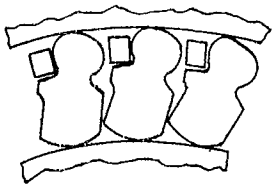

Overrunning

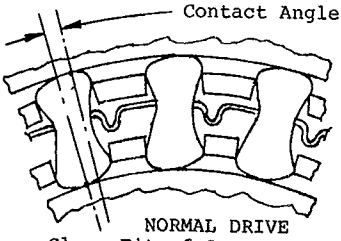

NORMAL DRIVE
Close Fit of Cages
Assures that all Sprags
Move in Phase

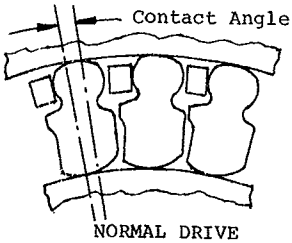

NORMAL DRIVE
Free Action of Sprags
Permits Individual
Positioning

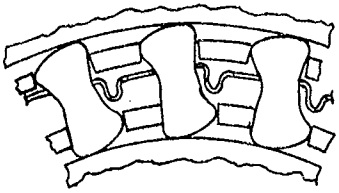

OVERTORQUE

Can Overturn When
Contact Angle is Zero
(Rise of Sprag Exceeded)

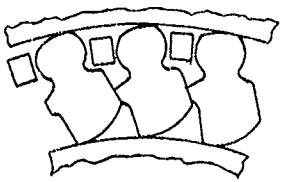

OVERTORQUE

Sprags Abut Each
Other, Forming a
Locked Assembly

Figure 5. The Principle of Operation of the Sprag Overrunning Clutch.

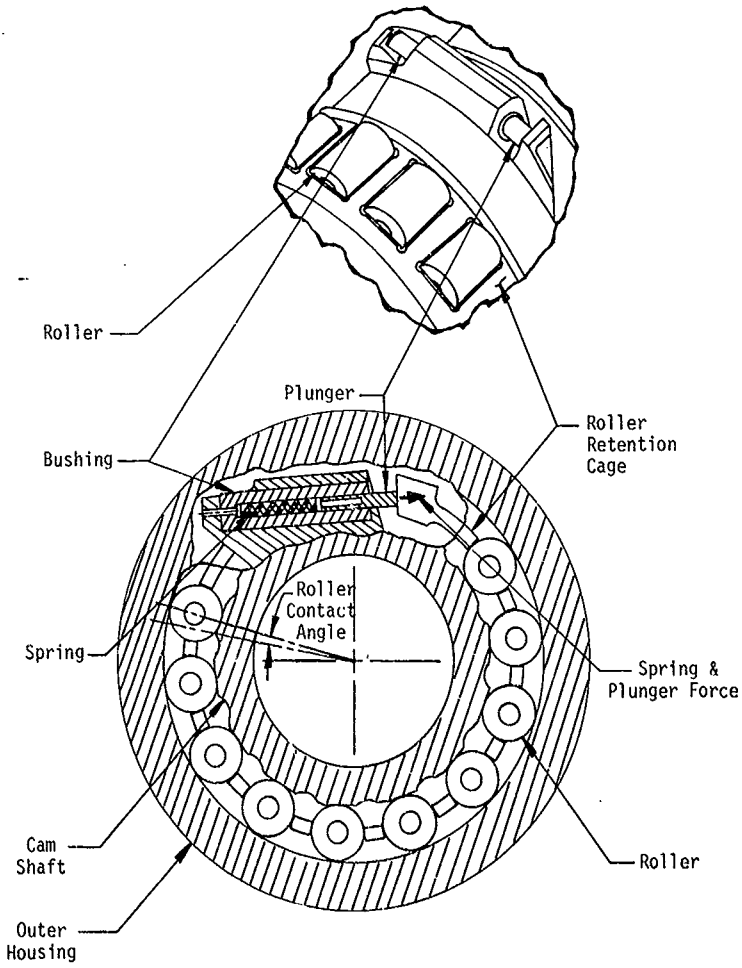

Figure 6. The Principle of Operation of the Ramp Roller Overrunning Clutch.

As with the sprag clutch, proper choice of the initial contact angle, commonly called the nip angle, is critical to the proper operation of the ramp roller clutch. This angle is shown in the force diagram of Figure 7.

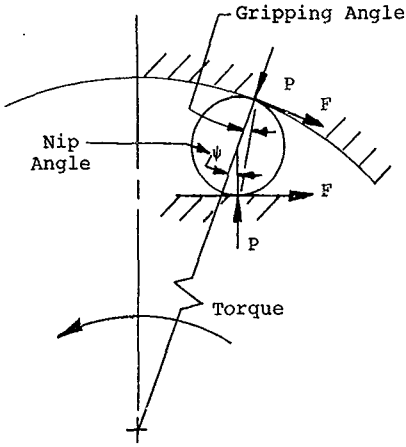

Figure 7. Ramp Roller Clutch Drive Forces.

The tangent of one-half of the nip angle, like that of the gripping angle of the sprag clutch, must be less than the coefficient of friction between the roller and cam. If the tangent of one-half of the nip angle exceeds the coefficient of friction, the rollers will not wedge properly, but will "spit out", thus preventing the transmission of torque. Another important consideration for the proper functioning of a ramp roller clutch is the design of the pin/spring mechanism, which keeps the rollers in constant contact with the outer housing. An improperly designed mechanism could lead to a jammed pin, which could either prevent clutch engagement or disengagement at the proper times. Frictional and centrifugal load considerations must be accounted for in the design of the pin and the spring. The cam shaft, cage, and outer housing require rigid tolerance control on those surfaces involved in the operation of the clutch. The circular grooves on the face of the cam shaft are used only in the assembly of the clutch. They serve no purpose in the operation of the ramp roller clutch.

The ramp roller clutch, like the sprag clutch, has become a highly refined unit through years of development and service. Among the more recent developments is the incorporation of hollow rollers. These rollers reduce Hertzian stresses considerably, thus leading to more compact clutches. Ramp roller clutches have been designed with one or two rows of rollers for a wide range of powers and speeds.

CLUTCH FIELD USAGE AND EXPERIENCE

Tables 1, 2, and 3 list the basic parameters for spring, sprag, and ramp roller clutches, respectively.

These clutches, in the cases of the sprag and ramp roller, have been in the field for thousands of hours and represent the state-of-the-art of helicopter overrunning clutches.

The charts are intended as guides to the ranges of applications of the clutches.

TABLE 1. SPRING CLUTCH DESIGNS.

Mfg	Model/Location	Torque (in-lb)	Design (hp)	rpm	D_o Outer Housing Bore Dia	b Spring Coil Width at Crossover	h Spring Coil Height at Crossover	L Spring Overall Length	Size Factor $\sqrt[3]{\text{Torque}/3570}$	Coil Tang Load at Crossover (lb)	Fa Axial Stress at Center Coil (psi)	Ft Total Stress at Center Coil (psi)	Centrifugal Diametral Growth
Sikorsky A/C	AAVLABS/Baseline	3,570	1,500	26,500	1.376	.397	.25	3.12	1.00	6,320	63,680	122,400	.0041
Sikorsky A/C	UTTAS/#1 Position	4,730	1,500	20,000	1.514	.437	.274	3.42	1.10	7,630	63,720	117,400	.00314
Sikorsky A/C	UTTAS/#2 Position	15,760	1,500	6,200	2.260	.65	.41	5.12	1.642	17,040	63,940	99,000	.00094
Boeing	UTTAS	12,910	1,520	7,419	2.125	.612	.385	4.80	1.54	14,840	62,980	117,800	.0012
Hughes	AAH	9,649	1,500	9,804	1.918	.552	.348	4.32	1.39	12,280	63,930	125,000	.0015
Boeing	HLH	44,220	8,368	11,502	3.163	.918	.578	7.22	2.313	33,930	64,000	137,700	.0095
Boeing	CH-47	27,350	4,600	10,600	2.711	.782	.492	6.15	1.97	20,800	64,500	137,100	.005
Sikorsky A/C	S-76	6,440	610	5,966	1.674	.483	.304	3.80	1.217	9,400	64,000	111,000	.00027

TABLE 2. SPRAG CLUTCH PRODUCTION DESIGNS.

Manufacturer	Model	Torque Rating (in.-lb)	hp	Speed (rpm)	Clutch Envelope Size		Sprag Elements				Strut Angle Degrees				Load Per Sprag		Stress - psi	
					Inner Race	Outer Race	Length	Size	Total No.	No. of Rows	Unloaded		Loaded		Tang @ OR	Norm @ OR	Outer Race Hoop	Inner Race Hertz
											V	W	V'	W'				
Bell	UH-1	10750	1100	6450	4.064	4.812	.470	.374	40	1	2.552	2.155	3.65	3.07	112	2080	48700	347400
Bell	209 & 212	17180	1800	6600	4.064	4.812	.470	.374	40	1	2.552	2.155	4.01	3.38	178	3020	69500	419000
Bell	204	10500	1100	6600	4.064	4.812	.415	.374	40	1	2.566	2.167	3.75	3.16	109	1980	52400	371200
Bell	206 & OH-4	3320	317	6000	1.957	2.613	.785	.328	22	1	2.653	1.987	3.35	2.50	115	2640	37400	331100
Hiller	FH-1100	3320	317	6000	2.274	2.930	.415	.328	26	1	2.569	1.994	3.50	2.70	87	1850	62700	378400
Hiller	HO-5	3320	317	6000	2.274	2.930	.415	.328	26	1	2.569	1.994	3.50	2.70	87	1850	62700	378400
Hughes	OH-6	2640	220	6000	1.500	2.156	.665	.328	18	1	2.703	1.880	3.26	2.26	136	3450	55800	422500
Hughes	369-500	2640	220	6000	1.500	2.156	.665	.328	18	1	2.703	1.880	3.26	2.26	136	3450	55800	422500
Hughes	269-A	4630	147	2000	2.274	2.930	.615	.328	26	1	2.608	2.024	3.84	2.97	121	2340	68700	348200
Kaman	H-43	10500	1100	6600	2.843	3.591	.790	.374	30	1	2.657	2.103	3.64	2.87	195	3880	54600	383700
Piasecki	16-H	20600	1960	6000	2.843	3.499	.790	.328	48	2	2.650	2.153	4.16	3.37	122	2080	83900	285700
Avco	Eustis	3560	1500	26500	2.156	2.904	.665	.374	20	1	2.722	2.020	3.55	2.63	122	2670	53400	343800
Boeing	CH-47A&B	26120	4970	11990	2.274	2.930	.790	.328	48	2	2.569	1.994	3.42	2.65	185	4010	55800	404200
Boeing	CH-47	2350	308	8257	1.500	2.156	.665	.328	36	2	2.703	1.880	2.71	1.88	30	920	15200	218200
Boeing	CH-47C	37310	7500	12668	2.843	3.591	.665	.374	60	2	2.638	2.088	3.77	2.98	173	3330	65900	376600
Boeing	CH-46	24280	3000	7600	2.843	3.591	.665	.374	60	2	2.638	2.088	3.44	2.72	115	2430	41300	321700
Boeing	HLH	91080	16620	11500	4.509	5.507	.835	.499	68	2	2.797	2.289	3.66	2.99	243	4650	61600	340300
Boeing	YUH-61A	25740	3030	7419	2.437	3.185	.935	.374	44	2	2.682	2.052	3.42	2.61	184	4040	37600	353200
Boeing	UUH-61A	660	62	5936	1.500	2.156	.320	.328	18	1	2.703	1.880	2.99	2.08	34	935	32600	317000
Robinson	R-22	2300	98	2139	1.500	2.156	.665	.328	18	1	2.703	1.880	3.26	2.26	118	3000	54100	393700
Hughes	AAH	9827	1533	9841	2.843	3.591	.665	.374	26	1	2.683	2.088	3.69	2.92	210	4130	54700	419400
Hughes	AAH	684	90	8216	2.274	2.930	.320	.328	26	1	2.569	1.994	2.93	2.27	18	457	28800	214400
Lockheed	AH-56	24000	5940	15600	4.014	4.762	.665	.374	38	1	2.554	2.153	4.22	3.54	265	4280	84000	419300
Lockheed	AH-56	3930	258	4141	4.622	5.370	.410	.374	20	1	2.527	2.175	3.54	3.04	73	1380	38900	301200
Hiller	360	12410	630	3200	2.277	2.930	.780	.328	48	2								
Sikorsky	Eustis	4730	1500	20000	1.750	2.406	.665	.328	36	2	2.527	2.004	3.44	2.50	55	2500	58400	354200

TABLE 3. RAMP ROLLER CLUTCH PRODUCTION DESIGNS.

Model/Location	Torque (in.-lb)	Design (hp)	rpm	"R" Outer Housing Bore Rad	"X" Cam Flat to C.L. (in.)	No. Rollers	Roller Di-	Roller Length	Tang Load/ Roller (lb)	Norm Load/ Roller (lb)	No-Load Nip Angle (deg)	Full Load Nip Angle (deg)	Outer Hsg Hoop Stress (psi)	Cam/Roller Hertz Stress (psi)
S-51/Main GB	12,330	450	2300	1.312	.998	12	.3125	.871	780	13,770	2.92	6.68	78,300	728,100
S-55/Input	17,330	700	2400	1.709	1.291	12	.4139	.871	845	15,440	4.23	6.27	68,500	664,900
S-56/	46,690	2100	2700	2.264		15	.6338	1.116	1370	24,800	3.94	6.32	60,000	608,400
S-56/	46,690	2100	2700	1.625		12	.6899	1.492	1720	36,700	3.19	5.38	50,100	611,700
S-58/Input	32,640	1525	2800	1.957	1.349	12	.6338	1.116	1370	25,300	4.07	6.20	59,000	616,400
S-58T(Turbine)/Input	11,630	1050	6000	1.875	1.496	16	.375	.875	370	8,650	3.95	4.90	40,000	524,000
S61 (SN3A)/Input	9,060	1200	8350	1.875	1.459	12	.4139	1.031	402	10,710	2.88	4.29	32,100	515,400
S61 (SN3D)/Input	10,500	1350	8100	1.875	1.459	12	.4139	1.031	466	11,860	3.42	4.50	36,100	539,000
S61/Tail Take-Off	2,990	144	3031	1.997	1.616	12	.375	.500	125	2,980	3.81	4.81	22,000	406,000
S61/Accessory Drive	1,990	144	8350	.969	.718	8	.250	.500	140	3,640	2.79	4.41	38,300	553,900
S-62/Input	7,350	670	5760	1.875	1.458	12	.4139	.750	326	7,860	3.49	4.75	44,900	517,300
S-62A Coast Guard/Input	8,160	730	5635	1.875	1.458	12	.4139	.750	362	8,460	3.49	4.90	49,800	544,200
S-64/Input	45,100	4650	4500	3.25	2.526	14	.720	1.800	1430	32,320	3.02	5.08	43,000	516,000
S-64/Tail Take-Off				1.997	1.618	12	.375	.500			3.81			
CH53A/Input	33,500	3200	6022	2.626	1.934	12	.6899	1.493	1063	26,260	2.46	4.65	38,200	515,600
S-65/Accessory	2,160	297	6022	1.635	1.258	12	.375	.500	110	2,860	3.16	4.42	28,400	430,200
RH53D/Input	47,100	4500	6022	2.840		14	.800	1.603	1184			4.50		
CH53E/Trc Eng Input	59,380	4380	4649	2.9608	2.040	14	.825	1.580	1480	36,340	2.19	4.66	54,400	540,000
Roller Gear Drive	18,940	1870	6223	2.526	1.900	14	.625	1.255	535	13,680		4.48	32,400	420,000
S65/APP Clutch	1,150	150	8233	1.085	.853	12	.250	.50	88	2,700	3.70	5.17	23,000	475,000
S-79/Input	16,110	1427	5833	1.982	1.401	14	.580	1.200	580	13,930	1.97	4.88	8,900	458,000
S76/Input (2 Row)	6,360	630	6053	1.219	.841	12	.375	.750	237	4,491	3.97	6.03	13,580	442,700
Eustis RAD	4,716	1500	20000	1.503	1.125	14	.375	.625	225	4,162	3.87	6.20	36,250	431,000

DESIGN REQUIREMENTS, CONSTRAINTS, AND CONSIDERATIONS

Structural Requirements

The overrunning clutch should be designed in as small a package as possible, consistent with structural requirements. Not only does this practice reduce weight and cost, which are primary objectives, but the reduced size also diminishes the centrifugal effects and the pitch line velocity effects. In operation, the freewheel unit is locked whenever the engines are driving. Stresses in the locked position are steady in nature and vary only with power and speed; thus, high cycle fatigue need not be considered in the design of the helicopter overrunning clutch.

The primary consideration for freewheel unit structural design is the maximum torque that the unit is expected to experience. Usually, this is the value of the maximum engine output torque. Although high cycle fatigue is not considered, low cycle fatigue (ground/air/ground or GAG) is considered in the design of the clutch members. For the material used on the input and output clutch shaft members, the stresses induced at maximum design power must be below the allowable limit of the material at the maximum number of expected starts. For general purposes, 10,000 cycles can be regarded as a typical low cycle fatigue design life. The design allowable stress can be chosen on the basis of the fatigue stress at those cycles, which represent the life of the aircraft. Since the load cycles are not truly vibratory in nature, stress concentration factors are usually not considered. As a rule of thumb for case carburized members, 40,000 psi can be considered a design allowable stress at maximum engine torque.

The clutch members must also be designed for static torque conditions that exceed the maximum torque output of the engine. Often two times the normal maximum torque is used as the limit torque. No failure or yielding of members is allowed at this condition. A 1.50 factor of safety is generally applied to the limit load to obtain the static ultimate stress, whereas a 1.15 factor of safety is applied to the limit load to obtain the static yield condition as shown by

$$\text{M.S.}_{\text{yield}} = \frac{\text{Fty}}{1.15 f_t} - 1 \qquad (1)$$

$$\text{M.S.}_{\text{ult}} = \frac{\text{Ftu}}{1.50 f_t} - 1 \qquad (2)$$

where

M.S. yield	=	static yield margin of safety
M.S. ult	=	static ultimate margin of safety
Fty	=	tensile yield strength - psi
Ftu	=	ultimate tensile strength - psi
f_t	=	combined stresses induced in component (see analysis section for method of combining stresses)

Maximum speed is determined by engine speed. Centrifugal effects must be ascertained at all speed conditions, including the maximum expected overspeed condition. Often, 120% overspeed is specified as the maximum speed condition and may be experienced during autorotation.

Overrunning Requirements

The use of overrunning clutches in helicopter drive trains is illustrated in Figure 8. As can be seen from this figure, there are basically three areas in the transmission where overrunning clutches are used: between the engines and the main transmission (main freewheel units), between the main transmission and the accessories, and between the main transmission the auxiliary drive unit.

Clutches that are used between the engines and the main transmission must be capable of operating at high speeds (up to 20,000 rpm) while transmitting high torques. In addition, they must be able to operate in the overrunning mode for relatively long periods of time with very little wear. Wear in the overrunning mode has always been a problem with overrunning clutches. Wear in an overrunning clutch is dependent on the pressure and the relative velocity of the contacting surfaces. These two parameters vary considerably as the differential speed between the input and output members varies. Figure 9 shows a theoretical wear factor that was derived for sprag- and ramp-roller-type overrunning clutches. The curve is based on the assumption that wear will be proportional to pressure times velocity. For a low input speed and an output at full speed, the sliding velocity between the two members is high, but the centrifugal force, which is proportional to pressure, is low. As the input speed increases, the sliding velocity decreases, but not as fast as the centrifugal force increases; hence, the wear factor increases to a maximum when input speed is 67% of output speed. After this, the decrease in relative velocity becomes the overriding factor and wear rapidly drops off, reaching zero in the locked position.

TYPICAL LARGE HELICOPTER
TRANSMISSION SYSTEM

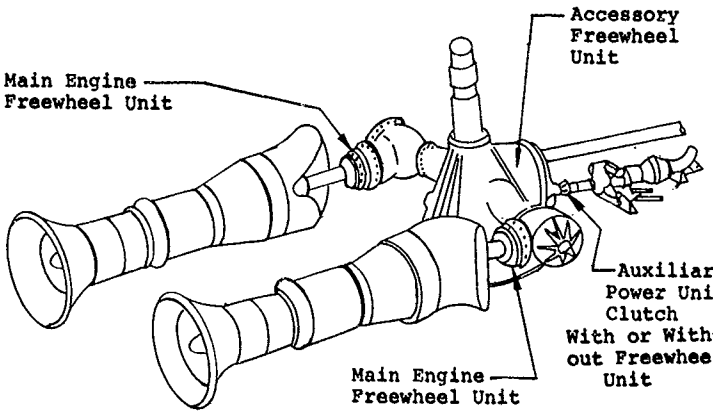

TYPICAL SMALL OR MEDIUM HELICOPTER
TRANSMISSION SYSTEM

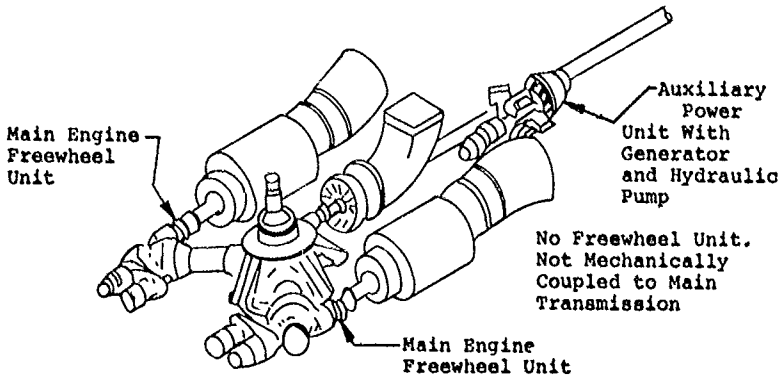

Figure 8. Location of Freewheel Units in Typical Helicopter Drive Trains.

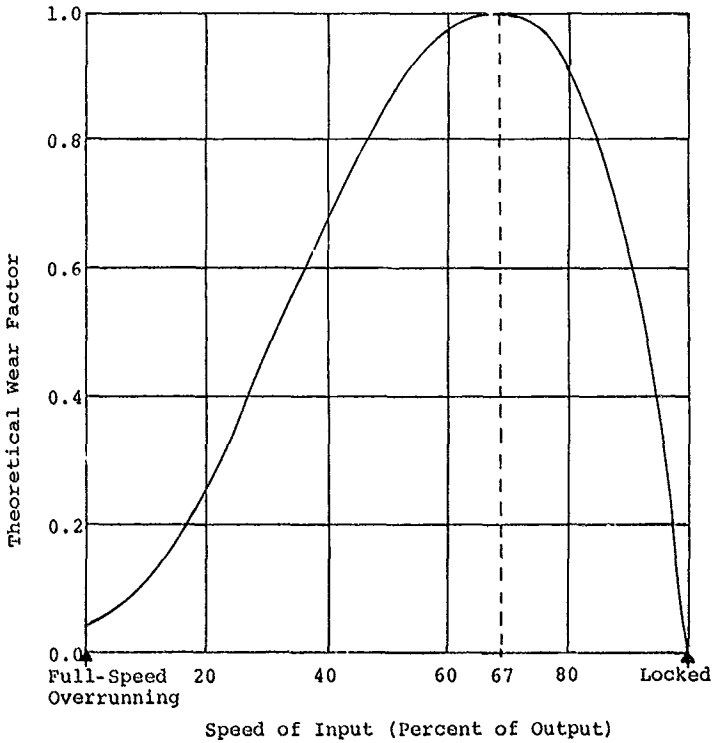

Figure 9. Theoretical Wear Factor for Ramp Roller and Sprag Clutches as a Function of Differential Speed.

Overrunning clutches, as used in the main drive train, operate except during transient conditions, in only three modes: locked, differential overrunning (input speed 50% to 70% of output speed), and full-speed overrunning (input speed 0 and output speed 100%). The locked position is, of course, the most common, occurring at all times when the engine is driving the transmission. Differential speed overrunning, which is by far the worst condition for wear, occurs mainly during practice autorotations with engines at ground idle, which is generally 50% to 70% speed or during start up. Full-speed overrunning occurs mainly during start up and in flight with one engine inoperative.

An estimate of overrunning clutch usage may be obtained from Table 4, which is derived from a survey of helicopter operation.

In determining the amount of time spent in autorotation (i.e., differential overrunning) during the life of an aircraft, the results of the survey were combined with the total aircraft flight hours for light, medium and heavy aircraft. The number of hours shown here for autorotation represents the average time an aircraft would be expected to operate in the autorotation mode during its life of 15 years. Since only practice autorotations are considered, this time may vary considerably from aircraft to aircraft, depending on their use. An aircraft used primarily for training purposes, for instance, will be operated in autorotation considerably more than an aircraft used for other purposes. It will be noted that heavy cargo aircraft are used in autorotation considerably less than smaller aircraft. This reflects the fact that standard procedure is to discourage practice autorotations in larger helicopters.

As can be seen from Table 4, the time spent in full-speed overrunning during start-up procedures depends on whether or not the particular aircraft has a rotor brake. In an aircraft equipped with a rotor brake, the standard practice is to engage the rotors after both engines are started; hence, there is no full-speed overrunning. In an aircraft not equipped with a rotor brake, full-speed overrunning occurs during the time between the start of the first engine and the start of the second engine. As is shown by Table 4, this amounts to a considerable length of time in full-speed overrunning over the life of the aircraft. However, it must be stressed that full-speed overrunning is not a severe wear condition for freewheel units, as is shown by Figure 9. Full-speed overrunning during flight with one engine inoperative (O.E.I.) was estimated to occur during one-tenth of one percent of the total aircraft flight time.

TABLE 4. MAIN DRIVE TRAIN CLUTCH USAGE SUMMARY

Aircraft Type	Service Life (yr)	Util (FH/mo)	Life Flt Hr	Avg Miss Time (hr)	Life Starts	Auto Time (hr/FH)	Aircraft Life Clutch Usage		
							Diff Over Auto (hr)	Full-Speed Over (Eng Start-up) (hr)	Full-Speed Over (OEI) (hr)
Light Observation w/Rotor Brake	15	70	12,600	2.0	6300	.01	126	0	12
Light Observation w/o Rotor Brake	15	70	12,600	2.0	6300	.01	126	378	12
Med Utility Trans w/Rotor Brake	15	69	12,420	1.8	6900	.01	124	0	12
Med Utility Trans w/o Rotor Brake	15	69	12,420	1.8	6900	.01	124	414	12
Heavy Cargo w/Rotor Brake	15	45	8,100	1.5	5400	.001	8	0	8
Heavy Cargo w/o Rotor Brake	15	45	8,100	1.5	5400	.001	8	324	8

Overrunning clutches for accessories and auxiliary drives are used mainly on larger helicopters. Referring to Figure 8, it can be seen that there are basically two configurations for accessories. The upper part of Figure 8 shows a configuration where a freewheel unit is placed between the main transmission and accessories. This freewheel unit permits ground operation of all accessories without the operation of the main drive system. Power is supplied to the accessories either from an auxiliary power unit (APU), which is mounted on the aircraft, or from a portable ground unit. When the accessories are operated independently of the main transmission, the freewheel unit, located between the accessories and main transmission, will be in the overrunning mode. Figure 10 shows graphically an estimate of the amount of time the accessory freewheel unit would be expected to operate in the overrunning mode during the life of a light, medium, or heavy helicopter.

If the aircraft is equipped with an APU, some type of mechanical clutch, often centrifugal- or multiple-disk-type, will be located between the APU and accessories. This is necessary since APU's generally do not generate enough power for the accessories until almost at full speed. There may or may not be a conventional overrunning clutch in addition to the mechanical clutch between the APU and accessories. This freewheel unit would overrun during all normal operation of the aircraft, such as flight; hence, the freewheel units used between the APU and the accessories overrun more than freewheel units used in any other location. In this type of application, sprag clutches have been used that are designed with centrifugal disengagement. If the inner race is connected to the APU and the outer race is connected to the drive train, these specially designed sprag clutches will lift off the inner race at approximately 50% speed (or higher). Thus, during normal operation, there is no wear since the sprags are not rubbing on the inner shaft. Of course, the APU cannot be engaged until the speed of the main transmission is reduced, allowing the outer race sprags to once again touch the inner race; hence, this type of design is only appropriate for an application such as an APU, which will never be used in flight.

The lower part of Figure 8 shows another transmission configuration, typical of a medium or small helicopter. Here, the only two freewheel units are located in the primary drive train at the engine inputs. The APU, which is used to drive a generator and a pump, is not mechanically connected to the main drive train, and hence, there are no accessory or auxiliary drive freewheel units.

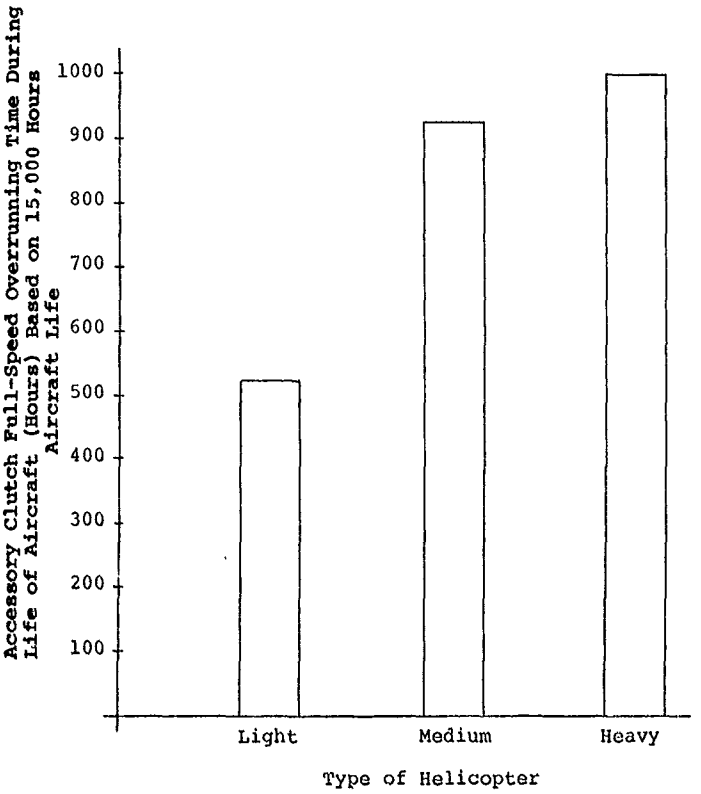

Figure 10. Accessory Freewheel Unit Overrunning Life.

During overrunning, centrifugal effects cannot be neglected, even at the relatively low speed of 3000 rpm. Assemblies that are inherently balanced by symmetry must be checked for distortions and stresses that can be induced by centrifugal loads. This is especially true in those cases where circular members have two opposing masses acting at 180° apart. Deflections are greatly reduced when four masses are used instead of two masses.

In the spring clutch, the spring should not expand and touch the outer housing until the relative speed of the members is reduced to the point where scoring cannot be induced. A good procedure is to design the spring so that it will not leave the spring arbor due to centrifugal force alone at maximum operating speed.

In the sprag clutch, the geometry of the sprag itself must be carefully designed to reduce overrunning drag and to reduce overturning moments on the sprag.

In the ramp roller clutch, the spring pin mechanism centrifugal effects must be analyzed. The centrifugal loads of the roller retention-cage lugs and the effects of distortions on cage clearance must be determined.

Environmental Requirements

Helicopter freewheel units, like all helicopter components, will be expected to operate satisfactorily over a wide range of environmental conditions. The various climatic extremes for military aircraft are covered quite extensively in such publications as MIL-STD-210B and AR 70-38, which should be consulted as a matter of course in the design of any helicopter component. The environments that are most likely to affect the operation of freewheel units are temperature and vibration. Corrosion is generally not a problem once the freewheel unit is installed in the helicopter since it is inside the transmission case. Present military helicopter freewheel units have been designed to operate satisfactorily over a temperature range of -65°F to +250°F. The temperature limits are usually defined in the aircraft detail specification or by a contractual requirement. With an operational temperature range of the magnitude generally experienced in helicopters, two areas of clutch design should be carefully examined: the use of dissimilar metals and lubrication.

While most clutch components will be of steel, there will be occasion to use other metals for freewheel unit components. For example, the use of bronze bushings is quite common in ramp roller clutches. With the use of such materials, special attention must be given to the effects of differential thermal

expansion or contraction on clutch operation. The clearances or the fits between all components of dissimilar metals should be checked at the temperature extreme that increases them, and the stresses or the clearances should be checked at the temperature extreme that decreases clearances. Bushings, for example, must be free to rotate under all temperature extremes.

In extreme cold, commonly used helicopter transmission lubricants undergo a marked increase in viscosity. This increase in viscosity can prove troublesome in that it can cause small clutch components to stick or move very sluggishly, thus affecting clutch operation, particularly on start-up. Good drainage should be provided so that, on shut-down, most of the oil will leave the clutch and drain into the transmission sump. If the clutch is positioned so as to be immersed in oil when the transmission is at rest, start-up difficulties could be experienced in cold weather. Hot oil has very little effect on overrunning-clutch operation other than the loss of lubrication film thickness due to the decrease in viscosity that comes with increased temperature.

One of the most important environmental considerations in the design of helicopter overrunning clutches is vibration. Basically, vibration should be considered from two standpoints in the design of freewheel units. First, the clutch should be considered as a receiver of vibratory energy from its environment. Second, the clutch should be examined as a potential source of vibration. The clutch as a potential source of vibration is only a function of clutch speed (1 per rev) and is a matter of component imbalance. Balance requirements are discussed separately.
The magnitude and frequency of the vibration an overrunning clutch will experience as a result of its environment is difficult to predict with accuracy. The vibration will be both torsional and lateral, with the transmission, airframe, and rotors all contributing in various degrees. The natural frequency of the clutch assembly must be removed from the operating environment of the helicopter transmission. Excitation sources include the gear clash frequencies, which can be high since they are a function of the number of teeth times the rotational speed. The most accurate method for determining clutch assembly natural frequency is by test. At the test stage of the clutch development, it may be too late to change the design drastically. Conventional transmission practices, which include damping treatments and changes to the masses of the components, can often change the natural frequency so as to remove the natural frequency from the operational range. A minimum margin of safety of 15% is suggested (i.e., the clutch natural frequency should be removed by at least 15% from the operating frequency).

Location and Orientation

The selection of the location for the freewheel unit in the transmission system of a helicopter is often based on past experience, as well as on the geometric considerations of available space and envelope. Based on weight alone, the freewheel unit should be located on the shaft with the highest speed. This will lower the required drive torque, which in turn reduces the size of the clutch components required to withstand the stresses induced by the drive torque. The highest speed in the transmission is usually the engine output speed (input to transmission), and the design with the overrunning clutch operating at engine speed will usually produce the lightest clutch package.

In the past, helicopter freewheel units did not operate at speeds above approximately 12,000 rpm. With the development conducted under contract DAAJ02-74-C-0028, overrunning clutches can now be operated at speeds up to 20,000 rpm.

The overall impact on the transmission system may be such that the weight alone does not dictate the clutch location. It is recommended that, in the early stages of any helicopter transmission design and development, alternate layout designs be prepared for the overrunning clutch: one with the clutch located between the engine and the transmission and one with the clutch located after the first stage of gearing. The attributes of each design can then be assessed, and the choice of clutch location can be made on this basis.

Once the location in the transmission system is known, the clutch operating speed will be established by the gear ratios involved. Hence, if the horsepower is known, the clutch design torque will also be known, from which the clutch can be sized based on structural design requirements.

There is no advantage or disadvantage for any overrunning clutch in regard to the direction of rotation. In the spring clutch, the direction of the spring winding can be right- or left-handed, which establishes the overrunning and driving direction. In the sprag clutch, since the driving envelope consists of concentric circular shafts, the freewheel unit can be made to operate in either direction. To accomplish this, one has merely to turn the sprag unit end for end and reassemble. In the ramp roller clutch, the direction of rotation is established by the hand of the cam and the pin/spring location on the lug of the cage. Thus, in the helicopter freewheel unit, the direction of rotation can be clockwise or counterclockwise and only requires care in the detail drawing phase to obtain the proper hand of spiral for the spring of the spring clutch or the proper hand of rotation for the cam and cage of the ramp roller clutch.

Each type of overrunning clutch has its own peculiarities concerning which member of the clutch should be the driving (or input) member and which member should be the driven (or output) member. In general, it is advantageous to have the innermost shaft of the clutch as the output member. During overrunning, the output member will rotate, and if the output shaft is also the innermost shaft of the clutch, lubrication can be fed by centrifugal force to all clutch components. If the input member is the innermost clutch member, the lubricant can only be fed by gravity or pressure feed in a sealed chamber since the input is stopped during overrunning.

The advantages and disadvantages of inner shaft output or input are discussed for the spring, the sprag, and the ramp roller clutches in the basic configuration sections.

Balance

Another important requirement, especially for clutches operating in excess of 6000 rpm, is the balancing of the clutch. Excessive imbalance in high-speed clutches can lead to accelerated wear of clutch components or failure of the clutch to operate satisfactorily. The vibration due to this imbalance can also cause premature failure of the clutch components, such as support bearings, and other dynamic components located near the clutch.

In general, it is advisable to balance high-speed components as complete assemblies. This practice is expensive because it creates matched sets, but it eliminates mass imbalances that may be introduced in assembling the hardware and eliminates the possibility of the small imbalances of the various components combining in the assembly. Unfortunately, the balancing of the complete assembly is not practical for overrunning clutches since the angular relationship of the input and output members changes constantly during overrunning. This necessitates balancing the input and output subassemblies separately.

There has been much discussion of the maximum degree of imbalance that should be allowed for high-speed helicopter components. A successful criterion, which has been used for production clutch input and output subassemblies, has been to balance so that the imbalance force produced is not greater than 10 pounds. The curve of Figure 11 shows the relationship of imbalance and speed for an imbalance force of 10 pounds. This curve is a plot of the following equation for a force of 10 pounds

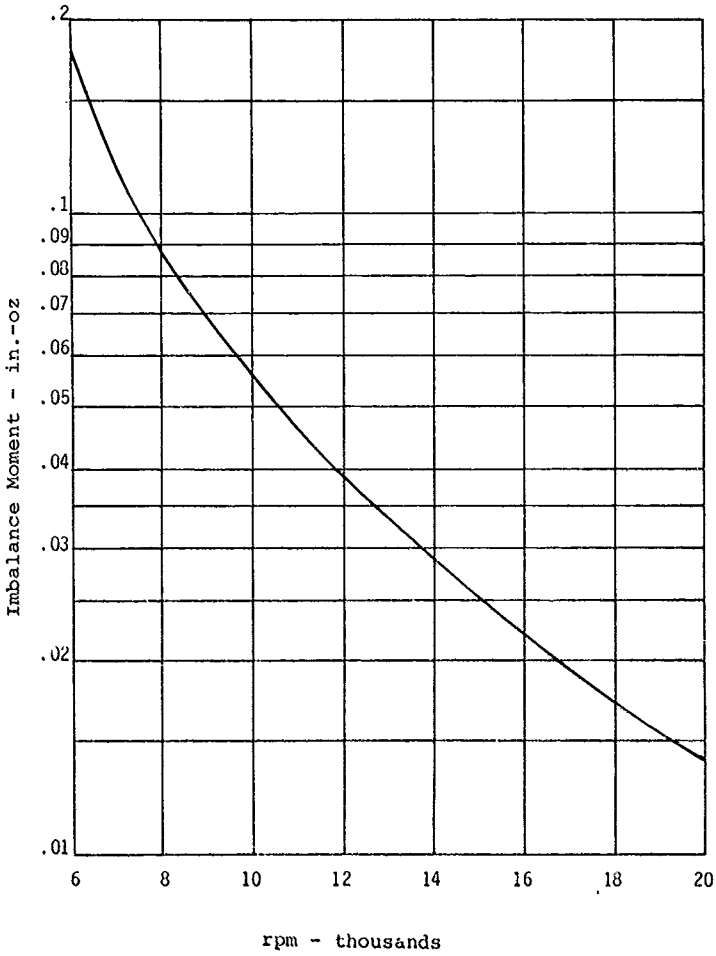

Figure 11. Drawing Balance Requirements for a Ten-Pound Force.

$$F = 1.776 \times 10^{-6} \text{ (in.-oz) (rpm)}^2 \qquad (3)$$

Closely related to balance is the consideration of critical frequencies, both lateral and torsional. In general, this is not a problem with helicopter overrunning clutches. The freewheel unit designs under consideration here are all inherently stiff both laterally and torsionally and thus have critical speeds well above those of normal operation.

CLUTCH SELECTION

Prior to selecting a particular type of clutch for a specific application, the design power and the clutch's location in the drive train must be known. The location in the transmission drive train will fix the clutch speed since the engine speed and reduction ratios are generally known. The testing accomplished in the Eustis Advanced Overrunning Clutch Technology program and reported in Reference 1 has shown that helicopter overrunning clutches can operate at up to 20,000 rpm. The spring clutch is capable of operation at even higher speeds, whereas the ramp roller and sprag are probably at their operating limits at 20,000 rpm. In fact, the ramp roller type of clutch is subject to centrifugal effects on the rollers, cage, and spring/pin mechanism that make development and operation difficult at 20,000 rpm. The operating limit should perhaps be set at 12,000 rpm for a ramp roller clutch because of centrifugal force effects.

Since torque is lower at higher speeds for the same horsepower, the overall clutch package will be smaller, weigh less, and be less expensive to manufacture if it operates at higher speed. If possible then, the helicopter clutch should be designed to operate at engine speeds and should be located at the transmission input. Possibly, it may be located within the first-stage pinion shaft.

To determine which type of clutch to use between spring, sprag, or ramp roller, it is suggested that layouts be made of each type. After a layout is made, factors such as weight and cost can easily be evaluated. A relative comparison of various factors for each clutch can be found in Table 5. The values shown are on the basis of 1.00 being the best, i.e., the lightest weight, least number of parts, etc. The actual numbers were derived during the design phase of Reference 1.

If the clutch is being designed for high-speed operation (above 12,000 rpm), the following overrunning clutch design check-off list should be followed:

Spring Clutch

1. Concentricity between spring, arbor, input bore, and output bore is critical.

---

1. Kish, Jules G., ADVANCED OVERRUNNING CLUTCH TECHNOLOGY, Sikorsky Aircraft, USAAMRDL Technical Report 77-16, Eustis Directorate, U. S. Army Air Mobility R & D Laboratory, Fort Eustis, Virginia (to be published).

TABLE 5. OVERRUNNING CLUTCH DESIGN SELECTION PARAMETERS.

Design Parameter	Spring	Sprag	Roller
Envelope Size	1.00	.85	.85
Weight	1.00	.85	.85
Development Cost	.88	1.00	.84
Manufacturing Cost	.85	1.00	.79
Speed Limitation	1.00	.57	.57
Number of Parts	1.00	.74	.75
Fail Safety	1.00	.50	1.00
Overrunning Wear Life	1.00	.72	.84
Torque-Carrying Capability	1.00	1.00	1.00
Confidence Factor	.80	1.00	.80
Maintainability	1.00	.90	.93
Centrifugal Effects	1.00	.97	.92
Lateral Vibration	.91	1.00	.87
Torsional Vibration	.56	.96	1.00
Transient Torque Capability	1.00	.93	.93
High-Temperature Operation	1.00	1.00	1.00
Low-Temperature Operation	1.00	.50	.50
Positive Engagement on Start-Up	1.00	1.00	1.00
Failure Modes	1.00	.58	.92
Unusual Test Requirements	1.00	1.00	1.00
Multi-Engine Operation	1.00	.93	.88
Bearing Brinelling	1.00	.30	.70

2. There must be a lubricant flow path on the overrunning end of the spring from the free end to the center of the spring, along the entire housing length. This can be accomplished by slots in the spring or slots in the housing.

3. Silver plating or other forms of plating on the overrunning coils should be avoided.

Sprag Clutch

1. Oil drainage should be such that when the clutch is at rest all oil in the sprag area is drained.

2. Clutch diameters should be as small as possible commensurate with stress levels. Thus, a tandem, two-row design should be considered. Smaller diameters reduce centrifugal effects.

3. The mounting arrangement with clutch bearings straddling the sprag unit is preferred.

4. The design should be centrifugally engaging. The drag produced by the centrifugal engagement must exceed the drag created by oil churning, i.e., drag should increase with increasing differential overrunning speed.

Ramp Roller Clutch

1. Circularity of the cage must be maintained at operating speed. The deflection of the cage due to centrifugal force on the cage lugs must not exceed the clearance between the cage and its mounting pilot on the cam.

2. The effect of centrifugal force on the pin/spring mechanism must be fully evaluated.

3. Hollow rollers are recommended to reduce centrifugal roller load and to lower Hertz stresses. Cage slot design must be such that a maximum material contact area exists between the end of the rollers and the end of the roller slots.

4. Clutch diameters should be as small as possible commensurate with stress levels. Smaller diameters reduce centrifugal effects.

As another aid to clutch selection, it is useful to examine comparative test results. Figure 12 shows clutch drag torque as a function of oil flow. As seen from the figure, the spring clutch is relatively insensitive to oil flow, whereas in the roller and sprag clutches, drag increases with increasing oil flow.

In Figure 13, clutch drag as a function of differential overrunning speed is shown. The ramp roller clutch tested displays a typical curve for this type of clutch. The sprag clutch, which was designed to be centrifugally engaging, should have a characteristic curve shape similar to that of the ramp. The curve actually obtained indicates that oil churning was actually overriding the drag from the centrifugally engaging sprags thereby lowering resultant drag torque. This is not a desirable characteristic in a sprag clutch. The spring clutch shows a characteristically flat-shaped curve.

Figure 14 is a plot of wear measurements versus test time for the testing in the Advanced Overrunning Clutch Technology contract and reported in USAAMRDL-TR-77-16 (Reference 1). For the ramp roller clutch, the wear measurement is the roller diameter. For the sprag clutch, the wear measurement is the depth of wear on the inner sprag radius, and for the spring clutch, the wear measurement is of the spring teaser coil radial wear. Note that the spring and sprag clutches project flat wear trends, indicating a long overrunning life, whereas the ramp roller clutch incurred a significant amount of wear during the turbine test phase of the program. The total allowable wear for all clutches is in the order of .005 inch, so that none of the clutches were in danger of failure by wear.

Figure 15 shows a similar type of wear curve for the ramp roller clutch only. This curve shows a peculiar type of wear experienced during testing on the end face of one particular roller. Only 3 rollers out of 14 experienced any wear at all. The roller with the highest wear is shown, while the other two that wore experienced less than one-half of the wear shown. The depth of wear is such that it significantly reduces the roller's overall length, thereby increasing roller stress. For future designs, this type of wear can be reduced by proper design of the roller retention cage slot end faces.

Figures 16, 17, and 18 show typical engagements for the spring, sprag and ramp roller clutches respectively. None of the clutches showed any significant differences in engaging or disengaging characteristics.

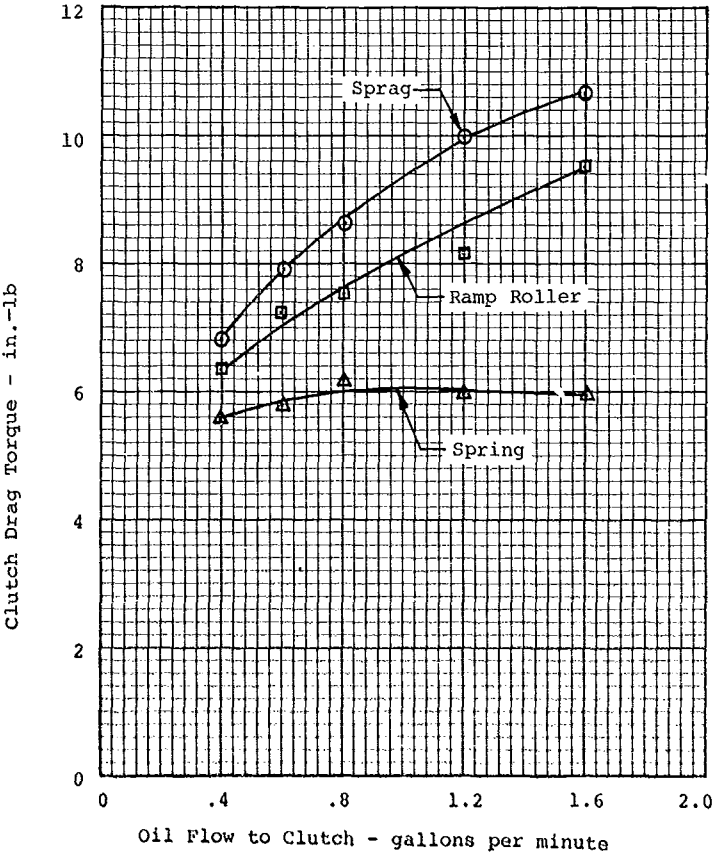

Figure 12. Test Results, Drag Torque versus Oil Flow at Full-Speed Overrun of Spring, Sprag, and Ramp Roller Clutches.

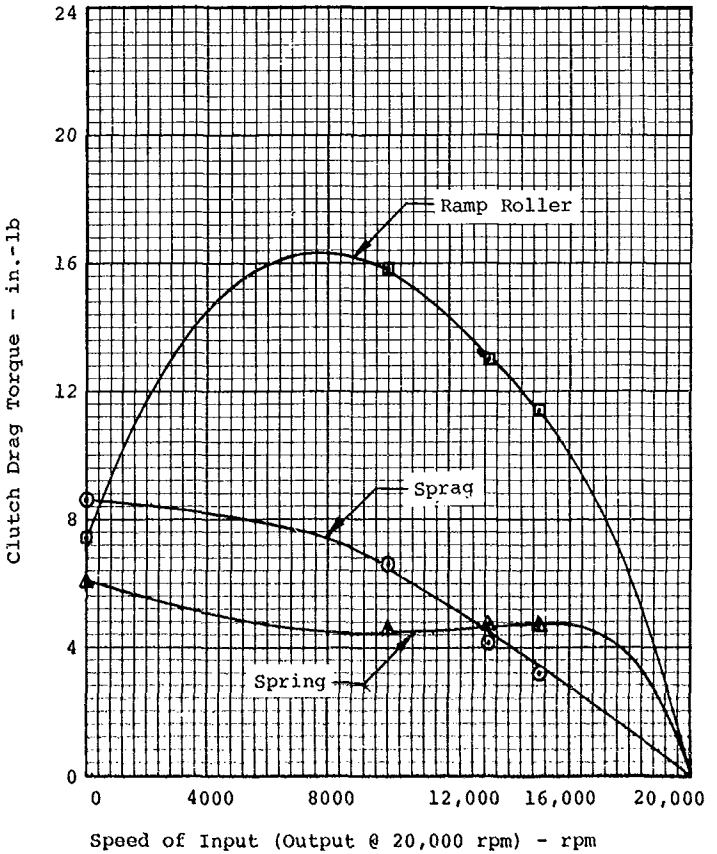

Figure 13. Test Results, Drag Torque versus Input Speed at 100% Flow, With Output at 20,000 rpm for Spring, Sprag, and Ramp Roller Clutches.

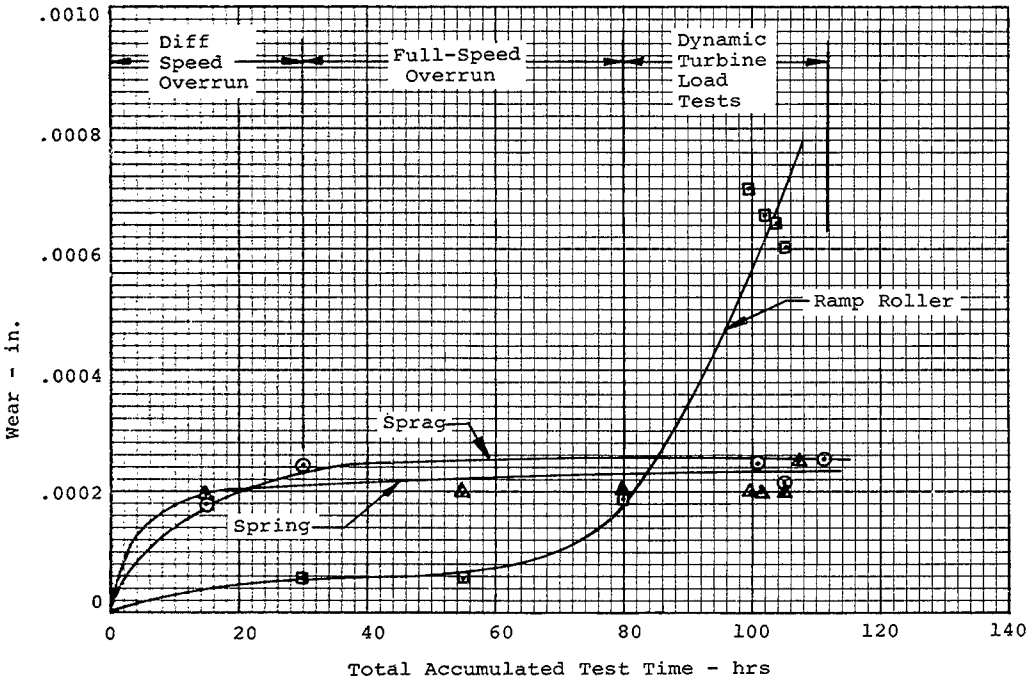

Figure 14. Test Results, Wear versus Time for Spring, Sprag, and Ramp Roller Clutches.

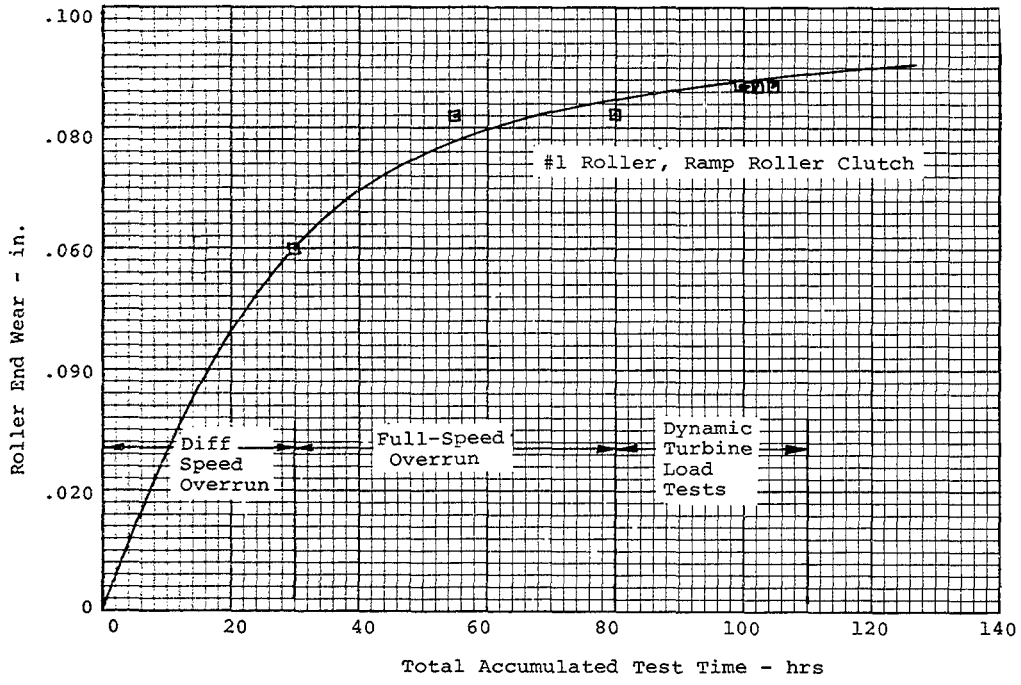

Figure 15. Test Results, Roller End Wear versus Time for a Ramp Roller Clutch.

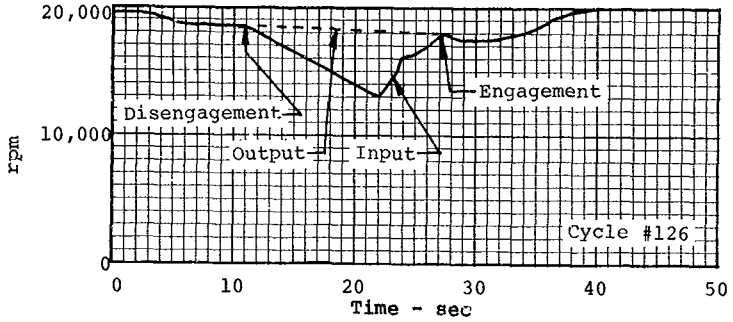

Figure 16. Test Results, Typical Engagement, Spring Clutch.

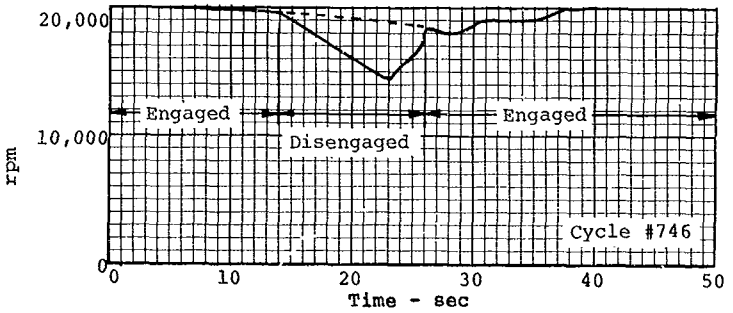

Figure 17. Test Results, Typical Engagement, Sprag Clutch.

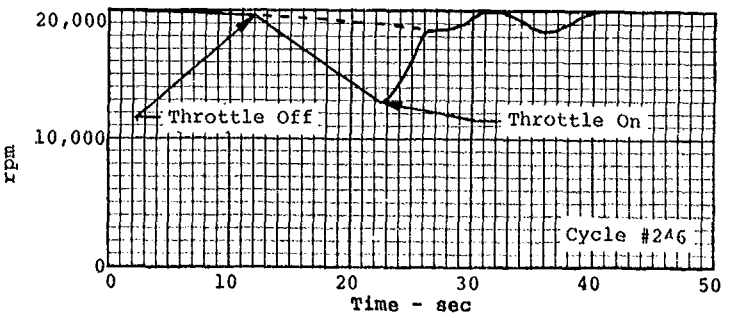

Figure 18. Test Results, Typical Engagment Ramp Roller Clutch.

Figure 19 shows clutch input and output torque with an induced vibratory torsional load on the input. Note the filtering effect on the output, which did not respond at the input vibratory torque magnitude. This was because the test stand included a flywheel that simulated the inertia of the rotor head, the transmission, and the blades of the helicopter. The inertia of the flywheel could not respond to the vibratory torque produced on the input. All three clutches reacted in a similar manner during this test.

Figure 20 is a plot of torque versus angular displacement of the input shaft relative to the output shaft. The large displacement of the spring clutch represents the spring unwinding from its arbor and expanding outward to the spring housing prior to torque transmittal. This is a typical characteristic of the spring clutch. Figure 21 is a curve of torque versus radial displacement of the clutch housings.

The spring clutch overload tests were stopped at approximately 12,000 inch pounds of torque because the spring slipped at this point and was unable to carry further load.

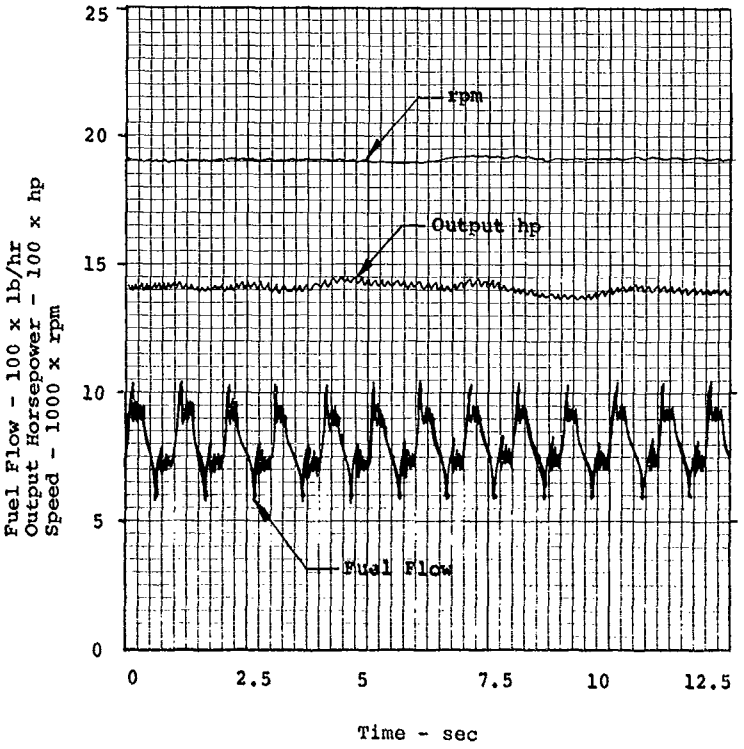

Figure 19. Results From Dynamic Cyclic Test, Typical Power, Speed, and Fuel Flow.

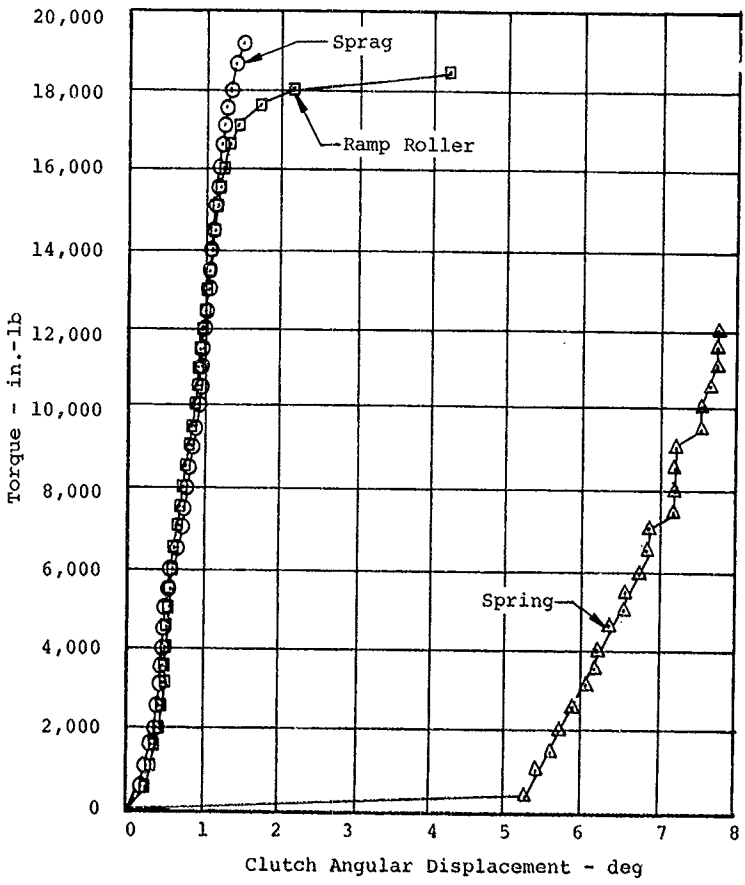

Figure 20. Test Results, Static Torque versus Angular Displacement for Spring, Sprag, and Ramp Roller Clutches.

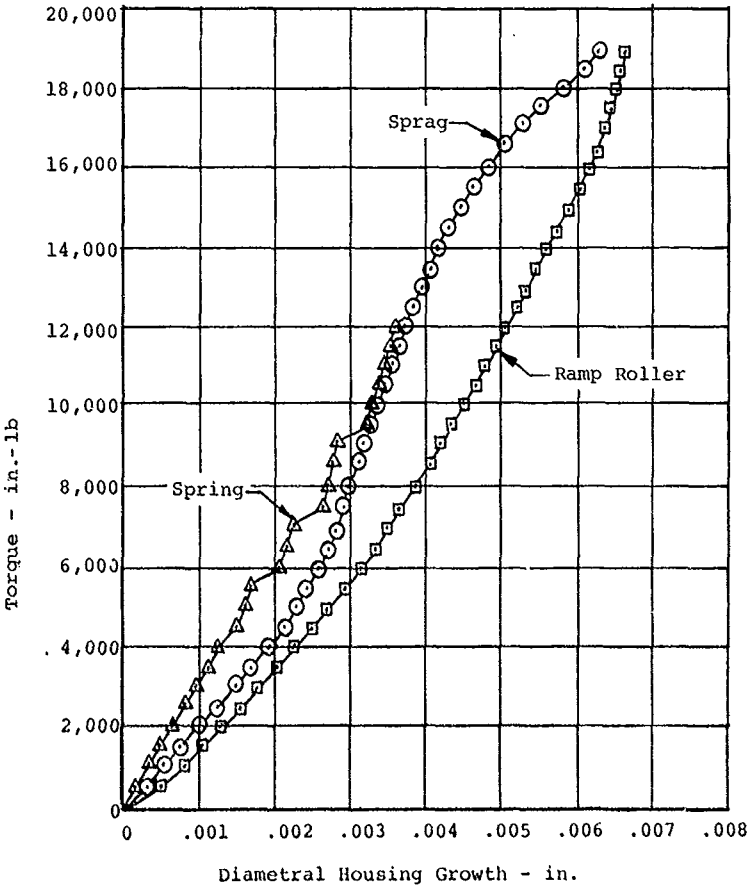

Figure 21. Test Results, Static Torque versus Radial Displacement for Spring, Sprag, and Ramp Roller Clutches.

SPRING CLUTCH DESIGN

Basic Configuration

The configuration and mounting of the spring clutch can take two basic forms. Early spring clutches were designed by the first method, wherein the spring was manufactured integrally with either the input or output housing. The second, most recent method, uses the symmetrical spring that is separate from both the input and the output housings.

The manufacturing of the integral spring design started with the machining of a thin, continuous slot between coil windings. The coils were then compressed and heat-treated so that they would remain compressed in the free state after heat treatment. This type of design has the serious disadvantage of constraint at the intersection of the housing and the spring. Whereas the spring wants to expand outward to the housing not attached to the spring, the integral housing attempts to restrain the spring from expansion. Tests conducted on this type of spring clutch have shown that it is very difficult to keep the stresses below the material endurance limit at the intersection of the spring and the housing because of the stress concentrations and the expansions involved.

The design that has proven successful is the symmetrical arrangement with its separate spring. The disadvantage of the integral spring design is completely eliminated in the symmetrical spring design. In this design, torque is gradually fed to the spring from the input housing by the action of friction and pressure. All the torque passes through the center spring coil to the output housing, where it dissipates in a mirror image of the way it was applied to the input housing.

These two configurations form the basic types of spring clutch design. The integral spring and housing design is not recommended because of the stress problem at the intersection of the housing and the spring. The symmetrical spring design eliminates this problem and is the recommended configuration.

In the symmetrical spring, the input and output housings must be free to rotate relative to each other and must be mounted concentrically. Usually, this is accomplished by duplex bearings mounted between the input and output housings. The overall clutch support is by bearings mounted on either the input or output, or the package can act as a quill shaft with splines on each end and supports to other transmission members. If one bearing is mounted to the input and one to the output, radial loads on the clutch must pass redundantly through the spring. This type of mounting is therefore not recommended.

Figure 22 shows the two basic types of spring clutch designs with a third design, which is the symmetrical spring with one bearing on the input and one bearing on the output. This third design is not recommended because any radial loads must be redundantly reacted by the spring. The recommended overall clutch support design has both support bearings on one shaft, either input or output, so as to form a rigid support.

In any type of spring clutch design, torque is transmitted to and from the unit by means of either gears or splines on the input and output shafts. If a gear is used, care must be taken in the design of the housing so that radial deflections of the housing do not influence the clutch's operation; i.e., the housing must be able to withstand the bending loads while deflecting an amount that will have a negligible effect on the spring.

In the designs shown in Figure 22, the input or output can be either from the left side or from the right side. The choice is merely a matter of assembly convenience. Also, the arbor can be mounted on either side of the unit. However, it should be pointed out that there are two reasons why the arbor should be mounted to the input side of the clutch. First, the input is stopped during full-speed overrunning and therefore there will be no centrifugal effects on the spring. Second, the output will always rotate, and since this is the shaft that is sliding relative to the spring teaser coil during overrunning, oil can be fed by centrifugal force past the teaser coils and out of the clutch. Also, the inner race of the duplex bearing should rotate with the output housing to provide lubrication flow to the bearing during overrunning.

The rotational direction of the spring clutch is immaterial. The direction is chosen on the basis of blade and engine requirements and the clutch's location in the drive train. In the detail design stage, the hand of winding of the spring (left hand or right hand) is chosen so as to provide proper operation.

The envelope of the spring clutch can be quickly determined during the preliminary transmission design phase of a project by sizing the clutch on the basis of maximum engine horsepower capability and clutch speed. A layout can readily be developed by using the basic sizes discussed in the next section, "Preliminary Sizing."

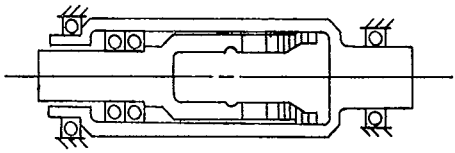

Spring Integral With Housing

(Not Recommended)

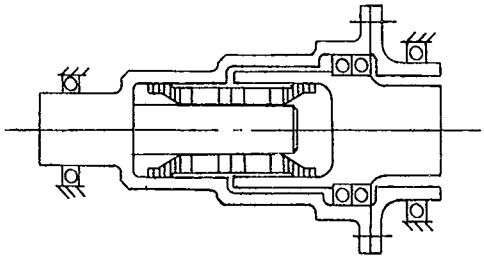

Symmetrical Spring - Support on Outer Housing Only

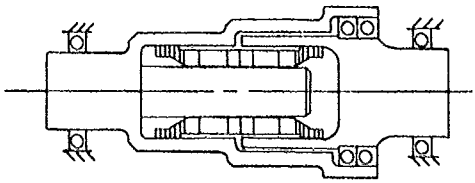

Symmetrical Spring - Support on Inner/Outer Housings
(Not Recommended)

Figure 22. Spring Clutch Mounting Arrangements.

Preliminary Sizing

Before starting the design of the helicopter spring clutch, the horsepower and speed must be known. These are usually available in a preliminary helicopter design when it is known what engine is being used. The spring clutch size will be based on the torque being transmitted. For reasons of cost and weight, it is desirable to keep the spring clutch as small as possible while keeping the stresses within allowable limits. The basic spring clutch parameters necessary for preliminary sizing are:

R	=	outer housing bore radius (in.)
T	=	clutch design torque (in.-lb)
d_m	=	spring mean diameter (in.)
L	=	spring length (in.)
b	=	center coil width (in.)
h	=	center coil height (in.)

When determining the basic size for the spring clutch, the problem is to define the spring envelope itself. A preliminary method has been developed that is based on the design of the original AAVLABS spring, which was designed for 3570 inch-pounds of torque (see Reference 2). All spring dimensions are found from a size factor (S.F.) found from

$$S.F. = \sqrt[3]{\frac{T}{3570}} \qquad (4)$$

where

S.F. = spring selection size factor

The baseline clutch has the following basic dimensions.

L_{base}	=	3.12	=	baseline spring length - in.
$d_{m\ base}$	=	1.126	=	baseline spring mean diameter - in.
b_{base}	=	.397	=	baseline spring coil width at crossover - in.
h_{base}	=	.250	=	baseline spring coil thickness at crossover - in.

The preliminary spring size is then found by multiplying the baseline sizes by the spring selection size factor as follows

---

2. Lynwander, P., Meyer, A. G., Chachakis, S., SPRING OVERRIDING AIRCRAFT CLUTCH, Avco Lycoming Division, USAAMRDL Technical Report 73-17, Eustis Directorate, U. S. Army Air Mobility R & D Laboratory, Fort Eustis, Virginia, May 1973, AD 769064.

$$L = L_{base}\ (S.F.) = 3.12 \sqrt[3]{\frac{T}{3570}} \quad (5)$$

$$d_m = d_{m\ base}\ (S.F.) = 1.126 \sqrt[3]{\frac{T}{3570}} \quad (6)$$

$$b = b_{base}\ (S.F.) = .397 \sqrt[3]{\frac{T}{3570}} \quad (7)$$

$$h = h_{base}\ (S.F.) = .250 \sqrt[3]{\frac{T}{3570}} \quad (8)$$

If this preliminary design procedure is followed, the spring center coil will have the same stress as the baseline spring center coil had at the crossover, which is approximately 63,000 psi at full torque. Of course, other spring designs may be developed once the preliminary sizes are known. The above-outlined procedure is presented only as a guide to obtain a starting point from which design iteration can be conducted. It is very possible to design a spring clutch with dimensions that do not fall within the range of values presented.

Figures 23 and 24 are plots of equations 5 through 8 to aid in preliminary clutch sizing. As an example of the preliminary design procedure, suppose it is desired to design a spring clutch for 15,000 inch-pounds of torque. From Figure 23, we find that $d_m = 1.82$, while, from Figure 24 using $d_m = 1.82$, we find $L = 5.03$, $b = .64$, and $h = .40$. With these parameters, the basic spring is defined, and a preliminary layout can be started.

Spring Stress Analysis

Spring clutches adhere to the classic capstan principle with regard to force or torque amplification; i.e., the torque transmitted by each successive wrap of the wire on the shaft is amplified exponentially such that the torque transmitted by the spring turn at the transfer point between shafts is an exponential function of the torque applied to the first turn. This function is expressed as

$$Tc = Te\ e^{2\pi\mu N} \quad (9)$$

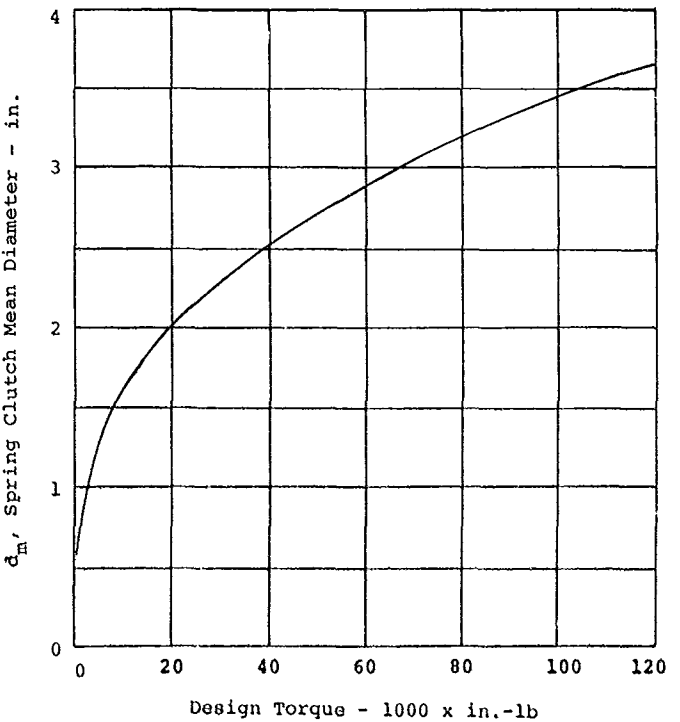

Figure 23. Spring Clutch Preliminary Sizing, Mean Diameter versus Torque.

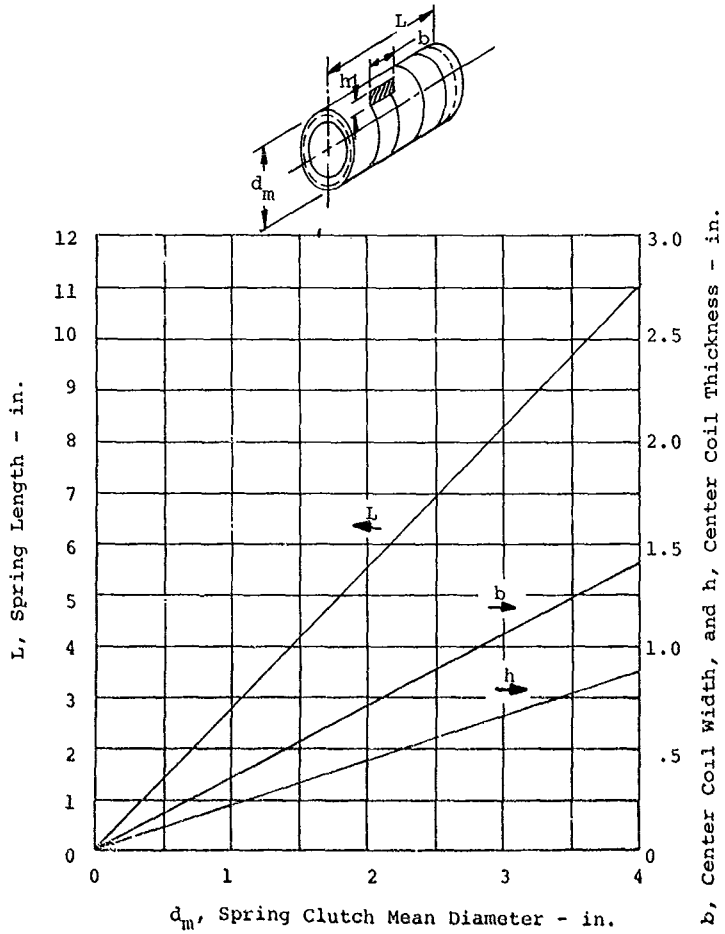

Figure 24. Spring Clutch Basic Dimensions as Functions of Mean Diameter.

where

To	=	output torque (total transmitted torque)
Te	=	energizing torque (torque at first turn)
μ	=	coefficient of friction between spring and shaft
N	=	number of spring turns engaged with the driving shaft

Equation 9 is valid only if the spring is in intimate contact with the housing. If the geometry of the spring used is near the size suggested in the Preliminary Sizing section, the stiffness will be such that the spring will be in contact with the housing at a small percentage of the design torque. Tests have shown that this point occurs at approximately 5% of the design torque. The expression $e^{2\pi\mu N}$ is the amplification or gain of the clutch. It may be noted that gain is greatly affected by increases in the number of coil turns since it is in the exponent of the gain function. For example, a spring clutch with 11 turns on the driveshaft will have a gain of 1000 assuming a coefficient of friction of 0.1. Thus, if the interference moment of the spring on the shaft is one inch-pound, the clutch will be capable of transmitting 1000 inch-pounds to the output shaft. In the overrunning direction, the drag torque applied to the driveshaft, assuming the output shaft is fixed, is only one inch-pound. Figure 25 shows the torque gain versus the number of coils for various coefficients of friction. Generally, 0.1 may be assumed for the design friction coefficient.

The stress in a spring of uniform cross section is a direct function of the torque transmitted by each element thereof. Therefore, if the torque applied by the spring varies exponentially along the wire turns, the stress also varies exponentially. In order to use the spring material efficiently, and to stress all elements equally, the spring cross section must be varied exponentially. The varying cross section is accomplished by varying the coil width while maintaining constant spring outside and inside diameters. This design permits a uniform clearance between the spring and the housing bores while the spring is wrapped down on the arbor. Tapering yields benefits in many designs since it is effective in reducing the weight and the size of spring clutches.

Stresses are produced when the spring transmits torque and are of two types: compressive stresses from the tangential force component of torque and bending stresses induced when the spring expands outward against the housing. The following discussion and formulas pertain only to an internal spring, which is the type commonly used because the spring will basically be in compression.

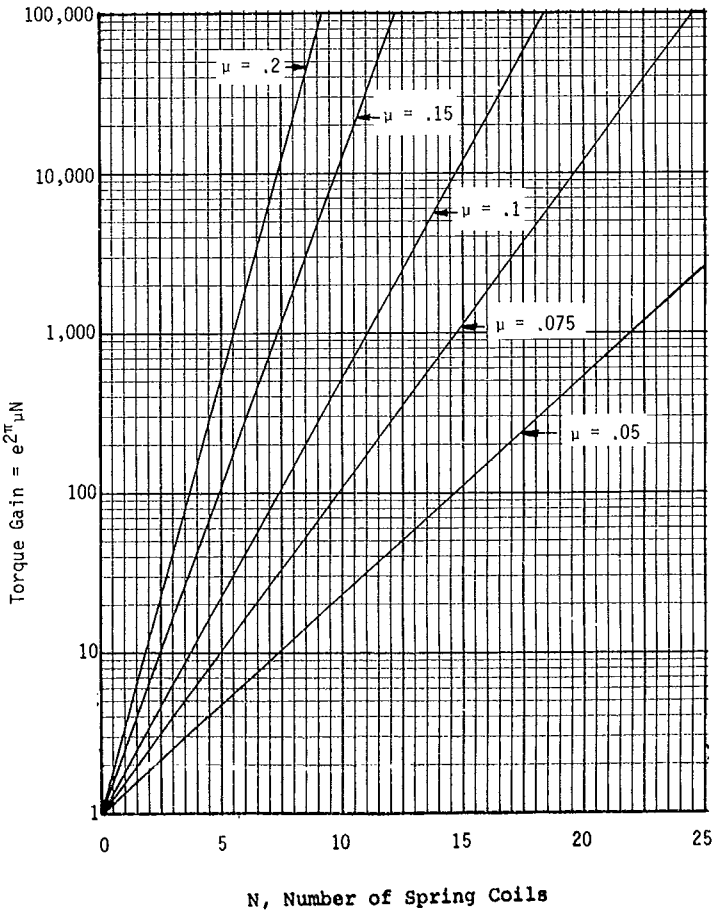

Figure 25. Spring Torque Amplification Factor.

The spring compressive stress from torque is critical at the center crossover coil and is given by

$$f_a = -\frac{P}{A} = -\frac{2T}{d_m b h} \tag{10}$$

where

f_a = axial stress in spring center coil - psi
T = total transmitted torque - in.-lb
d_m = clutch mean diameter - in.
b = spring coil width at crossover - in.
h = spring coil thickness at crossover - in.
P = spring center coil load - lb
A = area - $in.^2$

The axial stress at any coil, i, is found by knowing the torque at any coil and the coil dimensions

$$f_{ai} = -\frac{2T_i}{d_m b_i h_i} \tag{11}$$

$$T_i = \frac{T}{e^{2\pi\mu(N-i)}} \tag{12}$$

where

i = coil number, i=1, at either of the spring's free ends
N = number of coils from free end to crossover
f_{ai} = axial stress ith coil - psi
b_i = width of coil at ith turn - in.
h_i = thickness of coil at ith turn - in.
T_i = torque in coil at ith turn - in.

A spring bending stress will be induced whenever the spring is forced to expand from its initial position on the arbor to the outer housing. This stress is a function of the initial clearance between the housing's inside diameter and spring's outside diameter. When a curved beam is bent in the plane of initial curvature, the distribution of stress is not linear because of the different lengths of fibers on the inner and outer sides of the beam. The neutral axis of the beam does not pass through the centroid of the section. The change in neutral axis will be slight if the radius is large compared to the spring height, h; i.e., if h is about one-tenth of the mean radius. For the spring of the spring clutch, this is usually

not the case, and hence, a curvature correction factor is applied to the calculated stress. Reference 3 gives the following method for calculating the curvature correction factor

$$f_b = K \frac{E\ a\ h}{d_m^2} \qquad (13)$$

where

f_b	=	bending stress
a	=	diametral clearance between housing I.D. and spring O.D. - in.
E	=	Young's modulus for spring material - psi
K	=	curvature correction factor

Figure 26 shows the geometry used in the analysis of a spring section.

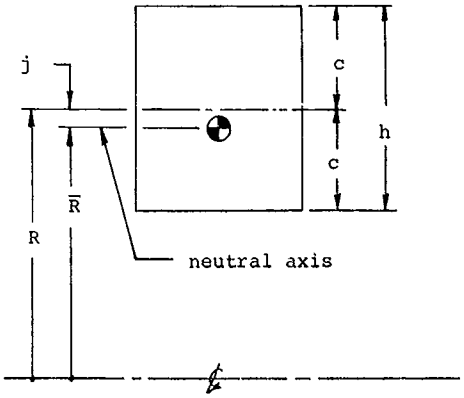

Figure 26. Spring Coil Geometry.

To calculate the curvature correction factors, the percent of neutral axis shift, j/c, is first calculated from Reference 3 by

$$\frac{j}{c} = \frac{d_m}{h} - \frac{2}{\ln\left(\frac{d_m/h + 1}{d_m/h - 1}\right)} \qquad (14)$$

3. Roark, Raymond J., and Young, Warren C., FORMULAS FOR STRESS AND STRAIN, McGraw Hill Book Co, New York, Fifth Edition, 1975.

$$Ki = \frac{1}{3j/c}\left(\frac{1 - j/c}{d_m/h - 1}\right) \quad (15)$$

$$Ko = -\frac{1}{3j/c}\left(\frac{1 + j/c}{d_m/h + 1}\right) \quad (16)$$

where

Ki = curvature correction for inside stress
Ko = curvature correction for outside stress

Note that the curvature correction factors and the neutral axis dimension, j, are independent of the coil width, b.

Figure 27 shows a plot of j/c versus d_m/h, while Figure 28 gives values of Ki and Ko for various values of j/c.

The spring bending stress will be compression on the outer fiber and tension on the inner fiber. Total spring stress is the sum of axial and bending stresses and is

$$f_o = f_a + f_{bo} \quad (17)$$

$$f_i = f_a + f_{bi} \quad (18)$$

f_a will be negative and is found from Equation 10; while f_{bi} will be positive. The outer and inner bending stress, f_{bo} and f_{bi}, are found from Equation 13 using the appropriate value of the curvature correction factor, Ko, for the outside, and Ki for the inside. Since the total spring stress is a function of torque, fatigue design is not considered except from a low-cycle ground-air-ground (GAG) standpoint, where each flight consists of one fatigue cycle.

The stresses on the outer fibers of the spring, being compressive in nature, have no effect on fatigue life. The inside fibers of the spring will be critical because the bending component of the total load is tensile. When the spring is fitted to the arbor, the inside fibers will be in tension, the value being given by Equation 13 with "a" equal to the interference fit between the spring and the arbor. When a small torque is applied to the spring, the spring will expand outward and conform to the outer housing. Again, the stress is found from Equation 13 with "a" equal to the housing inside diameter minus the spring's free outside diameter. Further application of torque reduces the stress since the compressive component from torque, f_a, subtracts from the tensile bending stress on the spring's inside diameter. During flight, the stress on the spring's inside diameter will be the difference between bending from expansion to the housing and

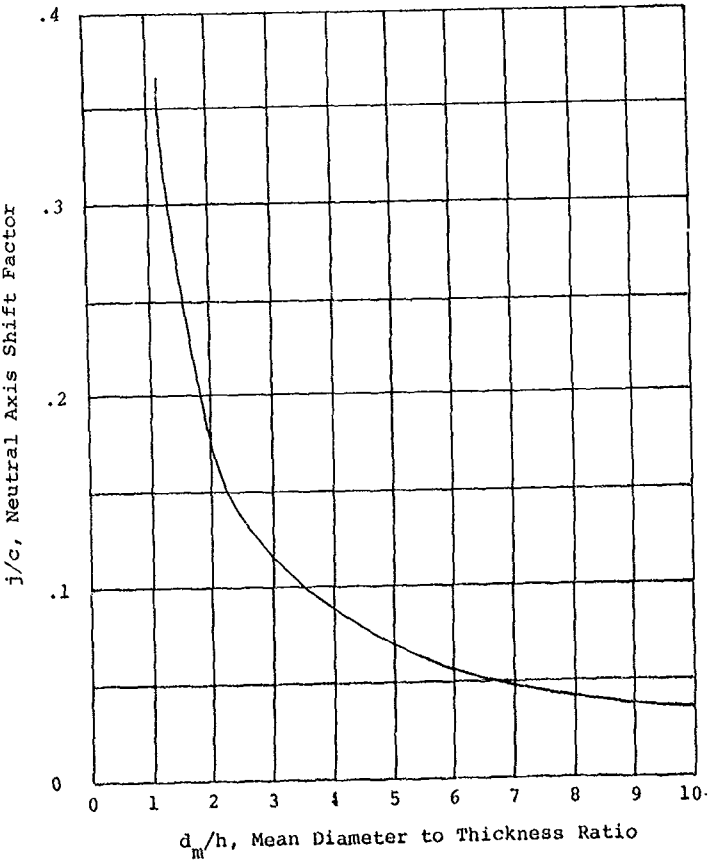

Figure 27. Neutral Axis Shift Factor for Curved Beams.

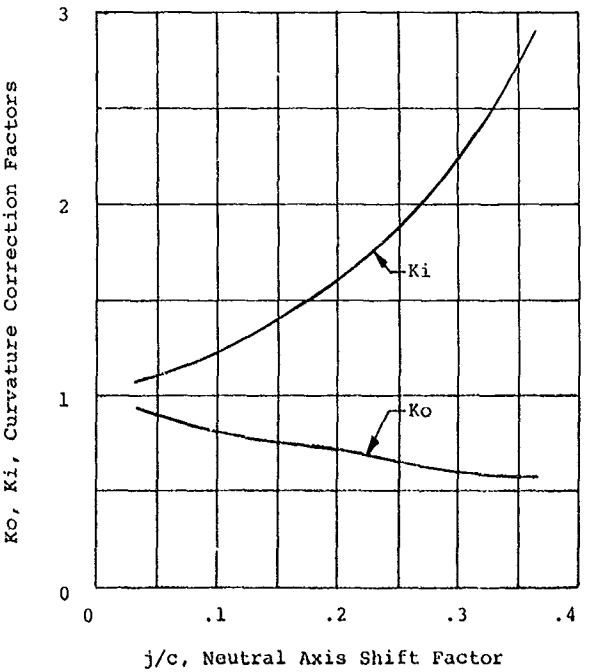

Figure 28. Curved Beam Inside and Outside Curvature Correction Factors.

compression from torque, and will usually be near zero because the bending and the compression are nearly equal. At the conclusion of the flight, the reverse procedure will occur, thus there are two fatigue GAG cycles per flight on the spring clutch. Figure 29 illustrates the stress/time relationship. The steady and vibratory stresses are found from

$$f_s = \frac{f_{bi} + f_i}{2} \tag{19}$$

$$f_v = \frac{f_{bi} - f_i}{2} \tag{20}$$

where

f_s = steady stress - psi
f_v = vibratory stress - psi
f_{bi} = bending stress on inside fiber from spring expansion (a = housing I.D. - spring free O.D.) - Equation 13
f_i = total stress on inside fiber - Equation 18

Allowable stresses are found from a fatigue stress versus cycle curve for the material, and from the desired life so noting that there are two stress cycle per flight.

Housing Hoop-Stress Analysis

The input and output housings of the spring clutch are subjected to tensile stresses as a result of the pressure created when the spring expands onto the housing during torque application. The pressure is calculated from the projected area of the spring and the tangential component of torque, and is given by

$$p_i = \frac{4\ T_i}{b_i\ d_m^2} \tag{21}$$

where

T_i = torque in coil at ith turn - in.-lb
p_i = pressure on housing at ith coil - psi
b_i = coil width at ith coil
d_m = clutch mean diameter - in.

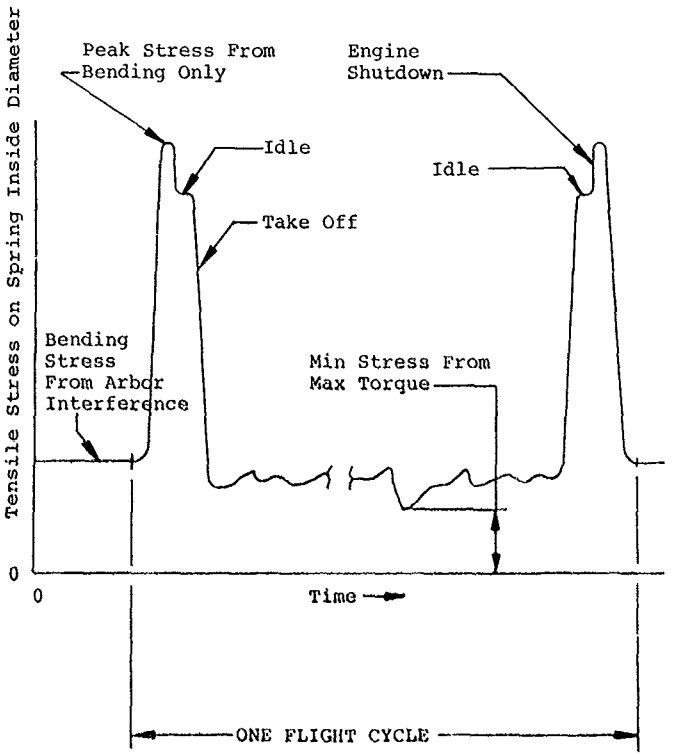

Figure 29. Spring Stress/Time Relationship

T_i in the above equation is found at any point in the spring from Equation 12 and is maximum at the center coil of the spring. After finding the pressure, the stress can be found by conservatively assuming that the maximum pressure (at the spring crossover) is constant across the width of the housing. If the spring has been designed for constant stress, the pressure will be constant. Using thick ring formulas as found in Roark (Reference 3) or other references, the housing hoop stress is calculated by

$$f_t = \frac{4\,T}{b\,d_m^2}\left(\frac{d_o^2 + d_i^2}{d_o^2 - d_i^2}\right) \qquad (22)$$

where

T	=	total transmitted torque - in.-lb
f_t	=	housing hoop stress - psi
d_o	=	housing outside diameter - in.
d_i	=	housing inside diameter - in.
d_m	=	clutch mean diameter - in.

Stresses in both the input and output housings of the spring clutch can be found with the above formula. In practice, the input or output spring clutch housing does not conform to a perfect cylindrical shape but may have a variable outside diameter. A conical shape is common for example. To find the stress in a housing with a variable outside diameter, a method is outlined here that may be used. The first step is to break the housing into a series of cylinders. The break points can be at changes of section or at changes of pressure. Figure 30 illustrates an outer housing that is essentially two basic sections as an example. Although the principle can be applied to any number of sections, two are shown for simplicity.

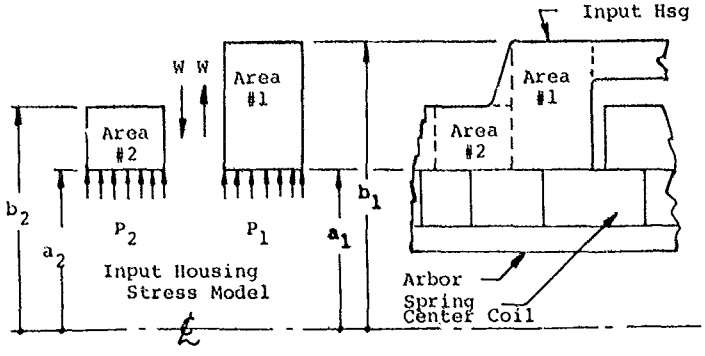

Figure 30. Mathematical Model for Outer Housing With Variable Outside Diameter.

Although W in Figure 30 is shown as a line load, it is assumed to be a pressure acting on each ring. If area 1 is stiffer than area 2, the direction of the equal and opposite loads, W, will be as shown in Figure 30 and W will subtract from P_2 and add to P_1. From Reference 3, for a ring subjected to internal pressure,

$$\Delta \text{ at "a"} = p \frac{a}{E} (\eta+\nu) \tag{23}$$

where

p = total pressure acting on area - psi
a = inside radius of area - in.
ν = Poisson's ratio
$\eta = \frac{b^2 + a^2}{b^2 - a^2}$
b = outside radius of area - in.

$$\eta_1 = \frac{b_1^2 + a_1^2}{b_1^2 - a_1^2} \tag{24}$$

$$\eta_2 = \frac{b_2^2 + a_2^2}{b_2^2 - a_2^2} \tag{25}$$

The deflection of area 1 due to P_1 plus W is equal to the deflection of area 2 from P_2 minus W. Substituting these values for p in equation 23, equating deflection, and simplifying,

$$(p_1 + W)\, a_1\, (\eta_1+\nu) = (p_2 - W)\, a_2\, (\eta_2+\nu) \tag{26}$$

from which

$$W = \frac{p_2 - p_1\zeta}{1 + \zeta} \tag{27}$$

where

$$\zeta = \frac{a_1}{a_2} \left(\frac{\eta_1 + \nu}{\eta_2 + \nu}\right) \tag{28}$$

For the special case where $a_1 = a_2$ and $p_1 = p_2$ (which is the usual case for a spring clutch).

$$W = p_1 X = p_2 X \tag{29}$$

$$X = \frac{1 - \zeta}{1 + \zeta} \tag{30}$$

Figure 31 is a plot of X versus η_1 for various values of η_2. X can be thought of as the percent of pressure relieved by the larger ring from the smaller ring.

After the pressure W is found by the above procedure, the stress is calculated from

$$ft_1 = (p_1 + W)\ \eta_1 \quad (31)$$

$$ft_2 = (p_2 - W)\ \eta_2 \quad (32)$$

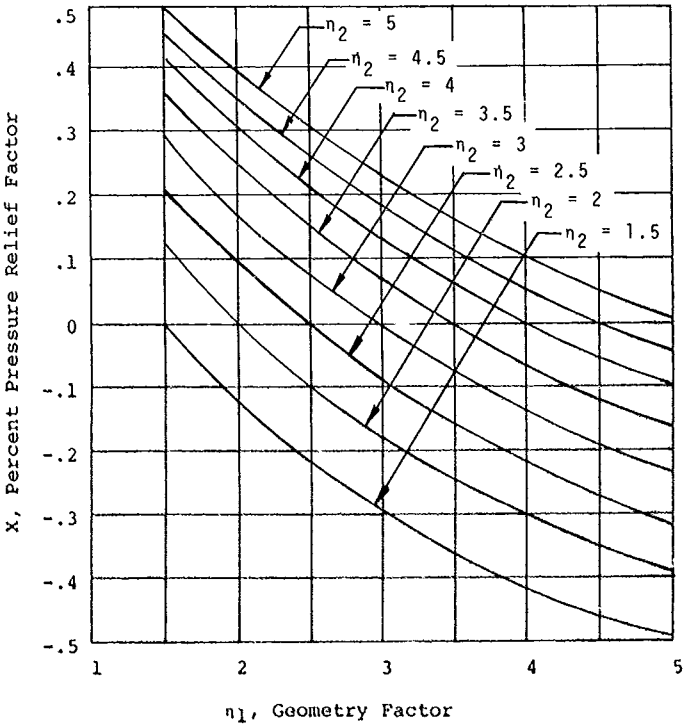

Figure 31. Percent Pressure Relief From Two Connected Rings Subjected to Internal Pressure.

Spring Growth from Centrifugal Force

When the spring clutch is operating in the differential speed overrunning mode, the spring will be subjected to the action of centrifugal force. The spring should be designed so that the centrifugal growth is less than the interference between the spring in the free state and the spring arbor. This will assure that the spring will not leave the arbor during differential overrun. If the spring should touch the housing bore before engagement, the end result could be an increase in drag torque or rubbing.

To calculate spring centrifugal growth, one-half of a spring coil is analyzed as a 180° curved beam with uniform outward pressure representing centrifugal pressure. The model for the analysis is shown in Figure 32.

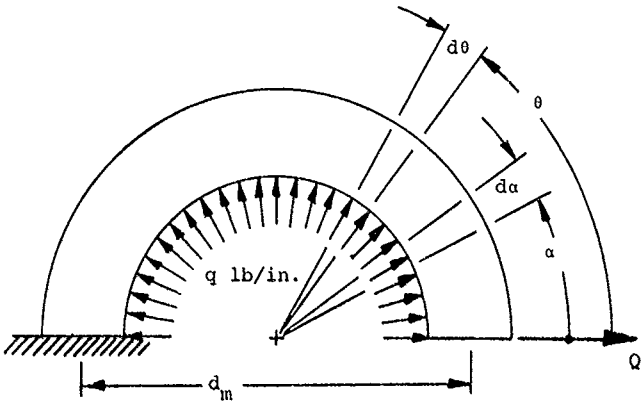

Figure 32. Spring Centrifugal Growth Mathematical Model.

An imaginary load, Q, is placed at the free end so that the theorem of Castigliano can be used to find deflection at the free end. The free end deflection will then be equal to the diametral growth of the spring due to centrifugal force. The uniform load, q, represents the spring weight from centrifugal force.

The bending moment is

$$M = Q \frac{d_m}{2} \sin\theta + \int_0^{\theta} F \frac{d_m}{2} \sin(\theta-\alpha) \qquad (33)$$

where

F = total force acting on the elemental length over $d\alpha$

Integrating leads to

$$M = Q \frac{d_m}{2} \sin\theta + q \frac{d_m^2}{4} (1 - \cos\theta)$$

M = bending moment at any section (34)

To find the deflection at the free end, the partial derivative of the strain energy, U, is found with respect to the load, Q

$$\delta = \frac{\partial U}{\partial Q} = \int_0^{\pi} \frac{M}{EI} \frac{\partial M}{\partial Q} \frac{d_m}{2} d\theta \quad (35)$$

Substituting the values of M and $\partial M/\partial Q$ into Equation 35 and setting Q equal to zero leads to

$$\delta = \frac{q d_m^4}{8 EI} \quad (36)$$

In the equation for centrifugal growth, q is the centrifugal force per unit length of circumference.

$$q = \frac{W}{g} \frac{d_m}{2} \omega^2 = \frac{\rho b h d_m}{2 g} \left(\frac{rpm \pi}{30}\right)^2 \quad (37)$$

I = moment of inertia = $\frac{bh^3}{12}$

Substituting the equations for q and I into Equation 36 and simplifying,

$$\delta = \frac{\rho d_m^5 \pi^2 rpm^2}{1200 E g h^2} \quad (38)$$

Assuming a steel spring with $\rho = .283$, $E = 30 \times 10^6$ psi, and $g = 386$ leads to

$$\delta = 2.01 \times 10^{-13} \frac{d_m^5 rpm^2}{h^2} \quad (39)$$

Equation 39 gives the spring diametral growth that, as previously stated, should be less than the spring and arbor interference fit. A suitable factor of safety, such as 2, should be applied to account for unknown variables.

Spring Geometric Considerations

The first geometric consideration in the design of the spring clutch is the end coil interference or the "teaser" coil design. The teaser coils at either end of the spring are designed to provide the torque necessary to either expand or contract the spring; i.e., to either transmit torque or allow the output shaft to overrun. The energizing torque is generated by making these coils, usually three in number at each end, with an interference fit with the housings. Sufficient diametral margin must therefore be provided for wear. Unlike the power coils, the teaser coils are not critical for stress, but are sized purely for this torque-generating capacity. The torque necessary to energize the clutch is

$$T_{ENERG} = \frac{T}{e^{2\pi\mu N}} \tag{40}$$

where

- T = design torque - in.-lb
- N = total number of coils from crossover to end
- T_{ENERG} = torque required on first coil to energize spring
- μ = coefficient of friction

Torque is established on the spring by the interference fit between the teaser coils and the housing bore. This torque is calculated with

$$T_{int} = \frac{E\, b\, h^3\, a}{6\, d_m^2} \tag{41}$$

where

- E = Youngs modulus - psi
- b = teaser coil width - in.
- a = interference between teaser coils and bore
- h = teaser coil height - in.
- d_m = teaser coil mean diameter - in.

The interference torque must always be greater than the energizing torque or the clutch will slip. When the interference torque is equal to the energizing torque, the clutch is on the verge of slipping. Thus, by equating torques and solving for a, one obtains the minimum diametral interference before slipping. Wear allowance will then be the initial diametral interference minus the final (with an appropriate margin of safety) and is found with

$$\Delta_{wear} = \left[a - \frac{6\,T\,d_m^2}{E\,b\,h^3\,e^{2\pi\mu N}} \right] \times \frac{1}{F.S.} \qquad (42)$$

where

Δ_{wear} = allowable clutch diametral wear on teaser coils
F.S. = wear factor of safety
a = initial diametral interference on teaser coils

The second geometric consideration in spring-clutch design is the tolerances, clearances, and interferences of the spring, arbor, and housings. Figure 33 summarizes the dimensions used in a typical clutch design. The important considerations are

1. Arbor/Spring Interference - The interference fit should be sufficient so that the spring will not leave the arbor under the action of centrifugal force during differential overrun. Tolerances should be considered; i.e., centrifugal growth should be less than the minimum arbor/spring inside diameter interference.

2. Running Clearance - The running clearances between the housing bores and the spring outside diameter when the spring is on the arbor should be enough so that the spring will never hit the housing bore.

3. Teaser Coil Interference - The teaser coils must be designed to provide sufficient interference torque for clutch energizing and to provide allowance for wear, but the interference must not be of such a magnitude that there is excessive drag or excessive wear. A factor of safety of 10 has been successfully used in part designs (ratio of interference torque to energizing torque).

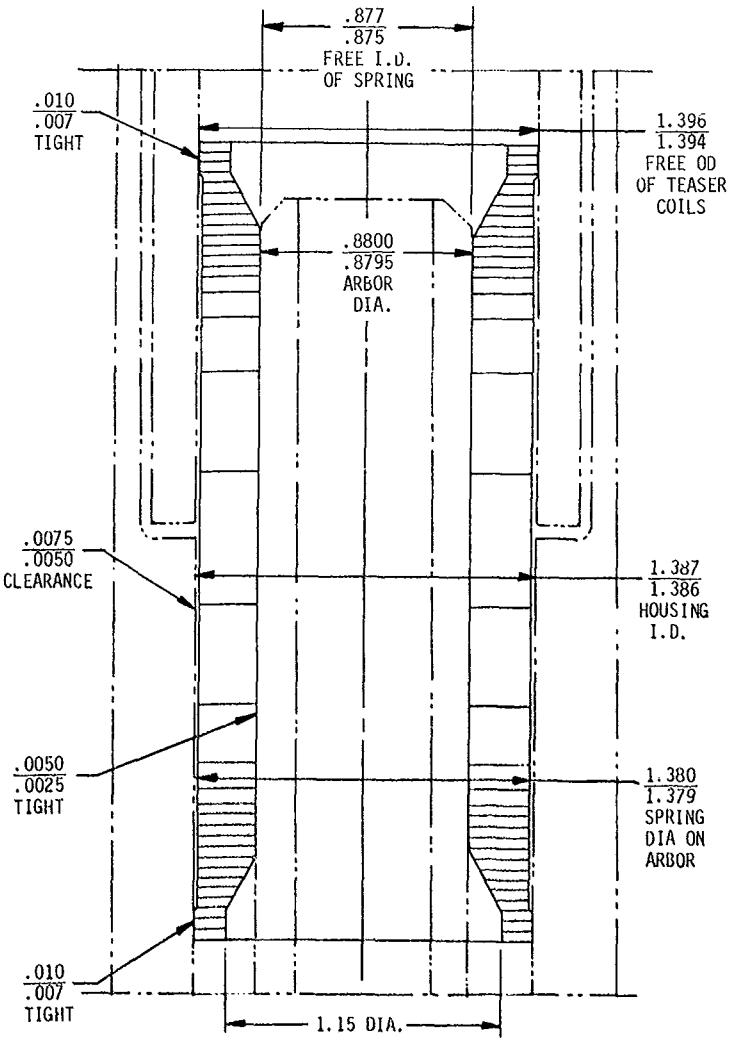

Figure 33. Typical Spring Fits, Clearances, and Tolerances.

Spring Design

The spring of the spring clutch is basically in compression when the clutch is driving. The bending component of stress is tensile on the inside of the spring and is induced as a result of the spring expansion onto the housing bores. The end "teaser" coils of the spring must continually rub on the housing bore whenever the clutch is overrunning. For this reason, the spring material must have a hard, smooth surface to minimize wear. Spring stresses change only when torque changes, and hence, the spring only operates in low-cycle fatigue conditions. The spring material does not necessarily have to be vacuum-melt steel for this reason, although springs used in helicopter overrunning clutches are usually manufactured from H-11 tool steel, AMS 6487, which is vacuum melt. This through-hardening steel can be heat-treated to Rockwell "C" 54 to 56 (Rc 54-56), which corresponds to an ultimate tensile strength of 275,000 psi.

There are a wide variety of spring materials available to satisfy the requirements of strength, availability, and special properties, such as corrosion resistance. Several steel materials that may be considered in a new design are listed in Table 6.

TABLE 6. TYPICAL PROPERTIES OF COMMON SPRING MATERIALS.

Name	Fatigue	Strength	Max Service Temp (^{O}F)
Music Wire - ASTM A228	Excellent	High	250
Hard Drawn - ASTM A227	Poor	Medium	250
Oil Tempered ASTM A229	Poor	Medium	300
Valve Spring ASTM A230	Excellent	High	300
Chrome Vanad AISI 6150	Excellent	High	425
Chrome Sil AISI 9254	Fair	High	475
Sil - Mag AISI 9260	Fair	High	450
Stainless 17-7 PH	Good	High	700
High Car AISI 1065	Excellent	High	250

The surface finish on the spring is generally held to RMS32 or better. The tolerance is critical on the three key diameters; i.e., the inside diameter, which mates with the arbor, the teaser coil outside diameter, which is fitted into the housing bores, and the spring central section outside diameter, which runs with clearance between the spring and housing during overrun and which wraps itself tightly to the housing bore during driving. These three critical diameters are generally held to a tolerance of $\pm$.001 inch. The tolerance along the spring's overall length is not critical. Sufficient axial clearance must be left between the housings, springs, and bushings for running with the .030-inch minimum being recommended.

Since the spring has an interference fit on the arbor, during overrunning it will remain with the shaft to which the arbor is attached. Slippage and sliding will then occur between the teaser coils and housing on the opposite member. Lubrication of the spring must be directed to this area. In a helicopter, the output member will be rotating all the time; hence, the arbor should be on the input so that the spring is at rest during full-speed overrunning. The path of lubricant flow is from the center of the rotating output member, past the spring teaser coils, and out of the clutch. It is recommended that the oil be permitted to pass from the teaser coils all the way to the center of the spring prior to draining from the clutch. In this way, any inadvertant rubbing of the central spring section during differential speed operation will not result in spring or housing distress since lubrication will be present. A convenient method for providing an oil passage is by means of slots in either the housing or in the spring. Each design must be evaluated to determine the best location for oil drain slots. Figure 34 illustrates the principle of teaser-coil lubrication with housing slots and shows, in cross section, a typical oil drainage slot design. If the slot depth is small, normal structural integrity should be unaffected.

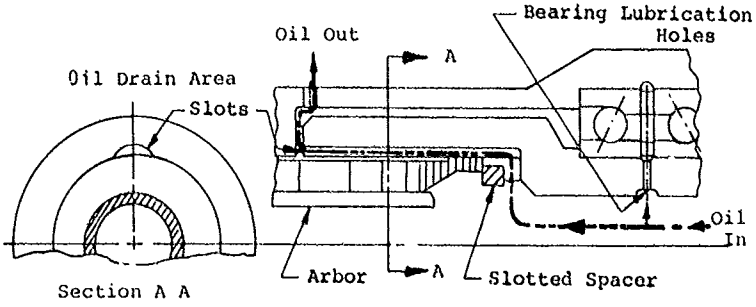

Figure 34. Spring Clutch, Lubrication Flow Path.

Housing Design

With the input and output spring-clutch members used in the symmetrical spring type arrangement, the two shafts serve the same purpose. They must transfer torque from one end of the shaft by means of friction and pressure, gradually into the coils of the spring. Both the input and output shafts must therefore be able to withstand the hoop tensions created by spring expansion.

Unlike the sprags of a sprag clutch or the rollers of a ramp roller clutch, the spring of a spring clutch spreads load, in the form of pressure, almost uniformly over the spring's entire outer surface. There are no concentrated line loads as in the other clutches. The depth of the surface hardness in the housings is therefore less critical in the spring clutch. The spring will rotate with the arbor during overrunning because of the interference fit. Usually the arbor will be attached to the input member, which forces the spring to rotate with the input member. There will be no relative motion between the spring and the housing on this member, and the material is not critical for this reason. However, the output member must withstand the wear of the spring teaser coils rotating on the housing during overrunning. A hard surface is recommended.

Previous spring-clutch designs used H-11 tool steel (AMS 6487) on both the input and output housings. This steel is a very hard steel with excellent fatigue properties and high temperatures properties. A minimum hardness of Rc 54 can be maintained in production.

Another possible material is case-carburizing steel. Surface hardness can be increased to Rc 58 minimum, which is better for wear prevention, but core hardness, on which strength is based, will be lower with case-carburizing steels. SAE 9310 (AMS 6260) or other case-carburizing steels are good alternate housing materials.

The surface finish on the housing bores should be maintained at RMS 32 or better. The tolerance on the bore is generally ±.0005 inch, which is an easily held tolerance for production grinding.

Lubrication passages must be provided in the input and output shafts for both oil supply and oil drainage. As suggested in the spring design section, the output housing or spring (assuming the spring arbor is attached to the input) should have lubrication slots. If the slots are in the output member, centrifugal force will assist the oil flow during overrunning. As a general rule of thumb, the velocity of oil in the slots should not exceed 5 feet per second. Thus, if the flow and area are known, the velocity can be calculated from

$$V = \frac{Q}{A} \qquad (43)$$

where

V = velocity ft/sec
Q = flow - ft^3/sec
A = area - ft^2

Spring-Guide Arbor Design

The spring-guide arbor is an essential component of the spring clutch. When the spring is rotating, centrifugal forces are induced that tend to expand the spring. For proper design, the initial interference between the spring and arbor is designed to be greater than the centrifugal spring growth. If the spring expands beyond the guide arbor during differential overrunning, the spring will be unstable in the housing.

Since there is never any relative motion between the spring and arbor and also since the pressure created by the interference is relatively low, the arbor material is not critical. Previous designs have used AMS 6415, SAE 4340, steel bar stock heat-treated to Rc 32-40. Any similar type of steel would be suitable.

The mandril's outside diameter tolerance is critical because it must mate with the spring's inside diameter and provide the proper interference fit and pressure. The tolerance is generally +.0000 to -.0005 inch, which will give close control over the fits with the spring.

Another important design consideration for the arbor is its attachment and mounting in the input housing. The arbor must be aligned with the housing bore when assembled so that the spring does not rotate eccentrically. In addition, the arbor must be restrained from axial movement. This has been done by dowell-pinning, but any suitable mechanical attachment may be employed. The dowell or other torsional restraint must be capable of transmitting a torque equivalent to the amount necessary to expand the spring center coil until it just touches the housing.

The arbor is not critical for stress and can be hollow to save weight.

Basic Configuration

The configuration of the support and the mounting of the sprag clutch is basically the same as that of a ramp roller clutch. For either the sprag or the ramp roller clutch, there are two basic bearing arrangements. The first pair of bearings are used to support the overall clutch package, while the second set of bearings are used to support the inner shaft on the outer shaft and to permit relative motion between the two.

The inner shaft support bearings can assume three configurations with respect to the sprag or roller orientation:

1. Straddle-mounted
2. Duplex left
3. Duplex right

With respect to the clutch overall support, the bearings can also assume three basic configurations:

1. Inner and outer shaft support
2. Supported on inner only
3. Supported on outer only

The permutation of the three inner support arrangements with the three overall support arrangements yields nine basic sprag or ramp roller clutch arrangements, as depicted in Figure 35.

In each support arrangement, the torque input to and output from the unit is by means of either a gear or a spline on the input or output shaft except in the cases of the three units that are supported entirely on the inner shaft. In this case, the outer housing must have a geared input or output member to transmit torque to or from the unit. In each of the other six designs, gears and splines are options.

When a gear is used to transmit torque to or from the clutch, great care must be taken in the design of the clutch support structure because the gear will induce a radial load on the unit. Deflections caused by the radial gear load can greatly influence the roller or sprag contact since the rollers or sprags of the clutch will form a redundant load path. If a gear is used as the torsional input or output, the radial deflection and the angular distortions of the support shafts must be negligible compared to the deflections induced by the normal roller or sprag loads. If a gear must be designed to be integral with the sprag or ramp roller clutch package, the most likely bearing arrangement is the support on the outer shaft only. In this case, the gear members would be mounted

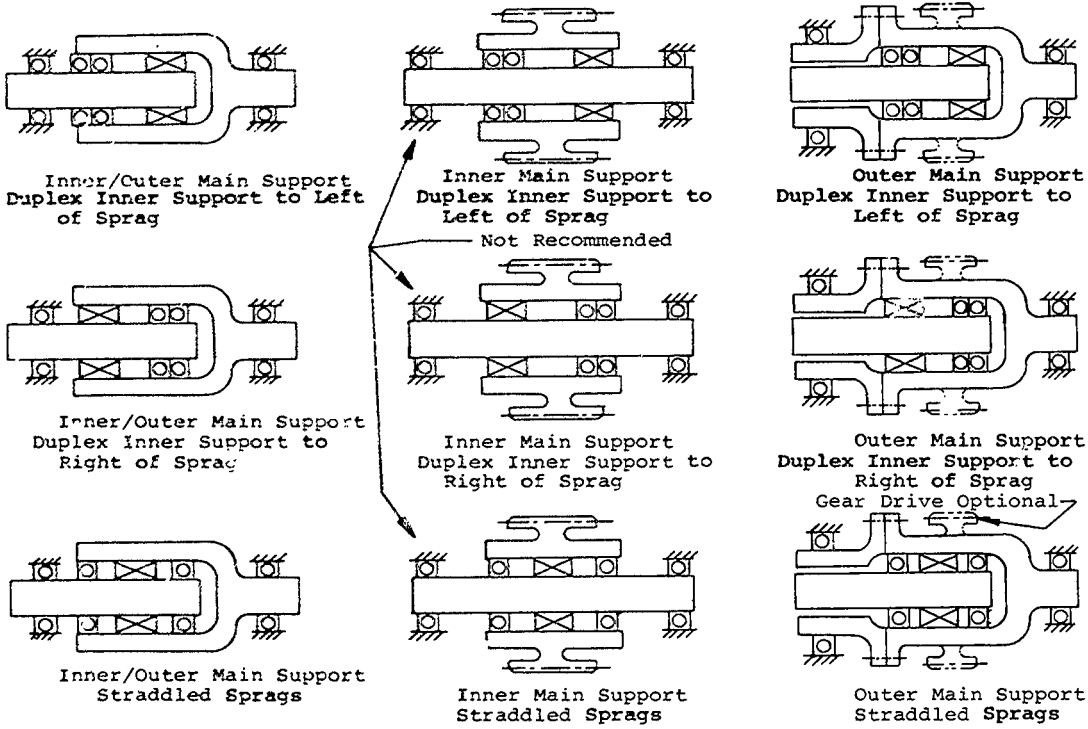

Figure 35. Sprag and Ramp Roller Clutch Mounting Arrangements.

on the outer shaft, and a direct load path to the support bearings is provided. A gear mounted on the outer shaft of an inner-shaft-supported unit is not recommended because the load must pass redundantly through the rollers or sprags to the support bearings. If this type of design is used, the rollers or sprags should be straddle-mounted as a minimum requirement. For this reason, an inner-shaft-supported unit is not recommended. Similarly, gear drives are not recommended on designs which support the shafting through the freewheel unit.

Of the nine mounting arrangements shown in Figure 35, the most preferable is the one having the bearings straddling the clutch with the outer race providing the total support of the clutch package. This bearing arrangement provides the optimum in concentricity and misalignment control between the inner and outer raceways. For proper clutch performance, the radial space between the two raceways must be closely controlled for two reasons: (1) to eliminate the scuffing of the cam surfaces of the sprags when in the overrunning mode and, (2) to minimize the minor shock loading created by the dwell period when the sprags themselves are forcing the races to assume a concentric position upon initial loading.

For a sprag clutch to allow lubrication to be centrifugal-assisted and to take advantage of the inertial forces of the clutch components upon engine accelerations, it becomes advantageous to have the outer race of the sprag clutch, the input member and the inner race of the sprag clutch, the output member, the latter being the opposite to that of a ramp roller clutch. All of the many modern helicopter applications that utilize a sprag-type clutch have the inner race as the output member. The rotational direction of the sprag-type clutch is immaterial since both races are cylindrical shafts. The sprag clutch can be easily assembled to obtain either direction of rotation by merely turning the clutch around, end for end.

The envelope of the sprag clutch can be easily determined in the preliminary transmission design stage by sizing the unit based upon the maximum engine horsepower available and the input speed. One should also consider the possibility of future power increases. A layout can then be made by using the next section, "Preliminary Sizing."

Since one of the major considerations involved in designing aircraft components is having the minimum weight consistent with high reliability, many of the larger helicopters utilize a tandem-type sprag clutch; i.e., a clutch containing two rows of sprags. This design concept also reduces the relative surface velocities, which is beneficial during overrunning conditions. With this type of clutch configuration, the race sections over and under each row of sprags, i.e., the race "back-up" material and geometry, must be the same to maintain the same degree of torsional stiffness in each row of sprags. If the race sections are not uniform, equal load sharing cannot be obtained. In theory, the idea of utilizing two separate clutches to overcome the torsional stiffness problem should correct the situation, but in reality, the combined full-rated torque capacity cannot be realized due to the possible out-of-phase (angular sprag relationship) condition between each row of sprags upon initial dynamic loading.

Preliminary Sizing

The sprag clutch is sized based on structural requirements. Before proceeding with the design, the power, speed, and safety margin must be known. This section deals with obtaining the basic sprag parameters from which a preliminary overrunning clutch layout can be constructed. These basic parameters are:

J	=	sprag section - in.
N	=	number of sprags per row
Do	=	outer shaft's inside diameter - in. $\approx$ Di + 2J
Di	=	inner shaft's outside diameter - in.
ℓ	=	sprag length
L	=	overall length including cages

Once these parameters have been established, a preliminary layout of the sprag clutch can be developed. To cover the total range of torque and race diameters that are typical of helicopter operation, four sprag sections have been made available: (1) .248, (2) .328, (3) .374, and (4) .500. The sprag section, J, is the nominal dimension across the sprag height and must be greater than the shaft annular clearance. The reason for the different sizes is to accommodate the variances in the Hertz stress, the gripping angles, and the amount of race stretch associated with the ranges in race diameters.

The characteristics of each size can be found in Table 7.

TABLE 7. SPRAG GEOMETRIC PARAMETERS.

Parameter	Sprag Section (J) - in.			
	.248	.328	.374	.500
Minimum circumferential pitch (Pc)	.265	.310	.340	.440
Recommended inner race diameter (Di) - minimum	.500	1.000	2.500	4.500
maximum	1.000	2.500	4.500	9.000
Recommended sprag length (ℓ) - minimum	.250	.300	.400	.500
maximum	.750	.990	1.100	1.500

The maximum number of sprags per row that can be used in a clutch of a given diameter depends on the size of the sprag section. Table 7 lists the minimum circumferential pitches necessary for sprags of different sizes, which take into account the proper cage and energizing-spring construction. Knowing the race sizes, the sprag section and the minimum circumferential pitch, the number of sprags can be arrived at by using the following formula:

$$N_{max} = \frac{(Di + J)\pi}{Pc} \qquad (44)$$

where

N_{max} = maximum number of sprags
Di = outside diameter of inner race - in.
J = sprag section - in.
Pc = minimum circumferential pitch - in.

Although it is not necessary to utilize the maximum number of sprags in a given clutch size, the practical problem is usually to obtain as much torque capacity as possible in a given space.

The maximum and minimum sprag lengths given in Table 7 are governed by the ability to heat-treat without distortion and the inefficient division of the axial space available for the necessary energizing spring. If the sprag length were to exceed the maximum length recommended in Table 7, the problem becomes one of unequal load distribution along the length of the sprag.

The actual sizes of the sprag clutch races are based on the Hertz stresses produced between the sprag and the inner shaft. Hertz stresses are always lower between the sprags and the outer shaft because of the negative radius of curvature, which makes the outer race conform to the sprag curvature. Thus, the inner race diameter controls the maximum Hertz stress. The equation for the calculation of sprag clutch Hertz stresses is derived from the equation for a cylinder on a cylinder and is given in terms of sprag clutch torque as

$$T = f_c^2 \frac{(1-\nu^2)}{E} \pi \ell N \frac{Di}{2} \tan V \left(\frac{d_i \, Di}{d_i + Di}\right) \qquad (45)$$

where

T	=	clutch torque capacity - in.-lb
f_c	=	allowable Hertz stress - psi
ν	=	Poisson's ratio
E	=	Young's modulus for sprag and shaft - psi
ℓ	=	length of sprag - in. (see Table 7)
N	=	number of sprags
Di	=	inner shaft's outside diameter - in.
V	=	gripping angle
d_i	=	2 ri = 2 times sprag's inner cam radius.

Equation 45 has been plotted as a function of torque versus inner shaft diameter in Figure 36. This curve assumes an allowable Hertz stress of 450,000 psi for case-carburized shafts and sprags and also assumes maximum sprag quantity and length. The inner sprag gripping angle is assumed to be 4.5 degrees, which is an estimate of the gripping angle under load. This angle includes allowances for the deflection of shaft, housing, and sprag members.

To conduct a preliminary clutch design, the torque, with safety factor included, must be known. The problem may be approached in two ways: (1) by designing a single-row clutch, or (2) by designing a tandem clutch containing two rows of sprags. The two-row design is generally preferred for helicopters since the overall clutch package will be smaller and lighter. However, many single-row designs have been used in the past. Often, other geometric constraints may dictate the number of rows, such as race sizes established by requirements other than clutch torque. This situation may arise when designing a clutch to fit within an existing gear member. In either case, the procedure followed is exactly the same. For a tandem design, the torque is divided in half, which assumes perfect load sharing. The procedure is then as follows:

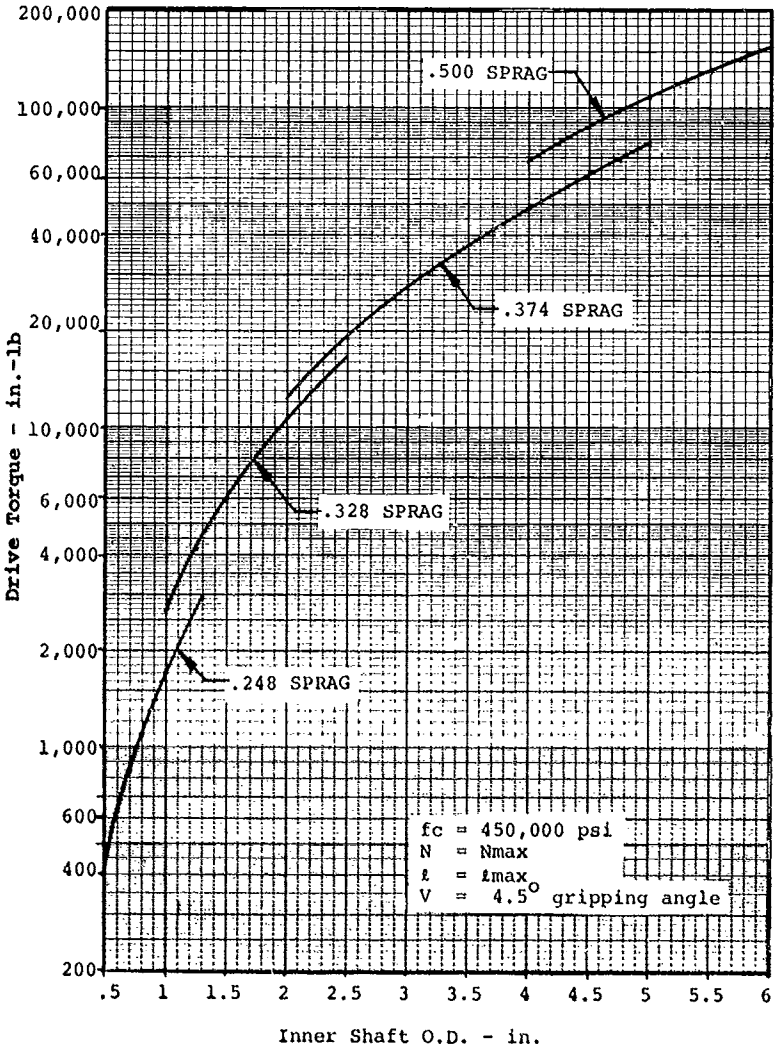

Figure 36. Sprag Clutch Preliminary Sizing Curve.

Step 1: Consult Figure 36 to determine the sprag section, J, and the inner race diameter, Di, based on design torque.

Step 2: Determine number of sprags

$$N_{max} = \frac{(Di + J)\pi}{Pc} \quad \text{(from Equation 44)}$$

Di is obtained from Step 1. J and Pc are found from Table 7 based on the sprag section chosen. N_{max} must be rounded to the next highest even whole number. An even number is chosen rather than an odd number because the manufacture of the sprag cage is easier with even numbers (broach may pass through).

Step 3: Solve for the exact inner-race diameter to re-establish correct pitch

$$Di = \frac{N(Pc)}{\pi} - J \qquad (46)$$

N is N_{max} from Step 2, and Pc and J are from Table 7.

Step 4: Solve for sprag length using the following equation for hertz stress:

$$\ell = \frac{2E\ (d_i + Di)\ T}{f_c^{\,2}\ (1 - \nu^2)\ \pi\ N\ Di\ \tan V\ d_i\ DI} \qquad (47)$$

or

$$\ell = \frac{(d_i + Di)\ T}{759\ N\ d_i\ Di^2}$$

for steel and V = 4.5 degrees (48)

The one last detail needed to complete the transmission layout is the overall width of the clutch, which varies in design depending on the configuration of the sprag-retention cages.

Basically, there are four designs available, two for each of the types of clutches, single row and double row, as shown in Figure 37.

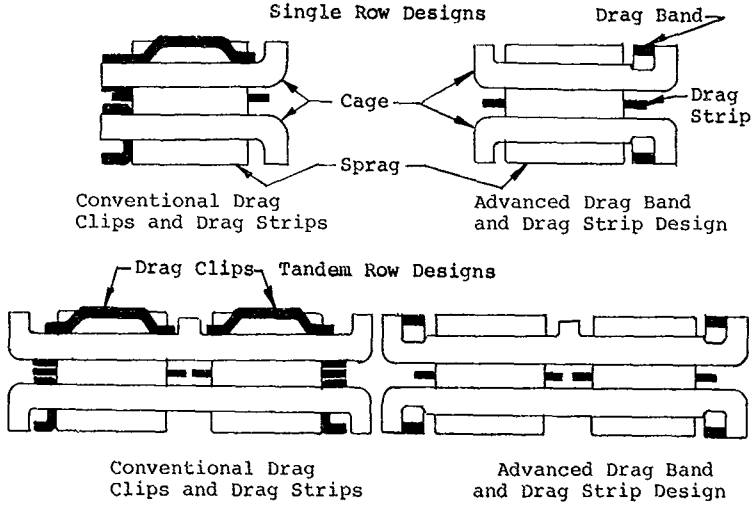

Figure 37. Sprag Clutch Cross Sections.

Figure 37 illustrates the conventional-type sprag clutches, which incorporate a number of individual frictional drag members called drag clips (attached to the outer cage) and drag strips (attached to the inner cage). The drag clip design offers the minimum overall widths. To obtain the actual width of a clutch, all that is necessary is to add .210 inch to the sprag length for the single-row type or .510 inch to the total sprag length (row-one length plus row-two length) for the double-row design shown.

Figure 37 also illustrates the advanced-type sprag clutches, which incorporate polygonally shaped, single-piece drag devices, bands on the outer cage, and strips on the inner cage. These clutches usually take up more space than the conventional-type clutches having individual drag members. The overall clutch widths can be obtained by adding .400 inch to the sprag length of the single-row design and .800 inch to the total sprag length (row one plus row two) for the double-row configuration.

NOTE: All the particulars of the contents of this chapter pertain to the "Fully-Phased" type of sprag clutch.

Since the "Positive Continuous Engagement" type of clutch can differ in the number of sprags and their length, both effective and overall, for a given clutch size, the theoretical torque transmitting capacities will also vary between the two.

Sprag Contact Angle Analysis

The objective of the sprag contact angle analysis is to determine the sprag gripping angles, V and W, under load. Once these angles are known, the sprag normal loads can be determined, after which contact stresses, housing and shaft hoop stresses, and race deflections can be found. The calculation of the contact angle is, therefore, the initial step in analyzing a sprag clutch.

The following assumptions are made in this analysis:

1. The stresses and the deflections of the housing and shaft members are derived from thick-wall cylinder theory with their effective lengths being equal to that of the overall sprag length. The strengthening effect of the housing material extending beyond the sprag length is conservatively neglected.

2. The radial sprag loads are converted to an equivalent fluid pressure since the chording effect of the sprags is small when the maximum number of sprags is utilized.

3. The loading of the housing due to centrifugal force on the sprags is neglected since its value is small compared to that of the loads imparted by the applied torque.

4. The races are assumed to be in concentric positions upon initial loading.

5. All sprags share the loads equally.

The evaluation of a clutch design is started by determining the relationship between an angle of sprag rotation, Ω, and the distance between the inner and outer raceways, J. Once this relationship has been established, the conditions of torque transmittal can be analyzed.

The sprag lies in the annular space between the two concentric races as shown by the enlarged layout of Figure 38. Both race centers are located at point O. The sprag cam centers are located at points A and B for the outer and inner cams respectively. By geometry, the point of contact or tangency point of any two circles lies on a line through their centers. Therefore, the outer cam contacts the outer race at point C, which lies on an extension of line A-O. The inner cam's contact point with the inner race is at point Q, which lies on line B-O. The angle between lines A-O and B-O is termed ψ.

As torque is applied to the inner race, it is transmitted to the sprag at point Q and from the sprag to the outer race at point C which defines the line of action Q-C.

By definition, the radial (normal) force must act along the lines A-O and B-O. Also by definition, the tangential force must act perpendicular to the normal line. Torque is the product of the tangential force and the radius at which it is applied. Also, the torque at the inner race must equal the torque at the outer race. Therefore, the tangential force (Fo) at the outer race must be smaller than the tangential force (Fi) at the inner race, as shown by the formula

$$T = Fi\ Ri\ N = Fo\ Ro\ N \tag{49}$$

where

T	=	applied torque - in.-lb
Fi	=	tangential sprag load on inner race - lb
Fo	=	tangential sprag load on outer race - lb
N	=	number of sprags

The included angle formed by lines B-Q and Q-C is defined as the gripping angle, V, at the inner race contact point. Also, the included angle formed by lines Q-C and O-C is defined as the gripping angle, W, at the outer race contact point. By geometry, it can be readily shown that

$$V = W + \psi \tag{50}$$

The term gripping angle is defined as the angle between the radial line and the line of action. For equilibrium, the vector sum of the tangential force and the radial force must lie on the line of action, Q-C.

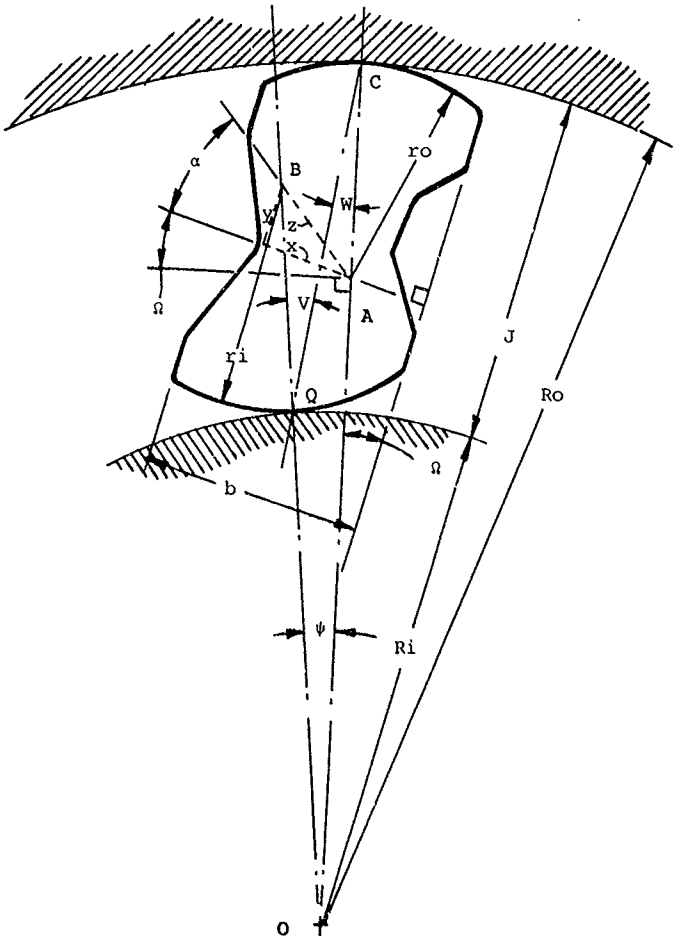

Figure 38. Geometry of a Simple Sprag.

Since the tangential force is a frictional force, its value is a variable quantity. That is, the frictional force is always equal and opposite to any applied force up to a certain maximum, which is found by the formula

$$F = \mu N \tag{51}$$

where

F = the frictional force
N = the normal force
μ = the coefficient of friction (static)

If the applied force should exceed the frictional force, slippage would occur. Substituting the value of N in terms of F and simplifying give the formula for no slippage as

$$\mu > \tan V \text{ (on inner race)} \tag{52}$$

$$\mu > \tan W \text{ (on outer race)} \tag{53}$$

When the tangent of the gripping angle is equal to the coefficient of friction, the clutch will slip or "spit out" as in a ramp roller clutch.

Initially, a small radial force is exerted between the sprag and races due to the energizing spring. When a torque load is applied, the radial force causes a frictional or tangential force between the sprag and the races. The resultant force then acts along a line whose angle with the normal line is greater than the gripping angles, V and W. These two resultant forces form a couple that causes the sprag to rotate. As the sprag rotates, its height increases, causing an increase in the normal forces by deflecting the races. Thus, the sprag becomes capable of carrying a greater tangential force. This process continues until the resultant of the normal and the frictional forces lies on the line of action, at which time the sprag reaches equilibrium.

The races must be designed with sufficient stiffness to provide the necessary normal forces for equilibrium or the clutch will fail in the "rollover" mode.

It must be pointed out here that wear causes the geometry of the sprag to change. This wear is caused by the sliding of the sprag over the race during overrunning. Eventually, the wear will cause the gripping angle to increase, at the initial locking height, to the point where slippage occurs, rendering the clutch inoperative.

When the output starts to rotate faster than the input, the sprag merely rotates to a smaller height, which is less than the mean radial height between the races; thus, the clutch is not capable of transmitting torque.

The initial step in the determination of the sprag gripping angle is the calculation of the deflection influence coefficients. The deflections and influence coefficients are summarized below

Δhsg = $\Delta cent + \Delta o$ = radial deflection of outer housing

$\Delta cent$ = centrifugal deflection of outer housing

Δo = deflection of outer housing from normal sprag load

Δi = deflection of inner shaft from normal sprag load

$\Delta sprag$ = deflection of sprag as a column or compression member

ΔHo = compressive (Hertzian) deflection between sprag and outer housing

ΔHi = compressive (Hertzian) deflection between sprag and inner shaft

The outer housing deflection includes centrifugal effects because they may become significant for high-speed freewheel units (rpm > 10,000). The centrifugal deflection is a function of the geometry, the physical properties of the material, and the rotational speed, and is independent of applied load. The centrifugal deflection is conservatively neglected on the inner shaft because the magnitude is reduced and the deflection acts in a direction that subtracts from the applied load deflections.

The deflection of the sprag acting as a column or compression member is the load times the height, divided by the area, and multiplied by the modulus of elasticity.

Compressive or "Hertzian" deflections are calculated from fundamental formulas for a cylinder in a groove (outer housing/sprag) and for a cylinder on a cylinder (inner shaft/sprag). The deflections, in terms of influence coefficients and loads, "No", acting normal to the outer housing surface, and "Ni", acting normal to the inner shaft surface, are

$$\Delta cent = \frac{Ro}{E} \frac{(3+\nu)}{4} \frac{\rho}{g} \left(\frac{\pi\ rpm}{30}\right)^2 \left[Rod^2 + Ro^2 \left(\frac{1-\nu}{3+\nu}\right)\right] \quad (54)$$

$$\Delta o = Co\ No \quad (55)$$

$$\Delta i = Ci\ Ni \quad (56)$$

$$\Delta sprag = C_s\ Ni = C_s\ No \quad (57)$$

$$\Delta Ho = No\ [C_2 - C_1\ ln\ No] \quad (58)$$

$$\Delta Hi = Ni\ [C_3 - C_1\ ln\ Ni] \quad (59)$$

The influence coefficients in the above formulas are found from

$$Co = \frac{N}{2\pi \ell\ E} \left[\frac{Rod^2 + Ro^2}{Rod^2 - Ro^2} + \nu\right] \quad (60)$$

$$Ci = \frac{N}{2\pi \ell\ E} \left[\frac{Ri^2 + Rid^2}{Ri^2 - Rid^2} - \nu\right] \quad (61)$$

$$Cs = \frac{Ro - Ri}{b\ \ell\ E} \quad (62)$$

$$C_1 = \frac{2(1-\nu^2)}{\pi\ \ell\ E} \quad (63)$$

$$C_2 = C_1 \left[\frac{2}{3} + ln\ \frac{\pi\ \ell\ E\ (Ro-ro)}{2\ (1-\nu^2)}\right] \quad (64)$$

$$C_3 = C_1 \left[\frac{2}{3} + ln\ \frac{\pi\ \ell\ E\ (Ri+ri)}{2\ (1-\nu^2)}\right] \quad (65)$$

where

Ro	=	radius from center of rotation to outer housing I.D. - in.
Rod	=	radius from center of rotation to outer housing O.D. - in.
Ri	=	radius from center of rotation to inner shaft O.D. - in.
Rid	=	radius from center of rotation to inner shaft I.D. - in.
ℓ	=	length of sprag - in.
N	=	number of sprags per row
rpm	=	revolutions per minute of outer housing
ρ	=	density of outer housing material - $lb/in.^3$

g	=	gravitational constant - 386 in./sec^2 at sea level
E	=	modulus of elasticity for housing and shaft parts - psi
ν	=	Poisson's ratio for housing and shaft material
b	=	width of sprag (circumferential)

Prior to beginning the procedure for solving for the gripping angles, which involves an iterative process, the basic sprag geometry that defines the sprag radii and the location of the radii centers must be known. The necessary information for the full-phasing type of sprag is given in Table 8.

TABLE 8. SPRAG GEOMETRY REQUIRED FOR CALCULATION OF GRIPPING ANGLES.

Parameter	Basic Sprag Sections (J) .248	.328	.374	.500
Sprag Width (b) in.	.147	.194	.214	.288
Inner Cam Radius (ri) in.	.128	.177	.198	.265
Outer Cam Radius (ro) in.	.132	.178	.195	.278
Distance between Centers (Z) in.	.0164	.0294	.0354	.0475
Angular Location of Centers (α) deg	31.264	49.821	49.574	49.268
Available Cam Rise in.	.009	.013	.015	.022

The following procedure may then be used to calculate the gripping angles

Step 1

$$\Omega = \arcsin \frac{(\bar{R}i + \bar{r}i)^2 - (Z)^2 - (\bar{R}o - \bar{r}o)^2}{2Z\,(\bar{R}o - \bar{r}o)} - \alpha \qquad (66)$$

Step 2

$$\phi = \arcsin \frac{Z \cos(\alpha + \Omega)}{\bar{R}i + \bar{r}i} \qquad (67)$$

Step 3

$$W = \arctan \frac{\bar{R}i \sin \psi}{\bar{R}o - \bar{R}i \cos \psi} \tag{68}$$

Step 4

$$V = W + \psi \tag{69}$$

Step 5

$$Ni = \frac{T \operatorname{ctn} V}{\bar{R}i\, N} \tag{70}$$

Step 6

$$No = \frac{T \operatorname{ctn} W}{\bar{R}o\, N} \tag{71}$$

Step 7

$$\bar{R}i = Ri - CiNi - \frac{Ni}{2}\,(C_3 - C_1 \ln Ni) \tag{72}$$

Step 8

$$\bar{r}i = ri - \frac{CsNi}{2} - \frac{Ni}{2}\,(C_3 - C_1 \ln Ni) \tag{73}$$

Step 9

$$\bar{R}o = Ro + \Delta cent + CoNo + \frac{No}{2}\,(C_2 - C_1 \ln No) \tag{74}$$

Step 10

$$\bar{r}o = ro - \frac{CsNo}{2} - \frac{No}{2}\,(C_2 - C_1 \ln No) \tag{75}$$

The procedure is repeated, starting with Step 1, until successive values of the angle Ω are within the desired accuracy. In Steps 1 through 10, $\bar{R}i$, $\bar{r}i$, $\bar{R}o$, and $\bar{r}o$ represent the deflected values of Ri, ri, Ro, and ro respectively. Thus, to obtain the no-load gripping angles, Steps 1 through 4 are performed using the undeflected radius values. The initial time through the procedure, the nondeflected values are used in place of the deflected values for $\bar{R}i$, $\bar{r}i$, $\bar{R}o$, and $\bar{r}o$.

After the gripping angles, V and W, are calculated, the remainder of the analysis can proceed.

If the sprag clutch has two rows of sprags instead of one, the torques in Steps 5 and 6 are reduced by 50%. This assumes perfect load sharing between rows. The actual structure is redundant, and load sharing between rows will be dependent upon the stiffness paths of the various clutch members. A comprehensive analysis of load sharing between rows is beyond the scope of this text and will not be presented.

Note that, in the sprag clutch analysis, a cylinder under the influence of pressure was assumed. If the inner or outer shaft has a variable diameter associated with it, the influence coefficients used in the ramp roller analysis may be used in place of those presented here.

Influence Coefficient for Cylinder Under Pressure	Influence Coefficient for Ring Subjected to "n" Loads
Ci	CK
Co	CR

Either Ci or CK may be used (for either analysis), and similarly, Co or CR may be used interchangeably. Moreover, the effect of Hertzian deflections have been neglected in the ramp roller clutch but may be included if desired.

The procedure outlined in Steps 1 through 10 will usually converge quite rapidly. Generally, four to six iterations are all that are required to obtain an accuracy in normal loads, Ni and No, within $\pm$.5 lb.

The above formulas pertain to a simple sprag; i.e., a sprag having only two cam radii, one at the inner race contact and the other at the outer race contact. However, the typical sprag used in a helicopter application is of the compound type, meaning that more than one radius is used to form either of the cam surfaces. Figure 39 depicts a sprag with a compound inner surface. The formulas previously defined are applicable to the compound sprag provided the proper inner radius is used. The inner radius is either ri or ei, depending on the rotation angle, θ, and the geometry of the sprag. Once the inner radius area of contact is known, the procedure is the same as for the simple sprag.

Once the gripping angles have been calculated, the sprag can be checked for "rollover." This is done by adding all the deflections as follows

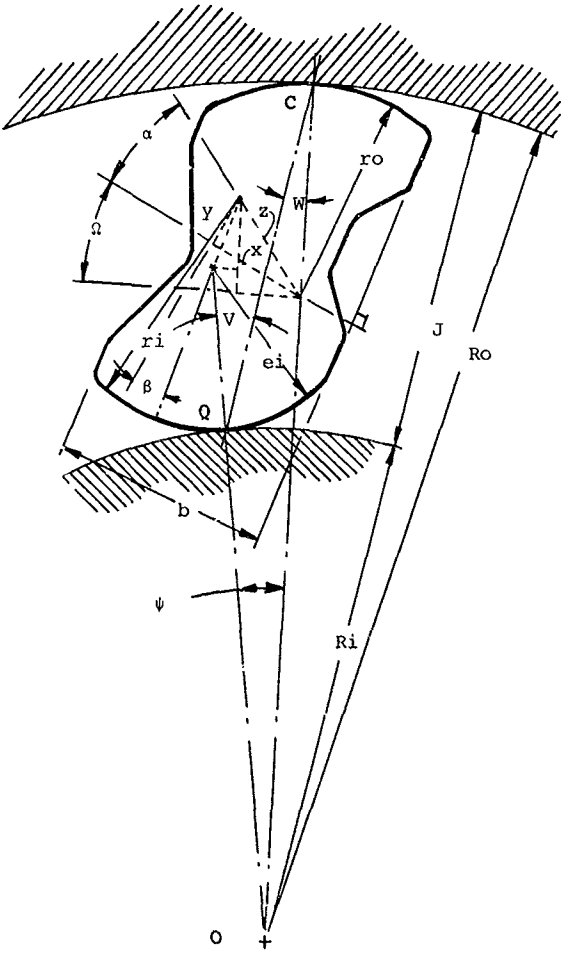

Figure 39. Geometry of Sprag With Compounded Inner Cam.

$$\Delta total = \Delta cent + \Delta o + \Delta i + \Delta sprag + \Delta Ho + \Delta Hi \qquad (76)$$

where

$\Delta total$ = summation of total radial deflections

Next the sprag characteristics table, Table 8, should be consulted for the available sprag cam rise. The available cam rise must be greater than the total radial deflections, $\Delta total$, as determined in Equation 76. If less, "clutch rollover" will occur, resulting in a failure to transmit torque. The total deflection, $\Delta total$, should preferably be 50% of the available sprag rise when using design-point data.

Sprag Hertz Stresses

The sprag will have stresses in it as a result of the loads acting normal to the surfaces of the inner and outer races. An isolated sprag with loads is shown in Figure 40.

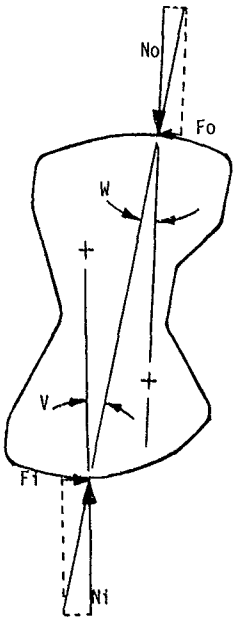

Figure 40. Sprag Loads, Free Body Diagram.

The contact stresses, or Hertzian stresses, are calculated from theoretical formulas for a cylinder on a cylinder (sprag contact on inner shaft) and for a cylinder in a circular groove (sprag contact on outer shaft). In determining the gripping angles, V and W, the normal loads, No and Ni, have been calculated from

$$No = \frac{T \text{ ctn } W}{Ro\ N} \tag{77}$$

$$Ni = \frac{T \text{ ctn } V}{Ri\ N} \tag{78}$$

The sprag Hertz stresses are then found from

$$f_{co} = \frac{No\ E}{2\pi\ell\ (1-\nu^2)} \left(\frac{Ro - ro}{Ro\ ro}\right) \tag{79}$$

$$f_{ci} = \frac{Ni\ E}{2\pi\ell\ (1-\nu^2)} \left(\frac{Ri + ri}{Ri\ ri}\right) \tag{80}$$

To avoid local brinelling due to the high Hertz stresses, the spragway surface should have a minimum surface hardness of Rc 60. This hard case should extend into the surface to a depth of .05 inch, at which point the hardness should not be less than Rc 50.

To prevant excessive race yielding under load, the hardness of the core supporting the case should be in the range of Rc 35-45. Experience with excessively hard cores (>Rc 50) has shown them to be prone to cracking at the outside diameter, and also, they were found to be very sensitive to stress risers.

An allowable Hertz stress of 450,000 psi has been used in previous clutch designs for helicopter applications.

Inner Shaft Hoop Stress Analysis

The inner shaft of the sprag clutch is subjected to compressive hoop stresses as a result of the pressure created on the shaft from the tangential and the normal sprag loads. The analysis is conducted by assuming the sprags are so closely spaced that their effect will be continuous. This assumption will allow the use of thick-wall cylinder theory under uniform external pressure.

To determine the magnitude of the pressure, the normal and tangential components of the sprag's load must first be calculated (see "Sprag Contact Angle Analysis"). The sprag normal load is then converted to pressure by

$$p_i = \frac{-N\ Ni}{2\pi\ \ell\ Ri} \quad \text{(negative sign indicates inward pressure)} \tag{81}$$

where

N	=	number of sprags
Ni	=	force from sprag acting perpendicular to inner race diameter - lb
ℓ	=	sprag length - in.
Ri	=	radius from inner shaft centerline to race O.D. - in.
p_i	=	equivalent pressure on inner race - psi

The perpendicular force of the sprag on the inner race diameter, Ni, is found by

$$Ni = \frac{T \cot V}{Ri\ N} \tag{82}$$

where

T	=	torque at which stress is desired - in. lb (per row)
V	=	gripping angle at inner race

Substituting for Ni from Equation 82 into Equation 81 and simplifying gives

$$p_i = \frac{-T \cot V}{2\pi\ \ell\ Ri^2} \tag{83}$$

Assuming the inner shaft is a cylinder under the influence of external pressure and conservatively neglecting the material which extends beyond the edges of contact between the sprags and the shaft, the stress can be calculated by

$$f_i = p_i \left[\frac{2\,Ri^2}{Ri^2 - Rid^2} \right] \qquad (84)$$

where

Rid = radius from inner shaft centerline to I.D. of inner shaft - in.
f_i = inner shaft compressive stress - psi

Equation 84 is useful for determining the stresses in the inner shaft for a true cylindrical shape. In practice, this may not be the case: very often the inner shaft I.D. may have two or more diameters. In this case, the shaft may be divided into a series of cylinders, and the method outlined in "Housing Hoop Stress - Spring Clutch", may be used. In effect, this method equates deflections of the various cylinders and solves for the loads required to produce this condition of equilibrium. Using this procedure, a more accurate picture of stress distribution may be obtained.

Keyways or splines located at the bore of the race beneath the spragway are considered stress risers, and the net area taken at the roots should be used conservatively in the above formulas. Rotational effects on stresses and deflections have been neglected since their values are small in comparison to those imposed by the torque being transmitted.

The deflection of the inner race under the influence of the external pressure, pi, can be calculated from

$$\Delta i = p_i \frac{Ri}{E} \left[\frac{Ri^2 + Rid^2}{Ri^2 - Rid^2} - \nu \right] \qquad (85)$$

where

Δi = radial deflection of inner race - in.
ν = Poisson's ratio

Outer Race Hoop Stress Analysis

The outer race of the sprag clutch has stresses induced into it in a manner similar to that of the inner race. However, in the outer race, the hoop stresses are tensile since the sprag loads act in an outward direction on the outer race. The analysis is conducted by assuming that the sprags are so closely spaced that their effect is continuous, and as with the inner race analysis, a uniform pressure is found from

$$P_o = \frac{N\ No}{2\pi\ \ell\ Ro} \quad \text{(positive sign indicates outward pressure)} \tag{86}$$

where

N	=	number of sprags
No	=	normal force from sprag acting perpendicular to I.D. of outer race - lb
Ro	=	radius from outer housing centerline to inside diameter - in.
ℓ	=	sprag length - in.
P_o	=	equivalent pressure on outer race - psi

The normal sprag load, No is given by

$$No = \frac{T \cot W}{Ro\ N} \tag{87}$$

where

T	=	torque at which stress is desired - in. lb
W	=	gripping angle on outer race

Substituting for No from Equation 86 into Equation 87 and simplifying

$$P_o = \frac{T \cot W}{2\pi\ \ell\ Ro^2} \tag{88}$$

Assuming the outer race is a cylinder under the influence of internal pressure and conservatively neglecting the material that extends beyond the edges of the area of contact between sprags and outer housing, the stress can be found from

$$f_o = P_o \left[\frac{Rod^2 + Ro^2}{Rod^2 - Ro^2}\right] \tag{89}$$

where

Rod = radius from outer housing centerline to outer housing O.D. - in.
f_o = outer housing hoop stress - psi

As with the inner shaft, Equation 89 pertains to a true cylindrical shape. In practice, the outer housing is outside radius, Rod, may have two or more different diameters associated with it. To determine the stress distribution with this type of outer housing, the method outlined in "Housing Hoop Stress Analysis in the spring clutch section may be used.

Keyways or splines located at the outside diameter above the spragway are stress risers, and the net area taken at the root diameter should be used conservatively in the above formulas. Rotational effects on stresses and deflections have been neglected since their values are small in comparison to the loads imposed by the torque being transmitted.

The deflection of the outer housing under the influence of the internal pressure, p_o, can be calculated from

$$\Delta o = p_o \frac{Ro}{E} \left[\frac{Rod^2 + Ro^2}{Rod^2 - Ro^2} + \nu \right] \qquad (90)$$

where

Δo = radial deflection of outer housing - in.
ν = Poisson's ratio

Sprag Centrifugal Effects

There are two basic types of sprags used in helicopter applications: those being "centrifugally engaging" and those being "centrifugally disengaging." The latter is used primarily in starter systems.

The disengaging type of sprag is designed to lift off the inner race so that overrunning wear is minimized and occurs only during the coastdown mode of operation. The speed at which disengagement takes place is predetermined and is usually just below that of engine idle speed. Once the sprag lifts off the inner race, it is impossible to engage the clutch. The only way an engagement can be made is to reduce the speed of the outer housing to the point where the sprag again makes contact with the inner shaft. Increasing the inner shaft speed to that of the outer will then result in an engagement. Note also that, with this type of sprag, a possibly dangerous

operating condition may result if the sprag disengages and the speed of the inner shaft is raised above that of the disengagement speed. In this condition, a shock engagement will occur if the outer shaft speed is reduced to that of the input. A system study should be performed to determine the possible consequences of such a condition.

Figure 41 shows how the lift-off effect is created and directed by centrifugal force when the sprag center of gravity lies outside the contact line "m." This relationship results in a moment Fc x a. When this moment is greater than the opposing moment of the energizing spring load and the friction, M_{spring}, the sprag will rotate towards the release direction until equilibrium is reached, at which time there is no contact between the sprag and inner race.

The engaging-type sprag is designed to continuously rub on the inner race during overrunning. This feature is necessary in the typical helicopter's main-drive and accessory-drive systems since the clutch must be capable of making dynamic engagements at all speeds.

As shown in Figure 41, the center of gravity of the engaging-type sprag lies on the opposite side of the contact line, "m." This results in a moment Fc x b that increases the contact pressure on the inner race as the outer race rotates and adds to the spring load and the friction. If the combined effects of centrifugal moment and spring force become excessive, the end result may be in the form of high sprag or raceway wear during overrunning. This is especially true with high-speed units since sprag centrifugal load is a function of speed squared:

$$Fc = \frac{Ws}{g} \bar{R} \left[\frac{\pi \text{ rpm}}{30}\right]^2 \qquad (91)$$

where

Fc	=	centrifugal force per sprag - lb
Ws	=	weight of sprag - lb
g	=	gravitational constant - $in./sec^2$
$\bar{R}$	=	radius from center of rotation to sprag center of gravity - in.
rpm	=	clutch outer housing revolutions per minute

The determination of the offset distances, a and b, is a complex geometric problem. Needless to say, the offset distances are dependent upon the spragway diameters, Di and Do, the sprag section, J, and the center of gravity location. Thus, it is seen that the effects of wear must be considered. Wear will result in a decrease of Di, an increase in Do, and a decrease in J. All of these parameters serve to increase

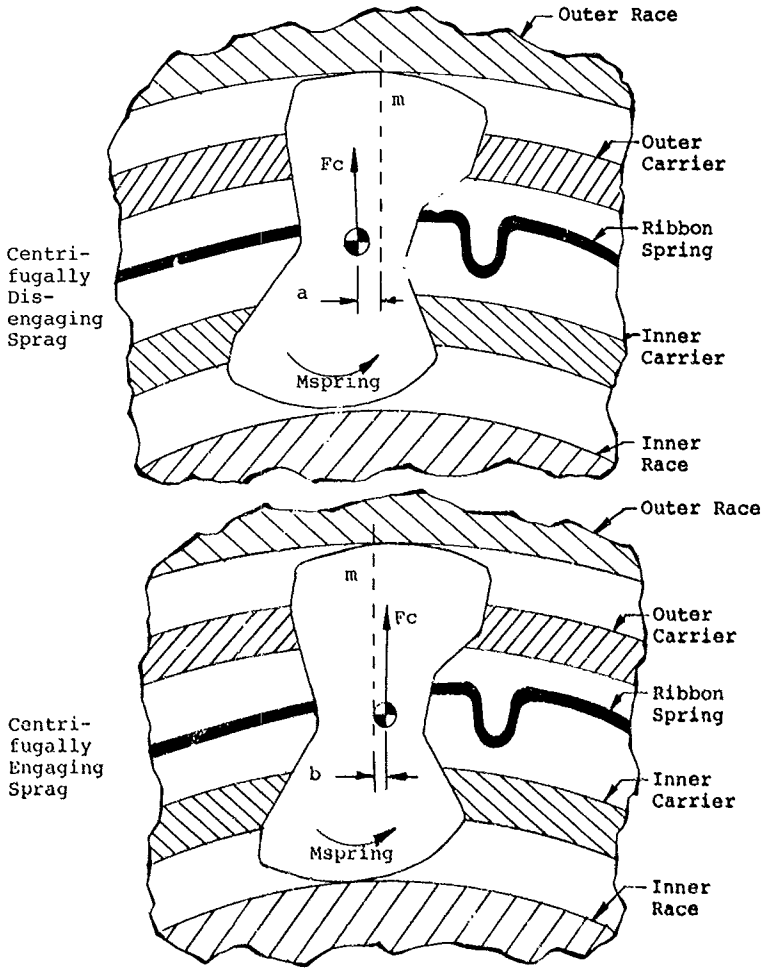

Figure 41. Sprag Centrifugal Effects.

the gripping angles of the sprag, and in effect, wear will decrease b and increase a.

With the engaging-type sprag, overrunning wear can be minimized to an acceptable level by the hydrodynamic effects of the oil coupled with the frictional devices attached to the cages of the clutch.

Outer Housing Design

To avoid local brinelling due to the high Hertz stresses generally found in aircraft clutches, the spragway surface should have a minimum surface hardness of Rc 60. This hard case should extend into the surface to a minimum depth of .050 inch, at which point the hardness should not be less than Rc 50.

To prevent excessive race yielding under load, the hardness of the core supporting the case should be in the range of Rc 35-45. Experience with excessively hard cores (greater than Rc 50) has shown them to be prone to cracking at their outside diameter's and also, they were found to be very sensitive to stress risers.

The race materials that are generally employed are of the nickel-chromium-molybdenum grade, such as S.A.E. 8620, 8640 and 9310. Other materials would work as well as these as long as the hardness and strength properties are maintained.

The surface finish of the spragway should be between 20-30 microinches. The taper of each side of the spragway should not exceed .0003 inch per inch of length of the sprags. A slight chamfer, about .03 inch x 30°, on the lead-in end of the spragway is usually necessary to simplify the assembly of the clutch.

The total accumulation of tolerances between the bore of the outer housing and the outside diameter of the inner shaft must be maintained within specified limits for proper operation. The maximum allowable radial variation in sprag space depends on the size of sprag section chosen (see Table 9).

TABLE 9. SPRAG RACEWAY TOLERANCES.	
Sprag Section	Max Allowable Variation in "J"
.248 in.	± .002 in.
.328 in.	± .003 in.
.374 in.	± .003 in.
.500 in.	± .004 in.

The tolerance of the spragway diameter of the outer housing should be held to ± .0005 inch.

Composite races consisting of pressed-in steel sleeves are not recommended due to their tendency to slip. Also, plating of the spragway should not be considered because of the high Hertz stresses encountered, which can lead to eventual failure by peeling or chipping of the plating.

If the configuration of the race is such that the cross-sections above and near the sprags are nonuniform, an allowance must be made for the bellmoutning effect, which, if present to a large degree, will reduce the effective length of the sprags and tend to skew them.

To obtain proper lubrication, oil dams are usually employed on each side of the sprag unit as shown in Figure 42. This design maintains a full head of oil within the clutch cavity when the outer race is rotating. Also, it is recommended that small oil drain holes be incorporated in the outer race over the clutch cavity to deter the accumulation of sludge deposits which have a tendency to accumulate due to the centrifuging effect. The quantity and size of these holes should be such that the level of the head of oil is not changed when the unit is at full speed. Thus, the oil input must be greater than the oil output through the outer housing drain holes while under the influence of centrifugal pressure at maximum head (see Lubrication-Pressure in a Rotating Dam of Oil).

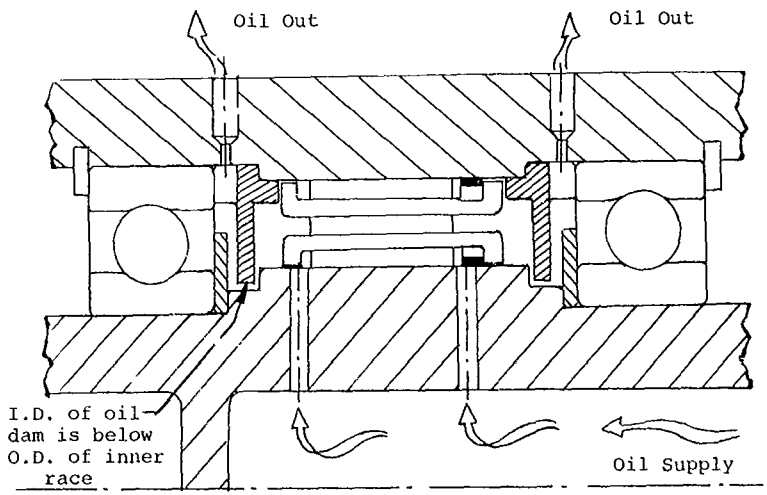

Figure 42. Sprag Clutch Lubrication Flow Path.

As shown in Figure 42, oil drain holes can be provided on the outboard side of the oil dams to reduce the quantity and, therefore, the churning encountered when the oil passes through the bearings while the clutch is in an overrunning mode.

Inner Shaft Design

The material, tolerances and hardness of the inner shaft and spragway are identical to those noted in the last section, "Outer Housing Design", the only differences being the tolerances for the diameters of the spragways of smaller clutches and the surface finish.

For smaller clutches, ranging in size from .500 to 2.500 inches in diameter, the tolerance of the spragway is usually held to a total of .0005 inch whereas in sizes greater than 2.500 inches, the tolerance is usually $\pm$.0005 inch.

Since overrunning takes place at the inner race on most sprag clutches, the surface finish should be held to within 10-20 microinches to minimize wear on the sprags.

Just as with the outer housing, a lead in chamfer should be incorporated on the spragway surface of the inner shaft for ease of assembly. This chamfer need not be any larger than .05 inch x 30^{o}.

To provide proper lubrication, the oil should be fed to the clutch via the bore of the inner shaft, as in Figure 42. A number of radial holes through the shaft section, in line with the clutch cavity, will allow the oil within the bore to feed into the clutch area by centrifugal force when the inner shaft is the output member.

It should be noted here that the customary practice of applying a phosphate treatment coating to bearings and other shaft surfaces should not be introduced in the area of the spragway since the effect will be to reduce the coefficient of friction, which the sprag clutch design is dependent upon. Black oxide, on the other hand, increases the coefficient of friction and is acceptable.

Sprag Design

The heart of the sprag design lies with the choice of the proper gripping angle at the point of initial engagement. This friction angle must be sufficiently low to break through the oil film and also to provide an allowance for wear generated when the clutch is in an overrunning mode of operation.

For economical reasons, the gripping angles on the various available sprag sections have been predetermined and cannot be changed at will without increasing the overall cost of the clutch by a large factor.

Sprags used in clutches for the aircraft industry are usually the high-temperature bearing-tool steels designated HTB-2, M-50 or AMS 6490. Sprags are also made from S.A.E. 52100 steel, but these are usually utilized in starter clutches where the sprags are disengaging in character. The hardnesses of these sprags are usually in the vicinity of Rc 63.

Nitriding, which is a recent development in the heat treatment of sprags, has lead to increased life from both the overrunning-wear and the gripping-angle-fatigue standpoints. The nitriding diffusion process results in a superior wear surface having a tough hardness value of Rc 77.

The intricate shape of the sprag is usually obtained by extruding the raw material through a series of dies. During this extrusion process, a surface finish of approximately 7 microinches is obtained. The tolerances across the cam surfaces are typically maintained at .0010 inch.

Because of the manner in which the sprags are further processed, the length tolerance is typically held to within .005 inch, which results in a maximum concavity along the length of the cam surfaces of .0002 inch.

In any given clutch, the sprags are individually measured and grouped in height to within .0003 inch, which allows for more uniform stress and wear distributions amongst the sprags.

Cage Design

Since sprag phasing in a clutch must be completely uniform, the "fully-phased" type of clutch employs two cages to maintain the proper angular and axial alignments of all sprags.

These cages, commonly called the inner and outer cages due to their close proximities to the inner and outer races, serve three purposes: (1) they limit the amount of sprag rotation in both directions, (2) they insure simultaneous engagement and disengagement of the sprags, and (3) they space the sprags equally, axially and circumferentially, around the associated races to provide a uniform stress distribution throughout.

The centralization of the inner cage with the inner race is provided by the integral internal flange or flanges, which act as a pilot on the inner race. At this interface, the diametral clearance is usually maintained at .002 to .014 inch.

The centralization of the outer cage with the outer race is also provided by an integral flange or flanges, which act as a pilot on the outer race. The diametral clearance at this interface is usually held to .001 to .013 inch.

In both cages, the width of the sprag hole (circumferentially) is designed with a .007-inch clearance with the sprag when the sprag is in a straight position. As the sprag rotates, either in the release or lockup direction, the .007-inch clearance reduces to about .003 due to the special shape of the sides of the sprags.

This clearance is necessary to overcome the tolerances associated with sprag widths, cage hole widths, and circumferential pitch errors inherent in any given clutch design.

The length of the sprag slots is also governed by manufacturing and alignment considerations, which dictate a clearance with the maximum sprag length of .003 to .008 inch.

Two basic types of cages are utilized in the aircraft industry: one type where the cages are made from deep-draw flat steel of the medium carbon range, like S.A.E. 1035-1045, and the other type where the cages are made from bar or tube stock usually of the S.A.E. 4340 aircraft grade.

In applications where a lower-cost clutch is desired, the clutch is usually designed with a minimum safety factor of 200%, and here, due to the large safety margin, the cages are fabricated from drawn cups and the sprag holes are formed by punch and die operations.

In special applications where the clutch is designed for minimum size, the cages are usually fully machined out of round or tubular bar stock. Due to their construction, the sprag holes are formed by a milling process followed by a broaching process. When this type of design is used, the number of sprags must be an even number to allow the broach to pass through the cage from one slot to the opposite slot, 180° apart. This type of construction results in increased durability and wear resistance.

All cages are given a heat treatment to obtain a hardness of Rc 35-45. With the fully machined type of cage, a subsequent nitriding heat treatment is employed. Nitriding provides a hard case of approximately Rc 55 and extends to a depth of about .012 inch. The hardened cage provides a superior wear surface at the interface where the cage crossbars contact the sides of the sprags. For raceway wear considerations, the nitrided layer on the inner cage flange (or flanges) is removed as a final manufacturing procedure.

As part of the overall clutch design, frictional devices called "drag clips" (or bands) and "drag strips" are attached to the outer cage and inner cage, respectively, as shown in Figure 43. The employment of these devices is usually referred to as "built-in drag".

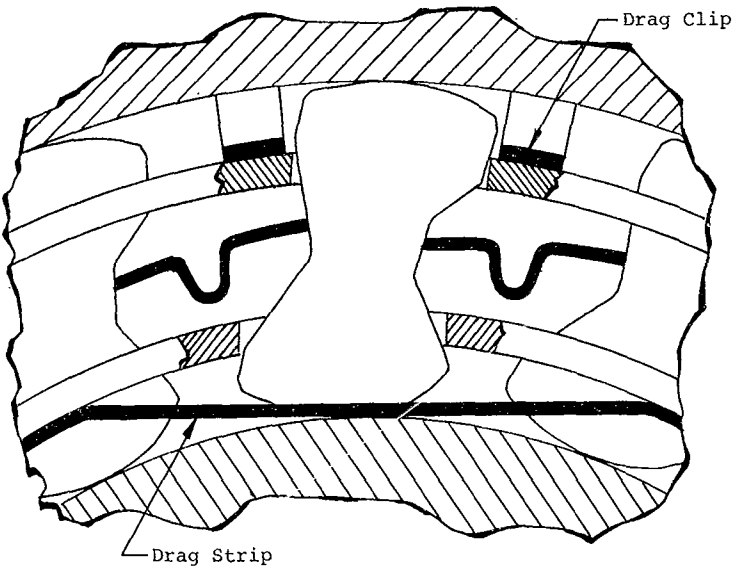

Figure 43. Sprag Clutch Frictional Drag Devices.

With the attachment of drag members to the outer cage, the sprag assembly is frictionally connected to the outer race. This is a necessary feature to overcome the inertial forces of the clutch and the components upon rapid acceleration or deceleration that could overcome the normal drag between the sprags and the races and prevent a normal engagement. These drag clips or drag bands are usually made from cold-rolled S.A.E.-type 301 stainless steel and are given a subsequent heat treatment after forming to relieve residual stresses.

The frictional drag torque necessary to overcome the inertia of the clutch is usually designed as a function of the number of sprags, their length, and the diameter of the inner race, and is expressed as

$$TDC = 4\ N\ D\ \ell \text{ (inch-ounce)}$$

which results in a value of 8 ounces per sprag per inch of sprag length at a radius of one inch. In the case of an extreme acceleration or deceleration, this value may be modified.

On the inner cage, drag strips are employed to obtain greater overrunning life and also to assist in the engagement of the sprags. During overrunning, the frictional forces oppose and subtract from the normal energizing-spring force on the sprags and thereby reduce the unit loading between the sprags and the inner race. During clutch engagement, the directionally sensitive forces add to the energizing spring force, thus providing a more positive and uniform clutch engagement.

Since a large amount of relative rotation takes place at the interface of the inner race and the drag strip, the latter is usually made from number-25 beryllium copper and given a heat treatment to obtain a hardness value of Rc 35. In some cases where the lubrication conditions are borderline, the drag strips may be given a further treatment, such as silver-plating to a thickness of .002 inch.

The drag torque usually employed here is 225% greater than the overrunning drag torque induced by the sprag energizing spring. Its value is found by

$$TDS = 2.25\ N\ D\ \ell \text{ (inch-ounce)}$$

This results in a value of 4.5 ounces per inch of sprag length at a radius of one inch. It can be deduced from the above that the normal overrunning drag torque is about two inch-ounces per inch of sprag length at a one inch radius or approximately 1/4000 of the rated torque capacity of the clutch.

RAMP ROLLER CLUTCH DESIGN

Basic Configuration

The configuration of the support and the mounting of the ramp roller clutch is very similar to that of the sprag clutch. The rollers are mounted between inner and outer clutch members just as the sprags of the sprag clutch are. Since the mounting is so similar to that of the sprag clutch, the "Basic Configuration" discussion given for sprag clutch design, also pertains to the ramp roller clutch. Please refer to that section.

The mounting of the duplex bearings on the right or the left side of the rollers is merely a matter of assembly and the choice is left to the designer. On any ramp roller clutch, either the driving or the driven members can be designed as either the cam or the outer housing. Each configuration has its own advantages and disadvantages. If centrifugal forces are to assist lubrication, it is advantageous to design the cam as the output. In a helicopter drive train, the output of the freewheel unit is the overrunning member, and therefore, the output is always rotating when the helicopter is in operation.

The ramp roller clutch of the type used in aircraft applications uses the innermost shaft as the cam member. The cam member guides the roller carrier and rollers. Centrifugal effects on the ramp roller clutch are, therefore, associated with the cam. For this reason, it is recommended that, for high-speed units, the cam should be the input member, while for low-speed units, the cam should be the output member for centrifugal lubrication. With cam input, lubrication to the cam surfaces is difficult. Pressurized lubrication chambers solve this problem and have been successfully used in aircraft applications.

The rotational direction of the ramp roller clutch is immaterial. The direction should be chosen on the basis of blade and engine requirements, and the clutch's location in the drive train. The cam and cage are designed to operate in the chosen direction in the detail design phase.

The envelope of the ramp roller clutch can be quickly determined during the preliminary transmission design phase of a project by sizing the unit on the basis of maximum engine horsepower capability and clutch speed. A layout can be developed easily using the guidelines in the next section, "Preliminary Sizing".

A recent development in ramp roller clutches, which has been used extensively in sprag clutches, is the two-row design. The detailed analysis of the two-row ramp roller clutch is beyond the scope of this design guide. Theoretically, if one were to obtain perfect load sharing, a two-row ramp roller clutch could be designed for one-half the torque of a one-row design. The number of parts and the axial length increase, but the diameter of the unit and the weight decrease. In practice, if the configurations of the clutch races are different, i.e., if the stiffnesses or the dimensions of the rows are different (even within the close machining tolerances used), equal load sharing cannot be achieved. A mandatory feature of a two-row ramp roller clutch is roller-retention cages that act independently of each other. This allows the rollers in each row to assume different "nip" angle positions if they so desire.

Preliminary Sizing

Before discussing the procedure for the preliminary sizing of a ramp roller clutch, it will be necessary to define some of the parameters associated with the design and analysis of ramp roller clutches. Before starting the design, the power and the speed must be known. Parameters necessary for preliminary sizing include the following

L	=	length of clutch rollers - in.
n	=	number of clutch rollers
R	=	outer housing bore radius - in.
T	=	clutch design torque - in. lb
ρ	=	roller radius - in.

It has been found from the geometry of the system that the optimum number of rollers for a ramp roller clutch is either 12 or 14 rollers. The optimum number of rollers is the most that will fit while still allowing cage clearance between rollers and the most that is compatible with the size and geometric considerations in designing and manufacturing cams. It is generally preferable to use the maximum number of rollers since this minimizes clutch stresses and allows a compact unit. With the number of rollers determined, it is first necessary to determine the radius of the rollers, ρ, that will be needed to transmit the design torque, T, within the allowable stress range for the rollers. Equation 92 is useful for a preliminary determination of roller radius.

$$\rho = \left(\frac{T}{730,000}\right)^{1/3} \qquad (92)$$

This equation may be used with Figures 44 and 45, which show the general relationships, ρ versus L and ρ versus R.

To illustrate the preliminary sizing procedure, let us assume that a design is required for a ramp roller clutch for 20,000 in. lb of torque. Substituting this value for T in Equation 92 gives us a roller radius of .30 inch. Using this value in conjunction with Figures 44 and 45, we find that an outer housing radius of 2.25 inches and a roller length of 1.00 inch are good first approximations for the clutch design. If we were to pursue this design, we would now have the necessary information to prepare a preliminary layout from which a stress analysis could be conducted; i.e., the roller and its position relative to the centerline are defined. Design iterations are then conducted from this initial layout.

It should be pointed out that the relations presented here are only approximate and should by no means be used as allowable ranges for the various parameters. It is very possible to design a ramp roller clutch whose parameters would fall outside the ranges suggested here. The empirical relationship for the roller size as a function of torque is derived from previous designs, while the ρ versus L and the ρ versus R relationships from Figures 44 and 45 are from actual helicopter ramp roller clutches in the field.

Roller Contact Angle Analysis

Torque is transmitted in the ramp roller clutch by frictional forces between the rollers, the cam, and the housing. The angle formed by the line between the rollers and the center of rotation and the cam flat perpendicular centerline is commonly termed the "nip" or roller contact angle (see Figure 46). The normal roller loads are proportional to the cotangent of one-half of the nip angle. Hence, the normal roller load becomes high and approaches infinity as the nip angle approaches zero. Cam, housing, and roller stresses are proportional to the normal roller load. It is, therefore, desirable to keep the normal roller load low. The tangential and normal roller loads are related by

$$F = P \tan \frac{\psi}{2} \qquad (93)$$

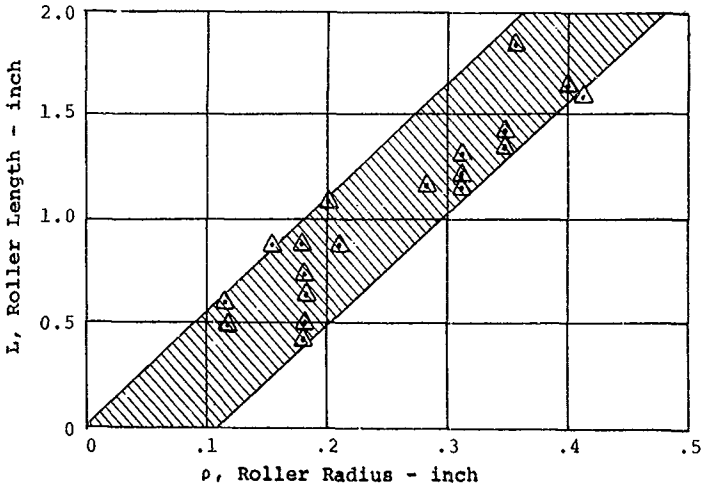

Figure 44. Roller Proportions, Historical Data.

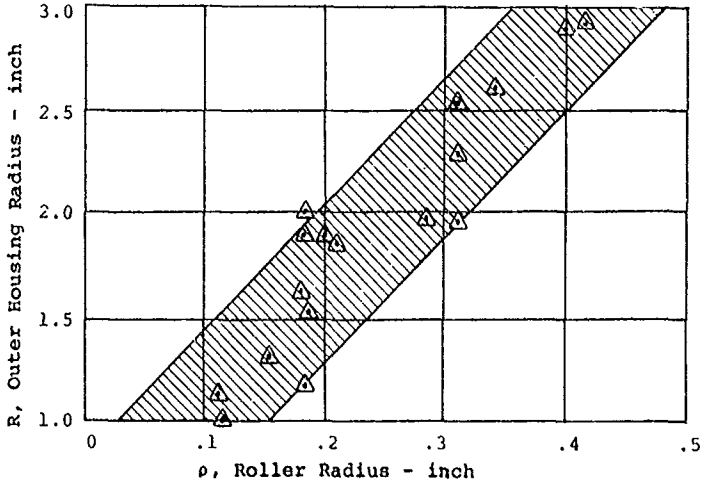

Figure 45. Roller Position, Historical Data.

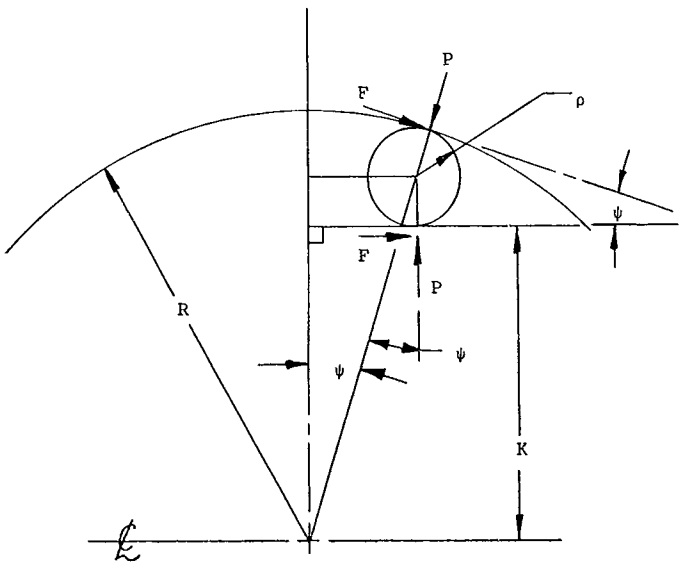

NOMENCLATURE

R = Radius of housing (undeformed)
K = Distance from centerline to cam surface (undeformed)
ρ = Radius of roller (undeformed)
ψ = Roller nip angle
F = Tangential roller load
P = Normal roller load

Figure 46. Roller Contact Angle Dimensions and Symbols for a Ramp Roller Clutch.

where

F = tangential roller load
P = normal roller load
ψ = nip angle

The maximum value that F can assume is P times the coefficient of friction.

$$F_{max} = \mu P \tag{94}$$

Since the torque transmitted is given by the following

$$T = n F R \tag{95}$$

it therefore follows that the maximum value of torque that can be transmitted in the ramp roller clutch occurs when the coefficient of friction is equal to the tangent of one-half of the nip angle; or, for transmittal of torque,

$$\mu \geq \tan \frac{\psi}{2} \tag{96}$$

If the coefficient of friction becomes less than the above value, the rollers "spit out;" i.e., the torque cannot be maintained. In practice, this usually occurs at a nip angle of approximately 12 degrees or greater (coefficient of friction 0.1 max).

As the components of the ramp roller clutch wear in service, the nip angle increases. It is therefore a good design practice to start with a nip angle that is low. By using a low initial nip angle, the clutch components can wear in service with no effect on clutch operation. A good starting value for a no-load nip angle is 3 or 4 degrees.

As torque is applied to the roller clutch, the nip angle increases because the outer housing deflects outward, the cam deflects inward, and the rollers compress. The nip angles under no load and load can be found from the following

$$\cos \psi o = \frac{K + \rho}{R - \rho} \tag{97}$$

$$\cos \psi f = \frac{K - \Delta cam + \rho - \Delta roller}{R + \Delta hsg - \rho + \Delta roller} \tag{98}$$

where

ψo = no-load nip angle
ψf = full-load nip angle
Δcam = cam radial deflection under load - in.
Δhsg = housing radial deflection under load - in.
$\Delta roller$ = roller radial deflection under load - in.
K = distance from centerline to cam surface - in.
R = radius of housing - in.
ρ = roller radius - in.

The cam and the housing deflections are determined using ring formula theory. Effective cam and housing areas for deflection analysis are determined by taking an axial cross section through the rollers of the clutch.

The effective areas used to find deflection may be different than the effective areas used to determine stress. In the interests of conservatism, the effective area for stress is usually smaller than the effective area for deflection. A typical effective area for a ramp roller clutch is depicted in Figure 47.

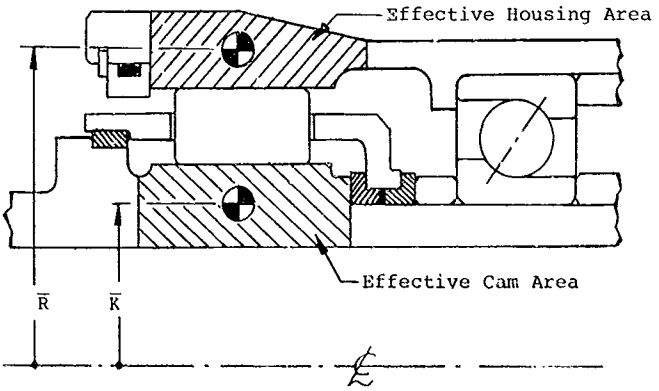

Figure 47. Typical Effective Cam and Housing Area Assumptions.

The areas to the right and left of the shaded areas of the cam and housing are conservatively neglected in the analysis. Once the effective cam and housing areas are established, the centroids, $\bar{R}$ and $\bar{K}$, are calculated. Next, the areas and moments of inertia of the area about the centroids are found. The influence coefficients for deflection are then calculated as follows

$$CR = \frac{A\,\bar{R}^3}{4\,E\,Ih} + \frac{B\,\bar{R}}{4\,E\,Ah} + \frac{3\,C\,\bar{R}}{10\,G\,Ah} \qquad (99)$$

$$CK = \frac{A\,\bar{K}^3}{4\,E\,Ik} + \frac{B\,\bar{K}}{4\,E\,Ak} + \frac{3\,C\,\bar{K}}{10\,G\,Ak} \qquad (100)$$

$$A = \frac{\theta}{\sin^2\theta} + \cot\theta - \frac{2}{\theta} \tag{101}$$

$$B = \frac{\theta}{\sin^2\theta} + \cot\theta \tag{102}$$

$$C = \frac{\theta}{\sin^2\theta} - \cot\theta \tag{103}$$

$$\theta = \frac{\pi}{n}$$

$$C\rho = \frac{rm^2}{\rho\ (1-H)\ L\ E\ er} \left\{ \frac{\pi}{4} - \frac{2}{\pi}\left[1 - \left(\frac{er}{rm}\right)^2\right] + \frac{2er}{rm} \left[\frac{2}{\pi}\left(1 - \frac{er}{rm}\right) - \frac{\pi}{8}\right] + \frac{15\pi\ er}{16\ rm}\right\} \tag{104}$$

where

H = I.D./O.D. of roller
L = total roller length
rm = $\rho(1 + H)/2$

$$er = \rho\left[\frac{(1+H)}{2} - \frac{(1-H)}{\ln(1/H)}\right]$$

Ih = effective housing moment of inertia about centroid - $in.^4$
Ah = effective housing cross section area - $in.^2$
Ik = effective cam moment of inertia about centroid - $in.^4$
Ak = effective cam cross section area - $in.^2$
n = number of rollers

The deflection of the roller is used only for hollow rollers. If the roller is solid, $\Delta roller = 0$. After the influence coefficients are found, the load and the deflection are found in the following manner.

Δhsg	= (CR)P	=	radial deflection of housing
Δcam	= (CK)P	=	radial deflection of cam
$\Delta roller$	= (Cρ)P	=	radial deflection of roller

From Equation 93

$$\frac{F}{P} = \tan\frac{\psi}{2} = \sqrt{\frac{1 - \cos\psi f}{1 + \cos\psi f}} \qquad (105)$$

Substituting for the cos ψf from Equation 98 and the expression for torque leads to

$$\frac{T}{n\,P\,R} = \sqrt{\frac{R - K - 2\rho + \Delta hsg + \Delta cam + 2\Delta roller}{R + K}} \qquad (106)$$

In Equation 106, the deflection terms in the denominator of the radical have been dropped because they are small compared to R + K; whereas in the numerator, the deflection terms cannot be neglected because R - K - 2ρ is almost equal to zero.

Equation 106 cannot be solved directly for P because the deflection terms also contain terms containing the load, P. A convenient way to solve the equation is by the Newton Rhapson iterative procedure:

$$f(P_i) = \frac{T^2(R+K)}{n^2 R^2} + P_i^2\,(-R+K+2\rho) - P_i^3\,(CR+CK+2C\rho) = 0 \qquad (107)$$

$$f'(P_i) = 2P_i\,(-R+K+2\rho) - 3P_i^2\,(CR+CK+2C\rho) \qquad (108)$$

$$P_{i+1} = P_i - \frac{f(P_i)}{f'(P_i)} \qquad (109)$$

For an initial guess, (i=1) P1 may be found from

$$P1 = \frac{T}{.05\,n\,R}$$

The procedure is then to start with i=1 and find P1 which is the initial guess for P_i. Substitute P1 for P_i in Equation 107 and 108 to obtain f(P1) and f'(P1), the function and derivative, and finally, P2 is found from equation 109 (P_{i+1}= P2). The value of i is then set equal to 2 and the procedure repeated until successive values of P fall within the desired accuracy. Usually, the above procedure conv rges very rapidly, and only two or three trials are required.

Once P is found, F is determined from Equation 95, and ψ is calculated from Equation 105. As a general rule, it is desirable to have the initial no-load nip angle, ψ_o, between 3^o and 5^o while the full-load nip angle, ψ_f, should be between 5^o and 6^o.

Housing Hoop Stress Analysis

The outer housing of the ramp roller clutch has normal and tangential loads induced by the rollers at "n" positions. In addition, a moment is produced that is the product of the tangential load and the distance to the effective housing area's center of gravity. Figure 48 depicts these loads.

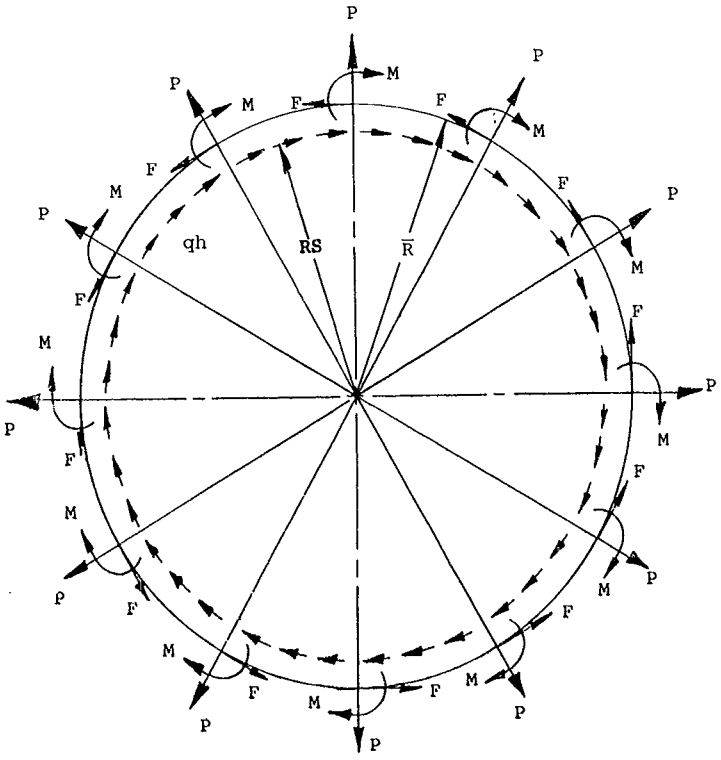

Figure 48. The Transfer of a Ramp Roller Clutch's Outer Housing Roller Loads to the Housing's Center of Gravity.

Torque on the outer housing is reacted by a shear flow and is assumed to be uniform. To determine stress, the internal housing loads are calculated. The directions and nomenclatures are shown in Figure 49.

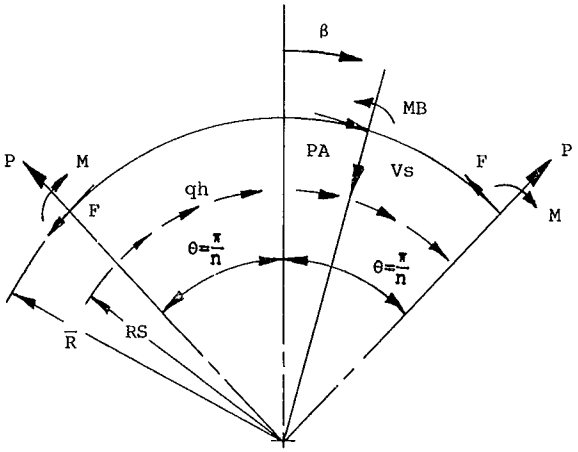

Figure 49. Ramp Roller Clutch Outer Housing Internal Loads.

The loads are calculated with the following equations:

$$MB = -\frac{P\bar{R}}{2}\left(\frac{1}{\theta} - \frac{\cos\beta}{\sin\theta}\right) - \frac{F\bar{R}}{2}\frac{\sin\beta}{\sin\theta} + \frac{T}{2\pi}\beta \qquad (111)$$

$$PA = +\frac{P}{2}\frac{\cos\beta}{\sin\theta} - \frac{F}{2}\frac{\sin\beta}{\sin\theta} \qquad (112)$$

$$Vs = -\frac{P}{2}\frac{\sin\beta}{\sin\theta} - \frac{F}{2}\frac{\cos\beta}{\sin\theta} + \frac{T}{2\pi RS} \qquad (113)$$

where

MB = internal bending moment - in. lb
PA = internal axial force - lb
Vs = internal shear force - lb

The internal loads must be evaluated for the range

$\beta = -\pi/n$ to $\beta = +\pi/n$

The stresses are then found from

$$f_b = \frac{MB}{Z} = \text{bending stress} \quad (114)$$

$$fa = \frac{PA}{Ah} = \text{axial tensile stress} \quad (115)$$

$$f_s = \frac{Vs}{Ah} = \text{shear stress} \quad (116)$$

$$Z = \frac{Ih}{y} \quad (117)$$

where

y = distance from c.g. to inner or outer fiber - in.

Ih = moment of inertia of cross section about c.g. - $in.^4$

For the housing, the sum of bending and tensile stresses should be kept below the material's endurance limit at the expected number of starts and stops in the life cycle. Again, the prime consideration is low cycle fatigue due to GAG cycles.

Cam Compressive Stress Analysis

Once the normal and tangential roller loads and the full-load nip angle have been calculated, the cam loads are found using Figure 50 and the following equations.

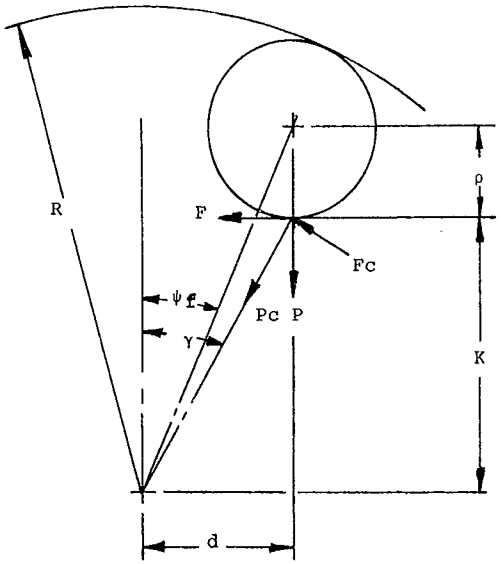

Figure 50. Ramp Roller Clutch Cam Loads.

From the figure

$$d = (R-\rho)\sin\psi f \tag{118}$$

$$\tan\gamma = \frac{d}{K} \tag{119}$$

$$Pc = P\cos\gamma + F\sin\gamma = \text{inward radial load} \tag{120}$$

$$Fc = P\sin\gamma - F\cos\gamma = \text{tangential load on cam} \tag{121}$$

$$Mc = Fc\left(\frac{K}{\cos\gamma} - \overline{K}\right) = \text{moment at cam c.g.} \tag{122}$$

After the cam loads are found, the cam is analyzed as a ring with "n" loads, as shown in Figure 51.

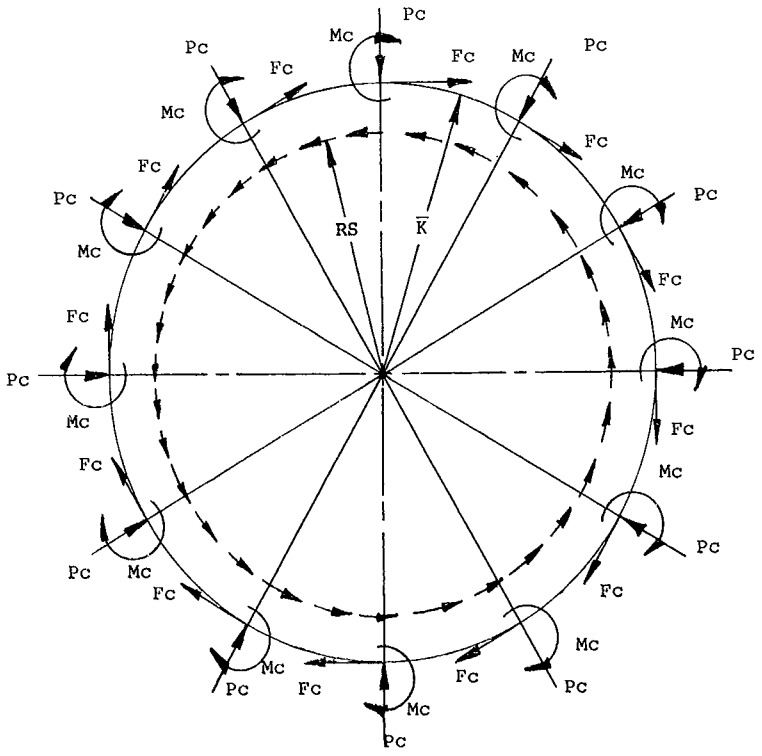

Figure 51. The Transfer of a Ramp Roller Clutch's Cam Roller Loads to Center of Gravity.

Torque on the cam is assumed to be reacted by a shear load acting at the shear radius, Rs. The shear radius is determined by examination of the cam's cross section. If the cam is splined to an inner shaft, the spline's pitch diameter can be assumed to be the shear diameter. Figure 52 depicts the internal loads on the cam.

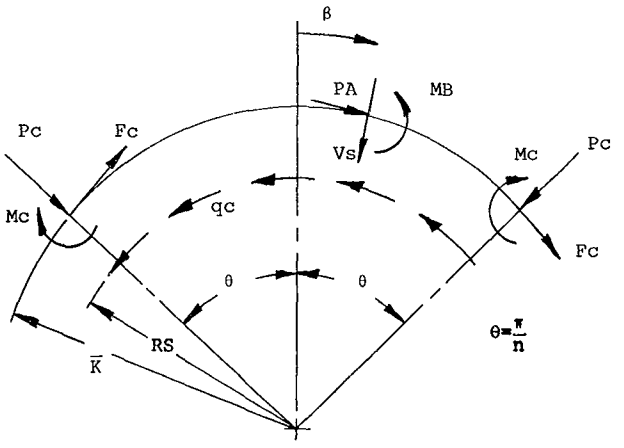

Figure 52. Ramp Roller Clutch Cam Internal Loads.

The following equations are used to calculate these forces and moments.

$$MB = + \frac{Pc\ \bar{K}}{2}\left(\frac{1}{\theta} - \frac{\cos\beta}{\sin\theta}\right) + \frac{Fc\ \bar{K}}{2}\frac{\sin\beta}{\sin\theta} - \frac{T\ \beta}{2\pi} \qquad (123)$$

$$PA = - \frac{Pc}{2}\frac{\cos\beta}{\sin\theta} + \frac{Fc}{2}\frac{\sin\beta}{\sin\theta} \qquad (124)$$

$$Vs = + \frac{Pc}{2}\frac{\sin\beta}{\sin\theta} + \frac{Fc}{2}\frac{\cos\beta}{\sin\theta} - \frac{T}{2\pi\ RS} \qquad (125)$$

where

MB = internal bending moment - in. lb
PA = internal axial force - lb
Vs = internal shear force - lb

The internal loads must be evaluated for the range $\beta = -\pi/n$ to $\beta = +\pi/n$. The stresses in the cam are then found from

$$f_b = \frac{MB}{Z} = \text{bending stress} \quad (126)$$

$$f_a = \frac{PA}{Ak} = \text{axial tensile stress} \quad (127)$$

$$f_s = \frac{Vs}{Ak} = \text{shear stress} \quad (128)$$

$$Z = \frac{IK}{y} \quad (129)$$

where

y = distance from c.g. to inner or outer fiber

The bending stress in the cam should be kept below the material endurance limit at the expected number of life-cycle starts since the critical consideration is low cycle fatigue due to GAG cycles.

Roller Stress Analysis

For a solid roller, hoop stress is not a design consideration. However, in a hollow roller, the prime design consideration is hoop stress, with allowable stresses being determined by low cycle fatigue (GAG) considerations. The point of maximum bending stress occurs under the load, P, at the inside periphery of the roller, as shown in Figure 53.

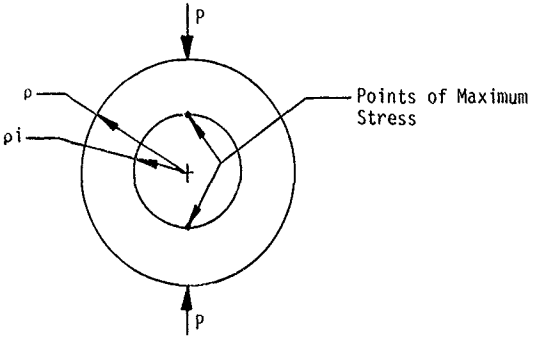

Figure 53. Hollow Roller Load and Stress Points.

There are several methods for determining hollow roller stresses analytically. A method, which was derived by photoelastic analysis, is presented in Reference 4. From this article, the stresses at various positions on the inside and outside of the hollow rollers are given by

$$f = K \frac{2P}{\pi L \rho} \tag{130}$$

where

P	=	normal roller load - lb
L	=	roller length - in.
ρ	=	roller outside radius - in.
K	=	factor dependent upon the position at which the stress is required and on the ratio of roller hollowness, H (ratio of inner to outer roller diameter)
f	=	annualar roller tangential stress - psi

A second method is presented in Reference 5 and is similar to the methods by (6) SKF, (7) Harris, and (8) Battelle shown below.

The Seeley and Smith method uses curved-beam theory. The results are in good agreement with the photoelastic analysis results except for rollers with small ratios of roller inside to outside diameters, H, (small hole in roller - approaches solid roller). The photoelastic method is more accurate for small values of H. The stress at a point on the inside of the roller and directly under the load is given by

---

4. Herger, O. J., FATIGUE TESTS OF SOME MANUFACTURED PARTS, Proceeding of the Society for Experimental Stress Analysis, Vol. III, No. II, 1946.
5. Seeley, Fred B., and Smith, James O., ADVANCED MECHANICS OF MATERIALS, Second Edition, New York, John Wiley and Sons, Inc., 1966, pp 177-182.
6. SKF Computer Program AE66Y004, ANALYSIS OF DYNAMIC PERFORMANCE CHARACTERISTICS OF CYLINDRICAL ROLLER BEARINGS UNDER RADIAL LOAD, King of Prussia, Pennsylvania SKF Industries, Inc.
7. Harris, T. A., and Aaronson, S. F., AN ANALYTICAL INVESTIGATION OF CYLINDRICAL ROLLER BEARINGS HAVING ANNULAR ROLLERS, ASLE Transactions 10, 1967.
8. Battelle Memorial Institute, ANALYSIS OF A ROLLER BEARING ASSEMBLY WITH HOLLOW ROLLERS, Columbus, Ohio, Battelle Memorial Institute.

$$f = \frac{P}{\pi \rho L}\left(\frac{1}{2 Z H} - \frac{1}{(1-H)}\right) \qquad (131)$$

where

H = inside diameter/outside diameter of roller

$$Z = -1 + \left\{\left(\frac{(1+H)}{2(1-H)}\right) \ln\left(\frac{1}{H}\right)\right\}$$

A comparison of the two methods is presented in Figure 54.

The hoop stress on the hollow roller should have a maximum value of 150,000 psi for the normal operating condition.

The equations for Hertz stress are derived from classical theory and are summarized in Reference 3. The Hertz stress is always higher between the cam and the roller than between the housing and the roller because the relative radius of curvature between the housing and the rollers permits a higher contact area than that permitted by the cam and roller radii. The Hertz stress is of course identical between two mating pieces because the band of contact and the load are the same on each part. For the ramp roller clutch, the Hertz stresses can be calculated as follows:

$$fcR\text{-}\rho = \sqrt{\frac{P E (R-\rho)}{2\pi L R \rho (1-\nu^2)}} \qquad (132)$$

$$fcK\text{-}\rho = \sqrt{\frac{P E}{2\pi L R \rho (1-\nu^2)}} \qquad (133)$$

where

$fcR\text{-}\rho$ = Hertz stress between housing and roller - psi

$fcK\text{-}\rho$ = Hertz stress between cam and roller - psi

ν = Poisson's ratio

dividing $fcR\text{-}\rho$ by $fcK\text{-}\rho$, one obtains

$$\frac{fc\ R\text{-}\rho}{fc\ K\text{-}\rho} = \sqrt{1 - \frac{\rho}{R}} \qquad (134)$$

It can be seen from the latter expression that the Hertz stress between the housing and roller is always less than the Hertz stress between cam and roller. The Hertz stresses between the rollers, the cam, and the housing should be limited to a maximum between 400,000 and 550,000 psi.

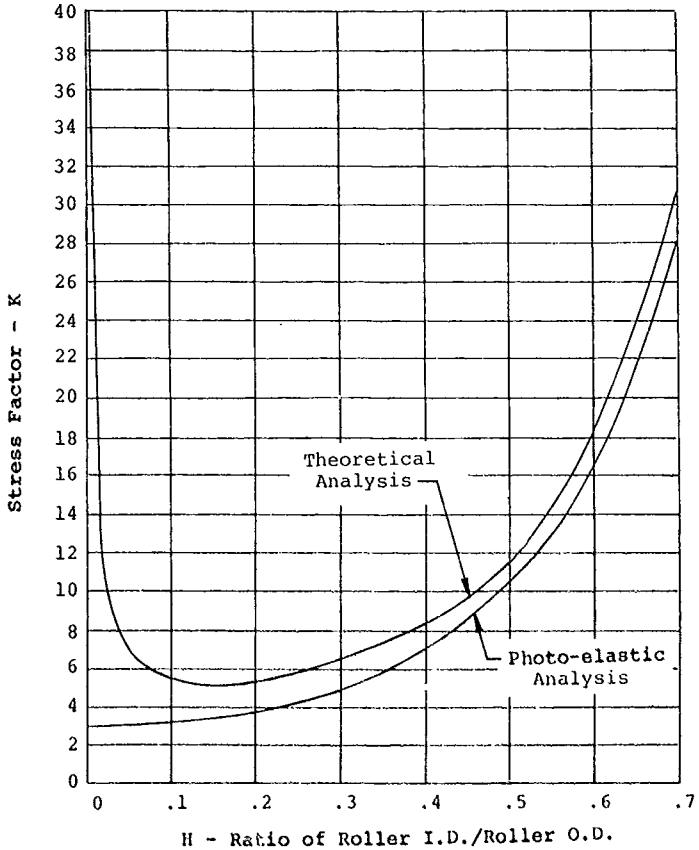

Figure 54. Stress Factors for Hollow Rollers.

Carrier Anti-Torque Requirement

As the ramp roller freewheel unit overruns, the rollers have two basic resistance forces acting on them, as depicted in Figure 55. Resistance torques are induced by rolling friction and also by viscous friction as the rollers roll through the layer of oil on the outer housing. The rolling resistance is a function of the roller's centrifugal force, which in turn increases with cam rpm; whereas viscous resistance is a function of cam and housing differential speed. Depending on which member drives and which member overruns, the maximum values of viscous and rolling drags can occur at either the same speed condition or different speed conditions. For example, if the cam is driving, rolling resistance is maximum at maximum cam rpm, while viscous friction is minimum. However, if the outer housing is driving, viscous friction and rolling resistance are maximum at full-speed overrunning, with the cam at full speed and the housing stopped.

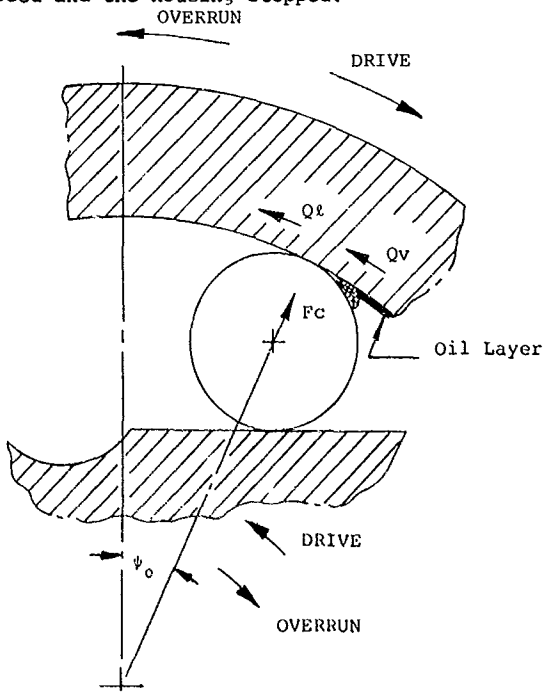

Figure 55. Roller Resistance Forces in the Ramp Roller Clutch.

The pin and spring assembly, which is discussed in the next section, induces a torque on the roller cage that overcomes the frictional drag created by the overrunning rollers. The minimum pin and spring force must exceed the viscous friction and rolling drag under all conditions of operation to reduce wear and permit smooth clutch engagements.

The total drag torque on the roller retention cage is

$$Q = Q1 + Qv \tag{135}$$

where

Q	=	total drag torque on cage - in. lb
$Q1$	=	drag torque from rolling resistance caused by roller centrifugal force - in. lb
Qv	=	drag torque from viscous friction - in. lb

The viscous and rolling drag are best estimated by empirically evaluated methods (Reference 9) used for bearings. Rolling drag, Q1, can be estimated from

$$Q1 = \mu_1 \, Fc \, R \, n \tag{136}$$

in which μ_1 is a factor that depends on bearing design and relative bearing load. For cylindrical roller bearings, Harris lists μ_1 as .00025 to .0003, which is the range of values best suited to the ramp roller overrunning clutch.

In Equation 136

Fc = roller centrifugal force - lb

$$Fc = M \left(\frac{d_m}{2}\right) \omega^2 \tag{137}$$

$$Fc = \rho_r \frac{\pi}{4} \frac{(d_o^2 - d_i^2)}{g} L \left(\frac{d_m}{2}\right) \left(\frac{\pi}{30} rpm_{cam}\right)^2 \tag{138}$$

where

ρ_r	=	roller material density - lb/in.^{3}
d_o	=	outside diameter of roller = 2ρ - in.
d_i	=	inside diameter of roller - in.
L	=	roller length - in.
d_m	=	clutch mean diameter = $2(R-\rho)$ - in.

---

9. Harris, T. A., ROLLING BEARING ANALYSIS, John Wiley & Sons, Inc., New York, 1966.

The viscous drag can be estimated from

$$Qv = 1.42 \times 10^{-5} \; fo \; dm^3 \left[vo \; \Delta rpm \right]^{2/3} \qquad (139)$$

where

vo = oil viscosity in centistokes
Δrpm = absolute value of differential speed between cam and housing = $|rpm\ cam - rpm\ hsg|$
fo = factor depending upon type of bearing and method of lubrication

Harris lists fo for cylindrical roller bearings as follows

fo = 1 to 1.5 for mist lubrication
= 2 to 3 for oil bath
= 4 to 6 for vertical mounting flooded oil lubrication or jet lubrication

Since the ramp roller clutch's rolling area on the outer housing is usually flooded, a value of fo = 5 can be used.

From Equations 135, 136 and 139, the cage drag can be estimated, and the requirement for pin and spring load can be established with a suitable load factor, such as 1.5.

Pin and Spring Analysis

The ramp roller pin and spring assembly is used to impart a torque on the roller retention cage in a direction that will keep the rollers in contact with the outer housing and the cam. When the rollers are in intimate contact with the cam and the outer housing, the ramp roller clutch is in position to engage. In addition, wear on the contacting surfaces is reduced because sliding is reduced (the rollers will theoretically roll on the outer housing).

Generally, two pin and spring assemblies located 180° apart are used for balance at high speed and also for a more uniform application of torque to the cage. Centrifugal effects on the pin and spring must be considered even at low speeds because improper design can cause the cage to become unloaded during differential overrunning, which can lead to shock engagement of the clutch. The pin is generally made with a central hole. This reduces pin weight and moves the center of gravity in a direction that reduces frictional effects.

The cage torque created by the pin and spring loads is dependent on friction between the pin, the spring, and the housing. During the design stage, it is useful to examine the resultant cage torque as a function of the expected range of the coefficient of friction. It is desirable to have a constant or a slightly increasing value of cage torque with speed. This will aid in keeping the rollers in intimate contact.

Figure 56 is a cross section of the pin and spring assembly showing the nomenclature used in the analysis.

Prior to starting the analysis, the geometry of the assembly must be known. A magnified layout such as 4x or 5x is recommended. As the analysis progresses, the geometry can be varied to obtain the desired results. The following geometric parameters are required

T = distance from bottom of spring to centerline - in.
S = distance from end of pin to centerline - in.

Note: End of pin is just touching cage stop when rollers are in the no-load position. It is desirable to examine the analysis from minimum S to maximum S. Maximum S can be assumed from a maximum allowable wear condition, such as rollers .010 undersize.

L = overall length of pin - in.
ℓ = depth of central hole in pin - in
D = outside diameter of pin - in.
d = inside diameter of pin - in.
Rp = distance from center of rotation to centerline of pin and spring - in.

In addition to the above geometry, the following spring data is required

f_s = free length of spring - in.
Ks = spring rate - lb/in.
hs = solid spring height - in.

Note: The spring must not bottom when the pin is pushed all the way into the spring and pin housing. In this position the rollers will be in the center of the cam undercut area.

d_o = spring outside diameter - in.
dw = spring wire diameter - in.
ρs = spring wire density = .283 lb/in.^{3} (for steel)

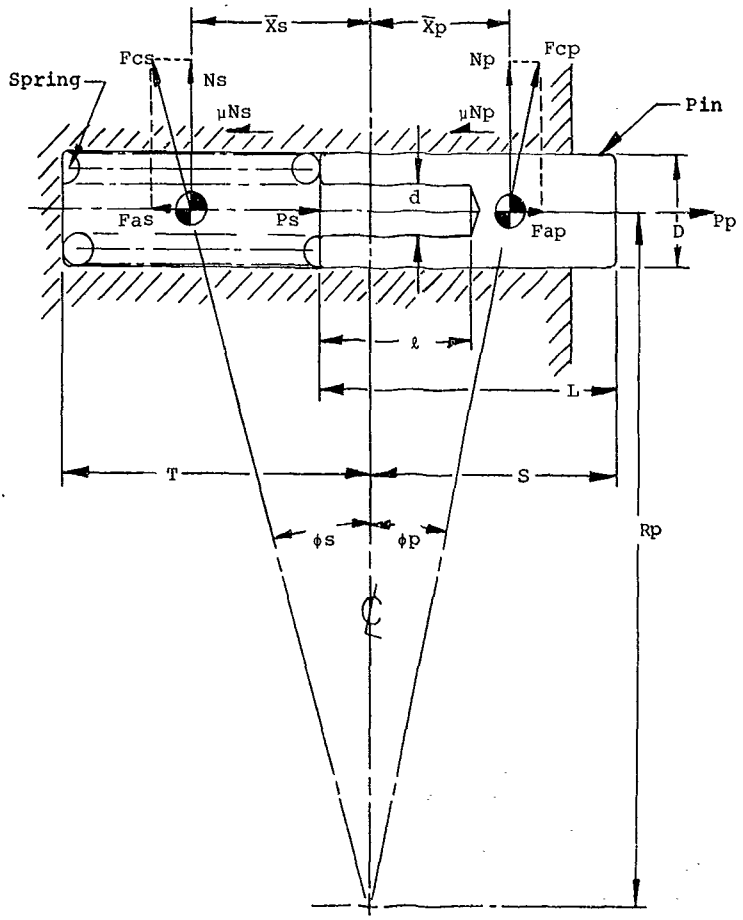

Figure 56. Roller Retainer Return Pin and Spring Assembly Geometry and Dynamic Forces.

The weight of the spring can be estimated from

$$Ws = \rho s \frac{\pi^2}{4} (d_o - dw)\, dw\, hs \tag{140}$$

The distance from the cam flat's centerline to the spring's center of gravity, in inches, can be found from

$$\overline{Xs} = \frac{T-S+L}{2} \tag{141}$$

The centrifugal force acting on the spring is given as

$$Fcs = \frac{\pi^2 Ws\ rpm^2}{900\ g} \sqrt{Rp^2 + \overline{Xs}^2} \tag{142}$$

where

g = gravitational constant = 386 in./sec^2
rpm = cam revolutions per minute
Fcs = centrifugal force on spring - lb

The normal spring force on the housing, in pounds, is found from

$$Ns = Fcs \frac{Rp}{\sqrt{Rp^2 + \overline{Xs}^2}} \tag{143}$$

The axial spring force, in pounds, is found from

$$Fas = Ns \frac{\overline{Xs}}{Rp} \tag{144}$$

The spring force, in pounds, at the installed position is given by

$$Fs = Ks\ (fs-T-S+L) \tag{145}$$

The resultant spring force, in pounds, acting on the pin in the axial direction is

$$Ps = Fs - (Fas + \mu\, Ns) \tag{146}$$

In this equation, Fas and Ns are dependent on cam rpm. At high cam speeds, it is possible that Ps in the above equation can be negative; that is, the spring will not act on the pin but will actually be forced to the bottom of the spring hole. This condition occurs when the axial component of centrifugal force exceeds the internal spring load. The speed at which this will occur is given by:

$$rpm_x = \frac{30}{\pi} \sqrt{\frac{g\ Fs}{Ws(\bar{X}_s + \mu\ Rp)}} \qquad (147)$$

where

rpm_x = rpm at which spring will be inoperative

The weight of the pin is found from

$$Wp = \rho p\ \frac{\pi}{4}\ (D^2 L - d^2 \ell) \qquad (148)$$

where

ρp = pin material density = .283 lb/in.^{3} (for steel pin)
Wp = weight of pin - lb

The distance from cam flat to the pin's center of gravity, in inches, is found from

$$\bar{X}p = \frac{D\ L^2 - d\ \ell^2}{2\ (D\ L - d\ \ell)} + S - L \qquad (149)$$

The centrifugal force exerted by the pin in the radial direction is

$$Fcp = \frac{\pi^2\ Wp\ rpm^2}{900\ g} \sqrt{Rp^2 + \bar{X}p^2} \qquad (150)$$

The normal load of the pin acting on the housing is

$$Np = Fcp \frac{Rp}{\sqrt{Rp^2 + \bar{X}p^2}} \qquad (151)$$

The axial pin force is found from

$$Fap = Np\ \frac{Xp}{Rp} \qquad (152)$$

The total load that the pin exerts on the roller carrier is the sum of the total spring load and the total pin load:

$$Pp = Ps + Fap - \mu Np \qquad (153)$$

It is this pin load, Pp, that should be designed for the drag load calculated in the previous section (Equation 135) with a factor of 1.5.

The carrier torque is the product of pin load and lever arm.

$$Tc = n\ Pp\ Rp = n\ Rp\ (Ps + Fap - \mu Np) \qquad (154)$$

where

n = number of pin and spring assemblies (usually 2)
Tc = torque on carrier - in. lb

Geometric Considerations

At the beginning of the detail design stage, it is recommended that an enlarged layout be made of a cross section through the cam, cage, rollers, and housing. This layout will be used to design several important features of the ramp roller clutch.

First, the enlarged layout is used to establish the cam's cross section. The cam is designed as a basic equillateral polygon having "n" sides. With this type of design, cam grinding is done perpendicular to the cam axis, which is the preferred orientation for rolling surfaces (grinding marks should align with rolling direction).

The undercut is established next. The undercut is used only for purposes of assembly. When the cage is all the way back, hitting its backstop, the roller centerline should be in the center of the cam undercut pocket. Figure 57 shows a typical example.

The dimension "X" is some small positive amount, such as .010 to .030, included so that there will not be a sharp edge. The dimension "y" is meant to keep the roller pocket from interferring with the rollers during overrunning. Usually "y" can be zero or very near the cam flat centerline. The radius, r, the locating dimension A, and the depth dimension B, are established by trial layout. The radius, r, should be slightly larger than the roller radius so as to allow the roller to rest in the bottom of the pocket during installation.

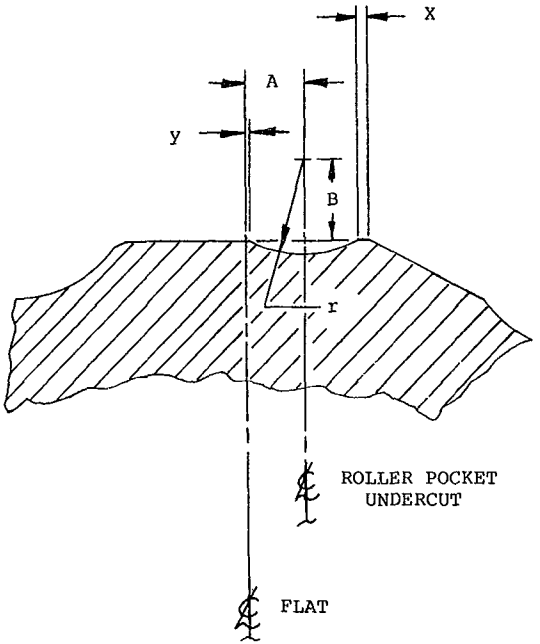

Figure 57. Ramp Roller Clutch Cam, Roller Pocket Undercut Geometry.

Once the cam cross section is established, rollers are layed out in various key roller positions, such as the minimum no-load initial position, the maximum no-load initial position, the average full-load position, and the maximum wear position. The no-load initial angular positions are calculated from

$$\cos \psi_{omin} = \frac{K_{max} + \rho_{max}}{R_{min} - \rho_{max}} \qquad (155)$$

$$\cos \psi_{omax} = \frac{K_{min} + \rho_{min}}{R_{max} - \rho_{min}} \qquad (156)$$

The maximum and minimum values are established from the tolerances to be used on the detail drawings. Typical grinding tolerances are used. The average full-load position is calculated using average dimensions and the method outlined in previous sections.

The maximum wear position is the no-load angle assumed when the rollers, the cam, and the housing have worn to the point where any further wear would cause roller "spit out" under load because the nip angle would be too large. A value of from 10 to 12 degrees may be assumed. If it is also assumed that the cam wear and housing wear are equal and are equal to one-half of the roller wear. The allowable wear can be calculated from

$$\cos \psi_{o\,max\ wear} = \frac{K_{min} - \Delta/2 + \rho_{min} - \Delta}{R_{max} + \Delta/2 - \rho_{min} + \Delta} \qquad (157)$$

from which

$$\Delta = \frac{2}{3} \frac{K_{min} + \rho_{min} - (R_{max} - \rho_{min})(\cos\psi_{o\,max\ wear})}{1 + \cos\psi_{o\,max\ wear}} \qquad (158)$$

where

Δ = maximum allowable roller radial wear - in.
$\cos\psi_{o\ max\ wear}$ = cosine for between 10 and 12° (assumed maximum wear nip angle)

For example, assuming a 10° maximum wear angle for the high-speed Eustis clutch, Δ is calculated to be .0057. Thus, the rollers can wear .011 inch (on diameter), the cam can wear .0028 inch and the housing can wear .0028 inch, which will result in a 10° no-load nip angle. The clutch will still be operable in this position but will be in danger of "spitting out" if further wear occurs.

Once the various roller angles are established, the cage's outside and inside diameters at the roller contact points can be found. The roller pockets in the cage are manufactured so that the front and back edges of the pockets are parallel to each other and are parallel to the roller pocket centerline. During all operating positions, the contacting point between the roller and the pocket of the roller retention cage should be in the flat area of the pocket face. This is illustrated in Figure 58.

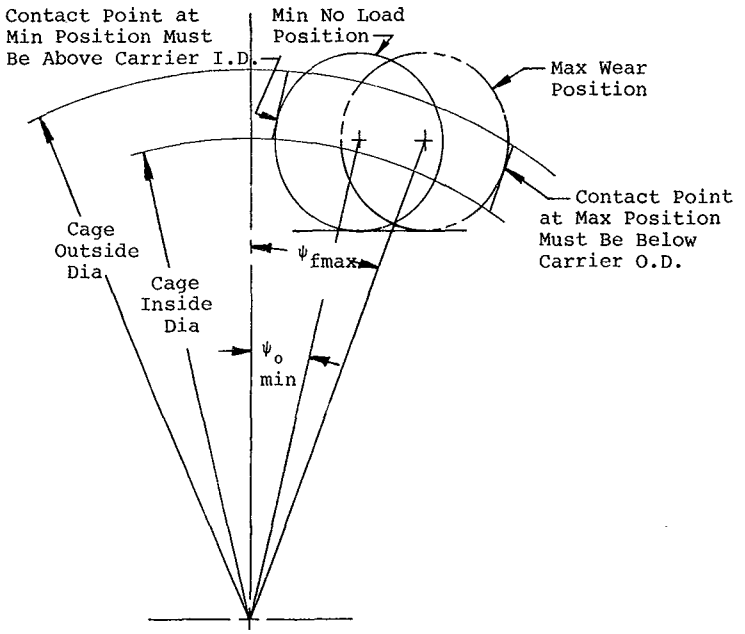

Figure 58. Carrier/Roller Contact Point Limits.

The next item to be established from the enlarged-scale layout is the pin and spring assembly design. The dimensions locating the pin and spring assembly to the cam flats and the dimensions locating the face of the stop to a roller pocket on the cage must be established from the layout.

The designer must work in conjunction with the analyst to determine the proper dimensions for the pin and the spring, which include centrifugal effects (the analysis is presented in a previous section of the design guide). The dimensions for the analysis are obtained from the layout. The end of the pin will contact the lug on the carrier at various angles, depending on the value of the nip angle. The cage lug will be flush with the pin if the angle is correct.

The angle at which the pin is flush with the cage lug should be the full-load nip angle. This is done for several reasons. First, during normal driving at full load, the pin is inoperative. However, if there are any vibrations present in the ramp roller assembly, the pin will tend to fret on the contacting face between the lug and pin. It is, therefore, desirable to have as much contacting surface as possible during this mode of operation. The second reason for choosing the full-load nip angle position for full-pin contact is that a new clutch will have a larger contact angle under load than during overrunning. However, as the new clutch "wears in", the contact angle can only increase and never decrease. Hence, by starting at a slightly larger angle than that required for overrunning, the clutch will eventually wear in to a flush pin attitude during the normal course of operation. Since the angles involved are very small, exact pin angular orientation is not critical.

Another item to check during this stage of the design is the insertion of the pin into the cam. At the maximum wear condition, no more than one-half of the pin should protrude beyond the support hole in the cam. Excessive protrusion will create overhanging moments that will tend to cock the pin in its hole and prevent proper operation.

At this stage of the design, the cage backstop is also designed. The backstop on the cage should hit the cam backstop flush when the roller's centerline is coincident with the centerline of the cam undercut radius. The backstop can be located at approximately 90° from the pin to cam interface or can be the pin to cam interface itself. Both methods have been used successfully. When the cage is against the backstop, the pin is pushed into its guide hole to the maximum position. In this position, the spring must not have reached its solid height.

All of the above geometric properties of the ramp roller clutch must be considered for the design to be successful.

Outer Housing Design

The outer housing of the ramp roller clutch is designed to withstand the hoop stresses created by the roller loads normal to the outer housing's inner bore. During overrunning, the rollers will roll on the outer housing and, if the cam is rotating, will also induce a centrifugal field that will act on the outer housing. Since the Hertz stresses will be high when the clutch is driving, a very hard surface with the high hardness extending well into the material is recommended for the outer housing.

Generally SAE 9310 case-carburizing steel is used. The surface is hardened to Rc 60-64, with an effective case depth of .060 to .100 inch, which is a very deep case for carburizing. It is usually not necessary to use vacuum melt material, such as AMS 6265, because there is no high cyclic fatigue loading on the outer housing; hence, AMS 6260, air melt steel, may be used. Other types of case-carburizing steel would probably work as well.

The surface finish on the roller contacting area is generally held to RMS 32 or better. The tolerance on the bore is generally $\pm$.0005 inch, which is an easily held tolerance for production grinding.

A lubrication dam is usually provided on the outer housing to assure good lubrication between the rollers and the housing. The height of the dam controls the level of oil in the outer housing's inside bore. Even at relatively low speeds, such as 6000 rpm, with a horizontally-mounted unit, the outer housing oil dam will provide a level of oil that is essentially parallel to the rotation axis due to the centrifugal force acting on the oil. The rollers must plow through this oil as they overrun, and hence, too high a level is undesirable. On the other hand, too low of a dam will not provide sufficient lubrication. A plot of outer-housing speed versus oil dam height (radial oil level) is presented in Figure 59. This curve is based on previous experience with ramp roller clutches and is recommended for design.

One end of the outer housing will be required to transmit torque from the roller, either from the input or to the output member. The design of the torsional connection, whether it be by bolted flange, spline, keyway, or other method, must follow conventional transmission design practice. The outer housing itself is usually "open ended"; i.e., one end is usually terminated at the oil dam, while the other end of the outer housing is connected to the torsional drive path. This configuration lends itself to unequal deflection along the length of the roller, commonly termed "bellmouthing." To minimize the effects of bellmouthing and to maintain a uniform radial deflection along the length of the roller, the cross section of the outer housing is usually made variable. The variable cross section will somewhat compensate for unequal radial deflection. Figure 60 illustrates the design principle.

An exact solution to the housing deflection is a difficult analytical procedure. Finite-element analysis may be used. However, the expense is not warranted as the amount of bellmouthing is generally very small and a design like that shown in Figure 60 will reduce the differential radial expansion to a negligible amount.

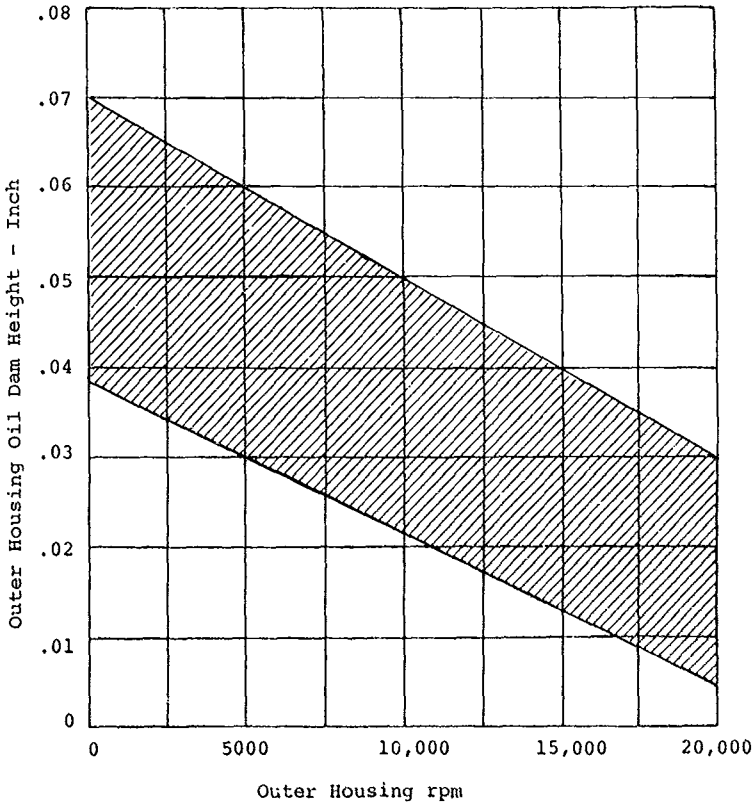

Figure 59. Ramp Roller Clutch Outer Housing Oil Dam Radial Height.

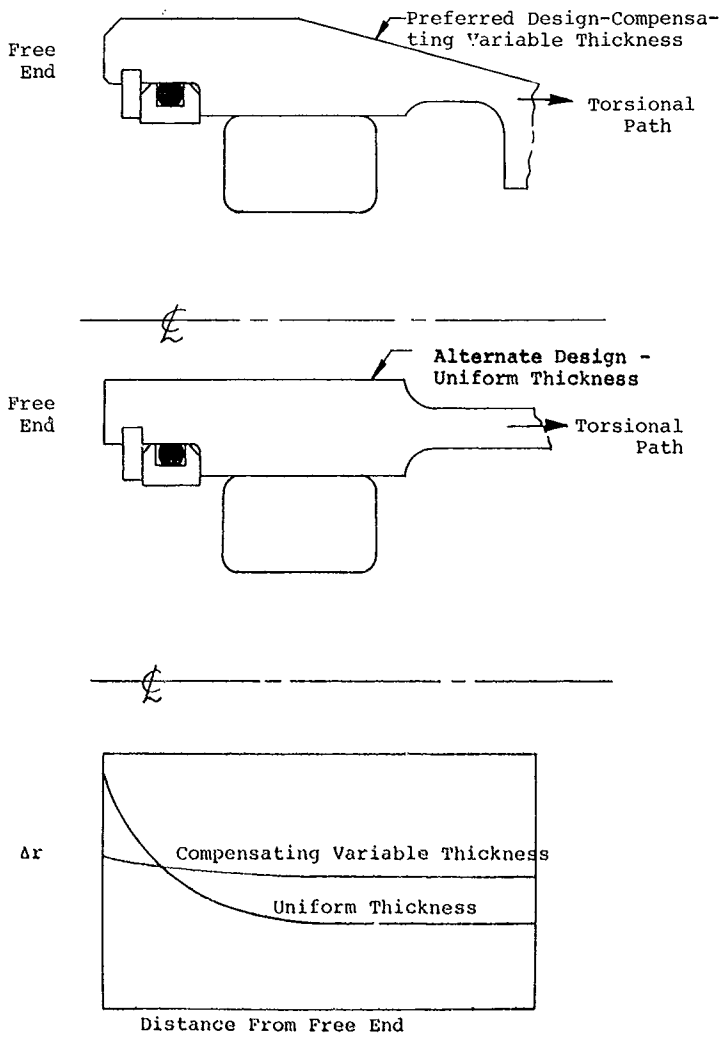

Figure 60. Compensation for Outer Housing Bellmouthing.

Cam Design

The function of the cam is very similar to the function of the housing: the cam must react the normal roller loads as a ring with "n" equally spaced loads. The cam is basically in compression while the outer housing is basically in tension.

Whereas in the outer housing the rollers are (in theory) in pure rolling, on the cam the rollers are in pure sliding, which is a more severe environment for wear. The Hertz stresses are also higher between the cam and the rollers than they are between the outer housing and the rollers. If a hard surface is required for the outer housing, the requirement is even more stringent on the cam. Thus, SAE 9310 or other equivalent case-carburizing steel is used for the cam. The surface is hardened to Rc 60-64 with an effective case depth of .060 to .100 inch. Because the cam does not feel high cyclic vibratory stresses, the material does not necessarily have to be AMS 6265, vacuum-melt steel, and hence AMS 6260, air-melt steel will suffice. Other types of carburizing steel will work as well. Through-hardening steels are not recommended because they obtain the high surface hardnesses of the case-carburizing steels. Nitriding steel is also not recommended because the surface stresses (Hertz stresses) of the ramp roller clutch are generally too high for nitriding steels, and brinelling may result with their use.

The surface finish on the cam is generally held to RMS 32 or better. The tolerance on the cam flat is generally held to +.0000/-.0005, with a total tolerance of .001 across two diametrically-opposed flats. In addition to the tolerance on the "K" dimension, the flatness, angularity, and true position of each flat relative to the other flats must be closely controlled to achieve good load sharing between the rollers.

The inside cavity of the cam is often used to supply lubricant to the roller area of the freewheel unit. If the cam is normally rotating (cam output), the lubricant can be centrifugally fed. It is standard practice to provide a minimum of one lubrication hole to each roller. If the speed is high (over 10,000 rpm), metering the lubricant may become a problem because it will exit from the metering holes as fast as it is being fed in, and thus, a lubricant head cannot be maintained. Under these conditions, it is easy to starve a particular area of oil because the tolerances on the hole location, etc.; i.e., lubrication design is more critical at high speed.

A recent development is the pressure-fed cam, which is used when the cam is the input member. When the freewheel unit is overrunning at full speed, the cam is fixed and no lubrication will be available from centrifugal force. In this case, lubrication can be fed to all the rollers if the center chamber of the cam is enclosed and fed lubricant under pressure. The pressure-fed cam should be used for high-speed freewheel units when gravity feed will not provide sufficient oil for the speeds involved (approximately 4000 rpm or higher).

Lubrication is also provided to the pin and spring assembly from the inside of the cam. The end of the lug on the cam must have a drain hole to relieve pressure.

Lugs are provided on the cam with reamed holes for the pin and spring assembly and a cantilevered extension that acts as the cage backstop. The location of the holes and the faces of the lugs must be closely controlled from the surface of a cam flat so that the pin and spring assembly will align in its proper position.

Care must be taken during the layout stage to provide for the ease of assembly of the clutch. A simple tool to hold the cage against the backstop may be required.

Roller Design

The design of the rollers of the ramp roller clutch follows practices established for rollers used in cylindrical roller bearings. The major difference between rollers of the ramp roller clutch and the rollers of the cylindrical-roller bearing is that the rollers of the clutch are stationary with respect to the cam and the housing when the clutch is driving while the rollers of the roller bearing are rolling under load. The stress environment is therefore less severe in the clutch rollers since high cycle fatigue loads are not induced. Thus, roller Hertz stresses can be much higher in a clutch roller than in a bearing roller. Along with the higher stress levels is the requirement for crowning in clutch rollers. Crowning reduces the peak stresses at the ends of the rollers, which would occur if the rollers were perfectly cylindrical. True circular crowns are difficult to manufacture with accuracy for the standard machine shop. However, companies that manufacture roller bearings are fully equipped for grinding roller crowns.

The crown drop is established by calculating the roller deflection under maximum load. When the roller is under load and in contact with the cam, the roller and the cam will deform, forming a mutual area of contact. Crowning the roller changes the area of contact under load. A good theoretical design goal is to aim for a perfectly rectangular area of

contact that has the property of uniform load. In practice, the eliptical contact area of the clutch rollers is used instead of the rectangular area.

The necessary crown drop of a freewheel unit roller is dependent on the roller radial load and the geometry of the roller to race contact. The contact stress and therefore the deflection is always higher on the cam to roller contact, and therefore, the housing to roller contact will not be considered in this guide. The roller to cam contact is shown in Figure 61.

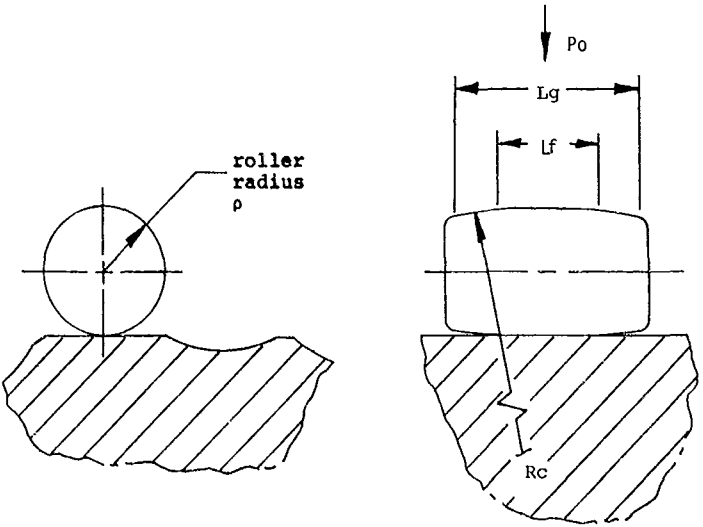

Figure 61. Basic Roller to Cam Contact.

In Figure 61, ρ is the roller radius, Po is the roller load, Lg is the roller gauge length, and Rc is the crown radius of the roller. The radius of the cam is infinite since it is a flat surface at the contact. A parameter, $\bar{A}$, is first computed by

$$\bar{A} = 2.025 \times 10^6 \frac{Lg^3}{Po\ \rho} \qquad (159)$$

With this parameter, the crown radius (Rc) is calculated by

$$Rc = \frac{2\rho\ \bar{A}}{2.77 + \ln \bar{A}} \qquad (160)$$

The crown length, Lc, is next expressed in the smaller of Equations 161 and 162.

$$Lc = .22\ Lg \pm .03\ Lg \tag{161}$$

$$Lc = 1.5\ \rho \pm .03\ Lg \tag{162}$$

where the tolerance on the crown length, $\pm .03$ Lg inch, is not greater than $\pm .030$ inch.

The flat length, Lf, is

$$Lf = Lg - 2\ Lc \tag{163}$$

To determine the crown drop per side, Δ, an approximation that is accurate to within .0001 is used

$$\Delta = \frac{1}{8\ Rc}\left[Lg^2 - Lf^2\right] \tag{164}$$

It is standard practice to specify that the gauge point, G, is .005 to .010 inch greater than the roller end radius, as shown in Figure 62.

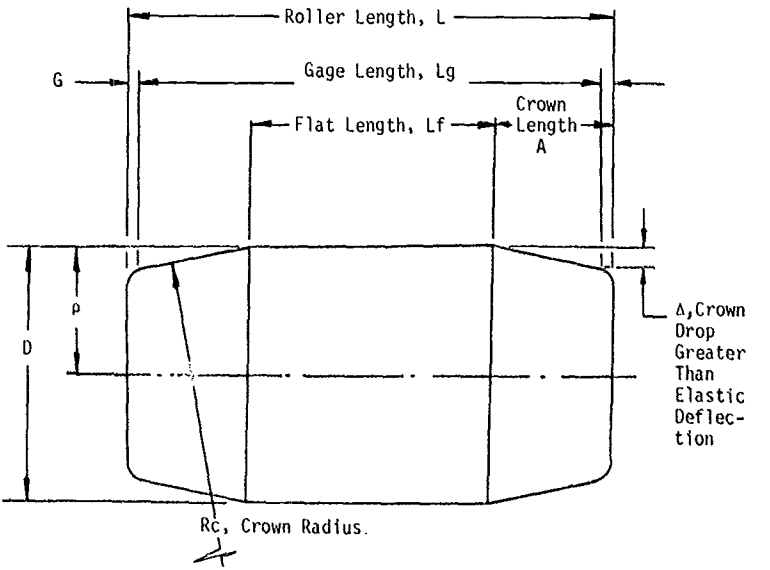

Figure 62. Roller Geometric Definitions.

Roller materials vary depending on the application. For solid rollers, through-hardened, AISI 52100 steel is often used. Since there is no high-cycle fatigue, to minimize costs, vacuum-degassed material is used rather than consumable-electrode vacuum-melt material. Hollow freewheel unit rollers are generally case carburized. AISI 9310, 8620, or other equivalent steels can be used. In hollow rollers, low cycle fatigue (GAG) stresses may control the design.

Generally, a surface finish of between 4 and 8 microinches is used on the rolling surfaces of the roller. The end faces are usually held to between 10 and 32 microinches. For the hole of hollow rollers, it is important to have a good surface finish. However, past experience has shown that this is difficult to achieve with current manufacturing methods. A surface finish of 125 microinches maximum has been used in previous designs.

Roller tolerances follow the standard practice of roller bearing manufacturers. The outside diameter is held to $\pm$.0001, while the length is generally held to $\pm$.0025 inch.

Carrier Design

The function of the roller retention carrier or "cage", as it is often called, is to position the rollers such that all rollers will touch both the cam and the outer housing simultaneously. A small torque is imparted to the cage by means of the pin and spring mechanism, which forces a minimum of one roller to touch the cam and outer housing. Because of tolerances, not all the rollers will be touching. However, the clearances of the remaining rollers will be very small. Under load, deflections of the members will force all the rollers into intimate contact. After a period of overrunning, the rollers, the cage, and the cam flats will wear to the point where all rollers will be touching at exactly the same points.

An even number of rollers is generally used so that the roller slots on the cage may be broached or shaped; the broach can pass through the cage, entering one slot and exiting at the slot 180° away.

The major mechanical distresses experienced by the cage are wear on the edges of the roller slots, wear on the support bushing surfaces, and wear where the pin hits the cage stop. To minimize the wear, a hard surface is required on the cage. Generally, case-carburizing steels are used with very shallow case depths to minimize distortion during the carburizing heat treatment.

SAE 9310 case-carburizing steel or an equivalent is recommended. The surface is hardened to Rc 58-64 with an effective case

depth of .010 to .020 inch all over. By case carburizing the cage all over, the need for masking in heat treat is eliminated.

The cage must be restrained from axial motion but must be unrestrained torsionally. This is easily accomplished by mechanical stops and bushings.

The cage must be supported by the cam. Usually an intermediate member, such as a bronze bushing, is used between the cage and the cam. This permits smooth rotation of the cage about the cam centerline, minimizes fretting, and also provides an inexpensive wear member that can be replaced during overhaul if required.

The bushings can be designed to provide a cantilever or a straddle-mounted arrangement with the rollers. Straddle mounting is recommended, but cantilever mounting has been successfully used in previous production designs. Straddle mounting has the advantage of being a more rigid support and, in addition, forms a trapped annulus that forces lubricant to flow through the clearances between the roller and cage pockets, which is precisely where the lubricant is required. In the cantilever-mounted cage, lubricant can escape from the end opposite the support end, and the lubrication is not as effective as it is in the straddle-mounted cage.

One end of the cage must also have a lug that has a surface designed to be perpendicular to the pin during operation. This surface acts as a stop for the pin and spring assembly and permits the pin to impart a tangential load onto the cage. A separate lug is used as a backstop; i.e., a stop in the direction opposite to the pin-load's normal direction. This stop is normally inoperative and only comes into play during assembly. When the cage is rotated so that the backstop on the cage rests against the backstop on the cam, the rollers should be aligned in the center of the "pocket" undercuts of the cams. The backstop lug and the pin lug can be combined into one lug. Usually two pins are used to provide the cage with an even distribution of load. For high-speed units, care must be taken that the lugs do not induce a centrifugal load of sufficient magnitude to create excessive deflections of the cage. Generally, excessive deflection created by centrifugal forces acting on the cage stops can be prevented by designing the cage with four equally spaced lugs, even though only two may be used.

The design of the roller slot involves having the proper clearance to allow roller advance and retard due to combined load or misalignment. Circumferential and diametral roller clearances are more critical than axial clearance. Testing may be required to select optimum clearances, but the values shown in Table 10 have been used successfully and may be used as guidelines.

TABLE 10. ROLLER POCKET DIMENSIONS.	
Item	Dimension (in.)
Cage pocket clearance on diameter	.005 (min)
Cage pocket width tolerance	+.005/-.000
Cage pocket clearance on length	.005 (min)
Cage pocket length tolerance	+.005/-.000

The pocket corners require reliefs to avoid sharp corners and to facilitate manufacturing. Two designs are shown in Figure 63. Design A is recommended when hollow rollers are used because it has the greatest coincident contact area on the end faces of the pockets. Design B has been used successfully with solid rollers, but with hollow rollers and high-speed applications, pocket end face wear has been a problem.

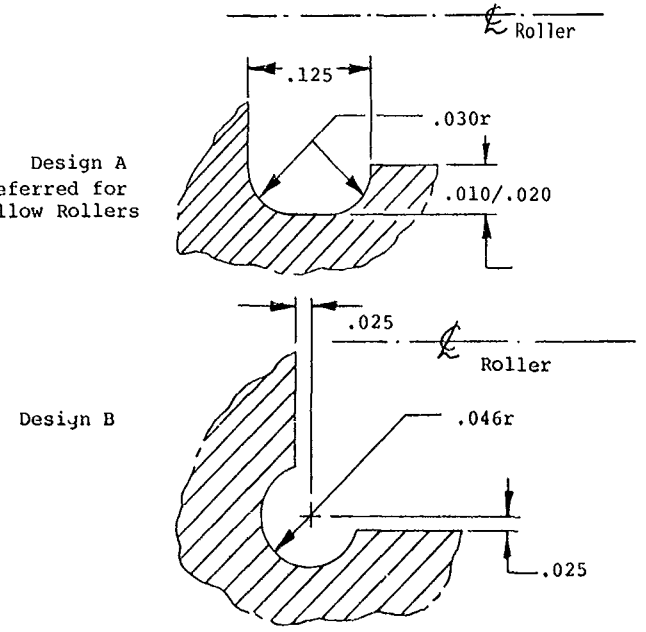

Figure 63. Roller Pocket Corner Relief Design.

Pin Design

The pin, or "plunger", of the ramp roller clutch transfers axial load from the spring to the roller carrier. The load on the roller carrier has a tangential component that produces a torque on the cage. This torque forces the rollers into contact with the cam and the housing. The pin must slide smoothly in the pin and spring hole.

The material is generally AISI 52100 through-hardened steel. The pin outside diameter is ground to produce a surface finish of 32 microinches. The tolerance on the outside diameter is $\pm$.00025, which is the same tolerance as that used for the pin and spring hole. The minimum clearance is usually .0005 inch on a diameter between the pin and the hole.

The pin is usually hollow to control the magnitude and direction of the centrifugal forces produced (see the Pin and Spring Analysis section). This is very important in high-speed ramp roller clutches and must always be considered to assure that the roller cage will always have a torque produced on it. The hole serves the purpose of moving the pin's center of gravity into a more desirable position while reducing pin weight.

Calculation of Flow Requirements

The lubricant that is fed to the freewheel unit serves to cool contacting surfaces and to lubricate the components. The critical period for the lubrication of the overrunning clutch is during the time it is overrunning. In the drive mode, the members are locked together and lubrication is not critical. The amount of oil required for lubrication is very small compared to the quantity required for cooling; thus, the cooling requirement generally dictates the design flow. Lubricant is required in the freewheel unit for support bearings, for inner-to-outer-shaft bearings, and for surfaces of the freewheel unit that rub during overrunning. Theoretical analysis of the oil flow rates required are difficult and not very accurate; thus, empirical relationships are generally used. Whenever possible, the oil flow rate to the freewheel unit should be determined by test. One method that has proven successful in the past is to conduct a test to determine the overrunning clutch's drag torque and temperature as functions of flow rate at full-speed overrunning. Full-speed overrun is generally the critical condition for lubrication. In general, the drag will decrease with decreasing flow, while the oil-out temperature will increase with decreasing flow. An operating flow rate should be chosen that produces a minimum drag torque with a corresponding oil temperature rise of from 20°F to 40°F. The oil temperature rise may be the best indication of proper oil flow. If the oil temperature rise is less than approximately 20°F, it indicates that the flow is too high: the oil does not get a chance to transfer heat from the parts to the oil. If the temperature rise exceeds approximately 40°F, it indicates that the flow is too low: the oil is heating up too quickly and parts may not be getting proper lubrication for cooling. Of course, these values are merely guidelines and may be exceeded in practice with good results.

The flow of lubricant to the overrunning clutch can be divided into two categories, the flow to the bearings and the flow to the overrunning clutch members. The flow to the bearings, which include the freewheel unit's outer- and inner-support bearings, can be calculated by conventional methods. However, each type of overrunning clutch has its own peculiarities concerning lubrication, and each is discussed separately. The spring clutch requires lubrication to the "teaser" coils on the overrunning side of the unit. The sprag clutch requires lubricant to either the inner or outer shaft surface, depending on which is the sliding surface. The ramp roller clutch requires lubrication to the rollers and the pin and spring mechanism.

The total flow of lubricant to the freewheel unit is the sum of that required for bearings and that required for the overrunning clutch.

A summary of the heat generated by the clutch bearings is presented in the following sections.

Bearing Lubrication

Lubrication requirements for antifriction bearings are dependent upon the amount of heat generated during operation. This energy is divided into two categories, (1) friction loss due to applied load, and (2) friction loss from viscous effects. The following method of analysis is presented in Reference 9, pp 446-451.

The friction loss created by applied load is

$$Ml = fl \; F\beta \; d_m \tag{165}$$

where

$F\beta$	=	bearing load factor - lb
Ml	=	bearing friction torque - in. lb
d_m	=	bearing mean diameter - in.

In Equation 165, fl is a factor depending on bearing design and relative bearing load. For ball bearings

$$fl = Z \left(\frac{Fs}{Cs}\right)^y \tag{166}$$

where

Fs	=	static equivalent load - lb
Cs	=	basic static capacity - lb
Z	=	coefficient of friction factor
y	=	exponent of friction factor

Values of the basic static capacity, Cs, are usually given in bearing manufacturers' catalogs along with procedures for calculating the static equivalent load. Values of Z and y are presented in Table 11 for various types of ball bearings. Table 12 presents values of fl for roller bearings.

TABLE 11. VALUES OF Z, COEFFICIENT OF FRICTION FACTOR, AND y, EXPONENT OF FRICTION FACTOR			
Ball Bearing Type	Contact Angle, α	Z	y
Deep Groove	0°	.0009	.55
Angular Contact	30°	.0010	.33
Angular Contact	40°	.0013	.33
Thrust	90°	.0012	.33
Self-Aligning	10°	.0003	.40

TABLE 12. f1, FACTOR FOR FRICTION COEFFICIENT FOR ROLLER BEARINGS.	
Roller Bearing Type	f1
Cylindrical	.00025-.0003
Spherical (Self-Aligning)	.0004 -.0005
Tapered	.0004 -.0005

$F\beta$ in Equation 165 depends on the magnitude and the direction of the applied load. For radial ball bearings

$$F\beta = .9\ Fa \cot\alpha - .1 \tag{167}$$

or

$$F\beta = Fr \tag{168}$$

whichever gives the highest value

where

Fa = applied axial load
Fr = applied radial load
α = contact angle

For radial roller bearings

$$F\beta = .8\ Fa \cot\alpha \tag{169}$$

or

$$F\beta = Fr \tag{170}$$

whichever is larger. For a cylindrical roller bearing, $\alpha = 0$. For a thrust bearing, either ball or radial, $F\beta = Fa$.

When calculating lubrication requirements for freewheel units, the critical condition occurs during overrunning. During overrunning, the only loads felt by the bearings are the weights of the clutch components. The rolling resistance created by the weight of the parts is generally negligible; hence, the only contribution to overrunning drag in a clutch bearing is from viscous friction.

The second contribution to drag torque in a bearing is created by the viscous effects of the bearing elements as they rotate through the lubricant. An empirical approach is presented by Harris in Reference 9, pp 447-451. For moderate speeds and not excessive loads, viscous friction torque can be expressed as

$$M\nu = 1.42 \times 10^{-5} f_o (\nu o \text{ rpm})^{2/3} d_m^3 \quad (171)$$

or

$$M\nu = 3.492 \times 10^{-3} f_o d_m^3 \quad \text{for } (\nu o \text{ rpm}) \leq 2000 \quad (172)$$

where

$M\nu$ = viscous friction torque - in. lb
νo = kinematic viscosity - centistokes

In Equations 171 and 172 above, f_o is a factor that accounts for the bearing type and the conditions of lubrication. Table 13 lists f_o as a function of the type of bearing and the lubrication.

The total friction torque is the sum of the viscous and load friction torques.

$$M = M\nu + Ml \quad (173)$$

The total friction torque is converted to heat by applying the appropriate conversion factors, as given in

$$H = \frac{M \times rpm}{1486} \quad (174)$$

where

H = heat generated in the bearing - btu/min

The required oil flow is then found from

$$Q = \frac{.13\ H}{Cp\ \Delta t} \quad (175)$$

TABLE 13. VALUES OF f_o, BEARING FACTOR.

Bearing	Configuration	Mist Lube	Oil Bath Lube Grease Lube	Vertically Mounted Flooded Oil Lube or Jet Lube
Deep-Groove Ball Bearing Self-Aligning Ball Bearing Ball Thrust Bearing	(Single Row) (Double Row)	.7 - 1	1.5 - 2	3 - 4
Filling Slot Ball Bearing Angular Contact Ball Bearing	(Single Row) (Single Row)	1	2	4
Angular Contact Ball Bearing	(Double Row)	2	4	8
Tapered Roller Bearing Spherical Roller Bearing	(Single Row) (Single Row)	1.5 - 2	3 - 4	6 - 8
Cylindrical Roller Bearing	(Single Row	1 - 1.5	2 - 3	4 - 6
Spherical Roller Bearing Tapered Roller Bearing	(Double Row) (Double Row)	2 - 3	4 - 6	8 - 12

where

Cp	=	specific heat of lubricant - btu/lb ^{o}F
Δt	=	change in oil temperature across bearing - ^{o}F
Q	=	oil flow rate - gpm

Spring Clutch Oil Flow

The total flow of oil to the spring clutch is the sum of that required for bearings and that required for the teaser coils of the spring during overrunning. Full-speed overrun (input fixed and output at maximum rpm) is the critical lubrication condition.

The best way to determine the clutch's flow requirement is to measure overrunning drag by test. An estimate of the spring teaser coil's drag torque can be made with

$$MSP = \frac{E\ b\ h^3\ a}{6\ d_m^2} \left(1 - \frac{1}{e^{2\ \pi\ \mu\ n}} \right) \qquad (176)$$

where

MSP	=	spring clutch drag torque - in. lb
b	=	width of teaser coils - in.
h	=	height of teaser coils - in.
a	=	diametral interference between teaser coil and housing - in.
d_m	=	mean diameter of teaser coils
n	=	number of teaser coils (usually 3)

The total drag torque on the clutch is the sum of the teaser coil's drag torque from Equation 176 and the support bearing's torques from Equation 171 or 172 and is

$$Mt = MSP + Mv \qquad (177)$$

This torque is assumed to be converted to heat; whereupon the flow is calculated by assuming an oil temperature rise.

Sprag Clutch Oil Flow

The lubrication of a sprag clutch is required to minimize wear on the sprag cams and on the inner race. This wear is generated during overrunning at full and differential speeds. The two primary functions of lubrication are to carry away excess heat and to provide a fluid for disengaging the sprags hydrodynamically.

The two most common types of oil used in aircraft applications are MIL-7808 and MIL-23699; although other types of oils have been used successfully. Oils containing extreme pressure (EP) additives are not recommended due to their characteristics, which include a lowered coefficient of friction on which proper clutch operation depends.

A sprag clutch employing engaging sprags can be made to disengage by the drag imposed by the oil during overrunning. As the outer and the inner race speeds approach each other, the hydrodynamic effect is lost, and the clutch is capable of transmitting torque at any absolute speed. Hydrodynamic disengagement requires that a complete film of oil be maintained around the circumference of the inner race during overrunning. This can be achieved by employing two oil dams adjacent to the clutch/sprag assembly, one on each side as described in the "Outer Housing Design" section for sprag clutches.

During overrunning in the differential mode (outer housing rotating), the clutch cavity is completely filled. The oil must therefore pass beneath the oil dams to escape, and since their inside diameter is smaller than the inner race outer diameter, hydrodynamic disengagement becomes possible.

Since the clutch cavity has a tendency to become a sludge trap in the arrangement described, several small radial holes directly over the clutch cavity in the outer race may be incorporated. These holes should be sized so as not to change the centrifugal head or level of the oil within the clutch cavity; i.e., the oil depletion must not exceed the input supply.

During full-speed overrunning (outer housing stopped), the centrifuging effect of the outer race is lost, which makes it more difficult to maintain a full cavity of oil. In this mode of operation, the oil supply must be great enough to again fill the cavity, which is possible if the sizes of the oil exit passages beneath the oil dams are held to a minimum.

Since the quantity of oil required by the clutch is far more than that required by the adjacent bearings, oil drainage passages are usually employed between the oil dams, the bearings and the radial holes in the outer race directly above the slots. This arrangement reduces the churning effects of the bearings, thereby reducing the heat generated.

The specific quantity of oil required by the clutch varies from application to application and usually depends on the size of the clutch and the speed at which it operates. To date there are no known, proven formulas for obtaining the oil requirement due to the many variables involved, such as actual

clutch drag, eccentricities, bearing clearances, and surface finishes. However, the quantity of oil is easily determined by a test in which the input member is fixed and the output member is rotated at 100% speed. The drag torque and the temperature rise are then measured as the flow is varied. An approximate preliminary flow may be calculated by

$$QS = Qsp + Qbrg \qquad (178)$$

where

QS = total flow to sprag clutch
Qsp = flow to sprag area only
Qbrg = flow to bearings that rotate during overrunning

The bearing flow, Qbrg, is calculated by the methods outlined in "Bearing Lubrication". As an estimate of the sprag flow, Qsp, Figure 64 may be used, which is a graph of flow versus torque and which was derived from previous experience.

Ramp Roller Clutch Oil Flow

The total oil flow to the ramp roller clutch is the sum of that required for the bearings and that required for the rollers of the clutch during overrunning. Full-speed overrun (input fixed and output at maximum rpm) is the critical lubrication condition.

As described previously, the best way to determine the ramp roller clutch lubrication requirements is by test. However, it is necessary to have some means of estimating what flows to use since the proper flow is not known until the completion of the test.

If we consider the rollers to be acting as a roller bearing during overrunning, the equations for bearings may be used to estimate the heat generated. The majority of the heat generated will be from viscous effects and is given by

$$MRR = 1.42 \times 10^{-5} \, fo \, (vo \, rpm)^{2/3} \, d_m^{3} \qquad (179)$$

where

MRR = the rollers' viscous friction torque - in.-lb

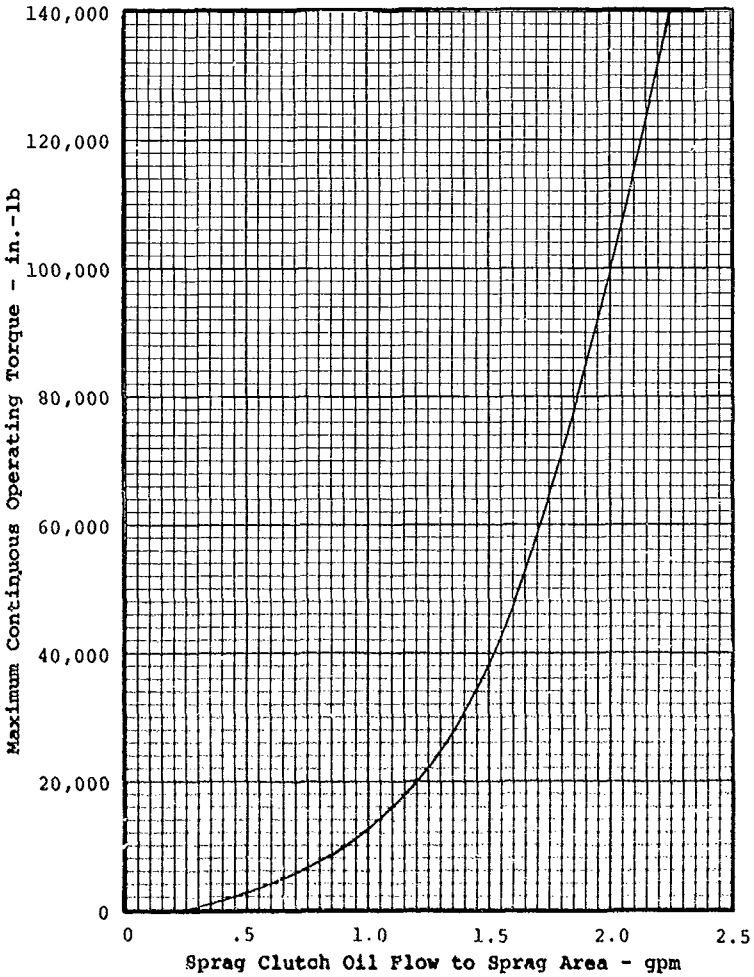

Figure 64. Preliminary Estimate of Oil Flow to Sprag Clutch.

When using Equation 179, if an fo value between 4 and 6 is used for cylindrical roller bearings and flooded oil lubrication, it will be found that low values of friction torque will be calculated. However, based on test data, a value of fo = 20 is more realistic.

Using a νo of 3 and an fo of 20 in Equation 179, gives

$$MRR = 5.91 \times 10^{-4} (rpm)^{2/3} d_m^3 \quad (180)$$

The total ramp roller clutch drag torque (Mt) is the sum of clutch roller and support bearing torques, and is

$$Mt = MRR + M\nu \quad (181)$$

This torque is assumed to be converted into heat, whereupon the flow is calculated by assuming an oil temperature rise.

Flow Through Orifice

In the design of a freewheel unit for helicopter operation, jets are often used for lubricating the bearings and overrunning clutch members. It is useful to review the method for calculating the flow through a jet as a means for sizing the jet diameters. The flow through a jet is given by

$$Q_m = C_v C_c A \sqrt{2 g p \gamma} \quad (182)$$

where

Q_m = theoretical flow - lb/sec
C_v = velocity coefficient
C_c = contraction coefficient
A = area of jet = $\pi d^2/4$
g = gravitational constant = 386 in./sec^2
p = pressure - psi
γ = lubricant density - lb/in.^{3}

The velocity coefficient, C_v, is defined as the ratio of the actual velocity in the jet to the theoretical velocity. The coefficient varies depending on the Reynolds number, geometry of the lines, etc., and is usually determined experimentally. The contraction coefficient, C_c, is the ratio of the area of the vena contracta of the orifice to the actual orifice area and is a function of the geometry of the orifice, etc. The product of the two coefficients is generally combined with a discharge coefficient, C, given by

$$C = C_V C_C$$

For initial design purposes, a C of .63 may be used. Also for preliminary design purposes, MIL-L-7808 oil at 210°F, a γ of .0301 lb/in.^{3} may be used. Substituting these values into Equation 182 and converting to gallons per minute

$$Q = 20.6\ d^2\ P \qquad (183)$$

where

Q = theoretical flow - gpm
d = jet diameter - in.

Pressure in Rotating Dam of Oil

In the design of the lubrication system for an overrunning clutch, a rotating oil distribution tube is often used. The oil distribution tube can be the inner shaft of the freewheel unit itself. If the speed of the rotating distribution tube is approximately 3000 rpm or greater, a rotating mass of oil will be formed in the tube with an oil level that is essentially parallel to the axis of rotation. The height of the oil within the rotating body will be established by the maximum radius on the part that will allow the oil to escape by centrifugal force.

Figure 65 shows a typical distribution tube with the nomenclature used in the analysis of the flow.

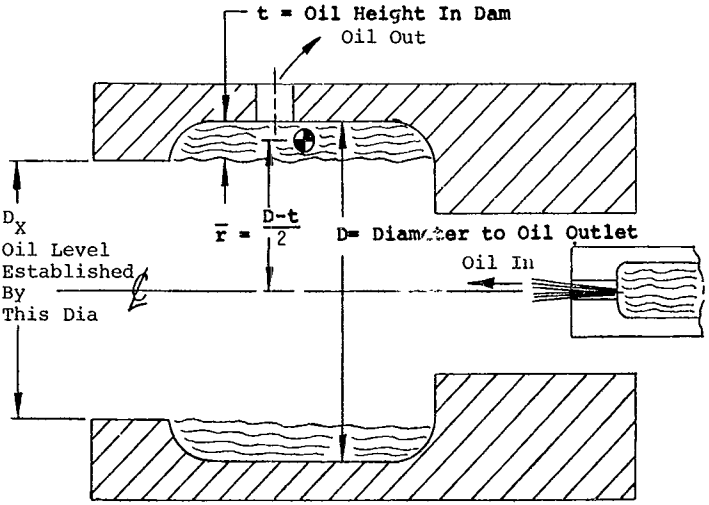

Figure 65. Nomenclature Used in Determination of Pressure in a Rotating Dam of Oil.

The pressure will be found from

$$p = \frac{\gamma\, t\, \bar{r}\, \omega^2}{g} \qquad (184)$$

where

γ = oil density lb/in.^{3}
ω = shaft angular velocity - rad/sec
p = pressure from centrifugal force acting on oil - psi

Once the pressure is calculated, the equations for flow through an orifice may be used to calculate flow.

Equation 184 assumes that the oil inlet will be greater than the oil outlet so that excess oil will flow past the end of the distribution chamber at diameter D_X in Figure 65. If this is not the case, if the flow of oil in is equal to the flow of oil out through the jets, the height of the oil, t, will be the only variable. Or, in another way of examining the problem, if the calculated flow out using the maximum value of t exceeds the flow in, the flow out will be equal to the flow in and the height of oil in the dam, t, will be less than $(D - D_X)/2$.

QUALIFICATION TEST PROCEDURES

Helicopter overrunning clutches are not subject to severe or stringent test requirements by the customer. Often the manufacturer will conduct tests on a new design to determine wear characteristics and strength. Both commercial and military test requirements do not cover overrunning. The clutch is substantiated structurally during the normal course of the transmission test. Specifications also refer to a required number of engagements for a clutch, usually from 100 to 300 being required.

Over and above the customer's requirements, any new clutch design should be tested in the overrunning condition. If an estimate is available of full-speed and differential-speed overrunning for the life of the helicopter, the main objective of the test plan should be to prove that the clutch will reach the projected life. Estimates of freewheel unit overrunning during the helicopter life are contained in the "Design Requirements, Constraints, and Considerations" section that may be used in the absence of more accurate prediction data.

After the overrunning life requirement has been established, a test plan can be developed to substantiate the life. The overrunning tests need not be for the entire predicted life but can be for some percentage of it. During the course of the test, measurements are made on the surfaces of the clutch components that are subjected to wear. For the spring clutch, these will be the spring end coils and the internal bore of the housing; for the sprag clutch, the sprags, and the internal, and the external shafts; and for the ramp roller clutch, the rollers, the housing and the cam flats. If several disassemblies are performed during the test so that wear measurements can be taken, curves of wear versus life can be developed. These curves will usually indicate a slope that can be extrapolated to the desired life.

The easiest type of overrunning test to conduct is the full-speed overrun test. The input is fixed to ground, and the output is rotated at rated speed. If a spring scale and arm are used to fix the input, drag torques can be measured. Drag torque can then be used to calculate the lubrication flow to the clutch by assuming that all the drag is transferred to heat, which is absorbed by the oil (see "Lubrication" section). A test duration of 50 to 200 hours will usually "wring out" the weak links of wear on the clutch.

The second type of overrunning test to conduct on a new clutch design is the differential speed overrun test. In differential speed testing, the output shaft is rotated at the rated speed, and the input shaft is driven at speeds below 100%. Usually, the range of 50% to 100% is used for the input shaft speed since this is the usual operating range of engines from ground idle to full speed. Of course, at 100% speed, an engagement will occur. Differential speed testing is more severe in terms of wear than full-speed overrunning testing. However, it is usually not done on a new design because of the complications of manufacturing a test stand incorporating a drive on both the input and the output. Full-speed overrun testing can be conducted on the standard transmission load test stand, whereas differential speed testing may require stand modification.

Load testing of a new clutch design is used to substantiate the structural integrity of the unit. The clutch is tested in the transmission system test. A static torque overload test of the freewheel unit assembly itself may be useful. From this test, the clutch's torsional spring rate and ultimate torque limit can be established.

Engagement testing is often specified by the customer. Engagements are of two types: start-up engagements and full-speed engagements. Engagement at start-up consists of picking up a load from rest, as would occur during a rotor engagement start. Full-speed engagements occur on twin-engine helicopters when one engine is driving the rotors and the other engine is brought up to rotor speed. When the second engine's speed reaches the first engine's speed, the overrunning clutch will engage. During the time the second engine's clutch input member is rotating below the speed of the output, the clutch will be operating in differential speed overrun. A test rig to conduct high-speed engagements is very costly, and therfore, the helicopter itself is usually used as the engagement test bed.

FAILURE MODES AND EFFECTS ANALYSIS

Tables 14, 15, and 16 present failure modes and effects analyses for the three types of clutches presented in this design guide. These analyses are only for freewheel units in the primary power train of a twin-engine helicopter. Accessory freewheel units are not considered. The failure modes and effects analysis only presents possible failure modes; the probability of occurrence is not considered in this analysis. It should be pointed out that some of the failure modes considered would have only extremely remote chances of happening in practice. The failure modes are divided into three categories, as follows:

Category I	Safety of flight failure mode: failures of this type lead to possible loss of aircraft, but none of the failure modes of the clutches was considered to be of this category because twin-engines were assumed. It is extremely remote that simultaneous clutch failures would occur on left and right inputs during the same flight.
Category II	Failure modes that would lead to unacceptable risks to the aircraft or the occupants if mission were to be continued.
Category III	Failure modes that result in the replacement of components, but do not affect mission capabilities.

TABLE 14. DESIGN FAILURE MODES AND EFFECTS ANALYSIS, SPRING CLUTCH

Part Name	Quantity Per Clutch	Function	Failure Mode	Failure Detection Method	Effect of Failure Mode on Clutch	Effect of Failure Mode on Aircraft	Failure Mode Category
Input Shaft	1	Transmits engine torque to spring	Fretting of Spline	None	Possible progression to spline shear failure	Complete failure of spline leads to loss of engine torque	II or III
			Excessive wear of bore in teaser coil overrunning area if arbor is attached to output	None	Clutch may slip or fail to engage	Possible loss of some or all engine torque	II or III
Output Shaft	1	Transmits torque from spring to transmission	Fretting of spline	None	Possible progression to spline shear failure	Complete failure of spline leads to loss of engine torque	II or III
			Excessive wear of bore in teaser coil overrunning area if arbor is attached to input	None	Clutch may slip or fail to engage	Possible loss of some or all engine torque	II or III
Spring	1	Transmits torque from input to output shafts; allows over-running of output	Excessive wear in teaser coil areas	None	Clutch may slip or fail to engage	Possible loss of some or all engine torque	II or III
			Fracture	Possible chip detector light activation	Clutch may slip or fail to engage	Possible loss of some or all engine torque	II or III
Spring Guide Arbor	1	Provides radial positioning of spring during overrunning	None				
Ball Bearing	2	Maintain relative position of input and output shafts; permit over-running of output member	Cage fracture	Chip detector light activation	Bearing siezure	Loss of overrunning capability	II
			Spalling	Eventual chip detector light activation	Debris generation leading to possible bearing siezure	Possible loss of overrunning capability	II
			False Brinnelling	None	Formation of slight pockets in bearing races due to lack of rotation	None	III

TABLE 15. DESIGN FAILURE MODES AND EFFECTS ANALYSIS, SPRAG CLUTCH

Part Name	Quantity Per Clutch	Function	Failure Mode	Failure Detection Method	Effect of Failure Mode on Clutch	Effect of Failure Mode on Aircraft	Failure Mode Category
Outer Race	1	Input or output member of clutch, transmits torque to or from sprag assembly.	Excessive Wear	None	Possible slipping or "roll over" of sprags in full phasing type. Possible slippage in PCE* type	Possible loss of engine torque	II or III
			Fretting of spline	None	Possible progression to spline shear failure	Complete failure of spline leads to loss of engine torque	II or III
Inner Race	1	Output or Input member of clutch; transmits torque to or from sprag assembly	Excessive Wear	None	Possible slipping or "roll over" of sprag in full phasing type Possible slippage in PCE* type	Possible loss of engine torque	II or III
			Fretting of spline	None	Possible progression to spline shear failure	Complete failure of spline leads to loss of engine torque	II or III
Sprag	Number depends on design	Transmits torque between input and output members; allows over-running of output	Excessive wear of sprags	None	Possible slippage or "roll over" of sprags in full phasing type. Possible slippage in PCE* type	Possible loss of engine torque	II or III
Retainer	1 or 2 depending on design	Retains sprags in proper position	Retainer fracture	Chip detector light activation	Sprags move out of position; causing failure of clutch. Possible secondary damage to other clutch components.	Loss of engine torque	II
Spring	1	Holds sprags in contact with input and output shafts.	Fracture	Possible chip detector light activation	Clutch fails to engage.	Loss of engine torque	II
Ball Bearing	2	Maintains relative position of input and output shafts; permits over-running of output	Cage fracture	Chip detector light activation	Bearing siezure and secondary damage to other clutch components	Loss of overrunning capability	II
			Spalling	Eventual chip detector light activation	Debris generation during overrunning possibly causing secondary damage to other clutch components	Possible loss of overrunning capability	II
			False Brinnelling	None	Lack of bearing rotation because of low overrunning time causes bearings to wear slight pockets in races. Usually does not affect clutch operation	None	III

* Positive Continuous Engagement

TABLE 16. DESIGN FAILURE MODES AND EFFECTS ANALYSIS, RAMP ROLLER CLUTCH

Part Name	Quantity Per Clutch	Function	Failure Mode	Failure Detection Method	Effect of Failure Mode on Clutch	Effect of Failure Mode on Aircraft	Failure Mode Category
Camshaft	1	Acts as input or output member depending on design by transmitting torque to or from rollers	Fretting of spline	None	Possible progression to spline shear failure	Complete failure of spline leads to loss of engine torque	II or III
			Excessive wear of cam flats	None	Eventual failure to maintain rollers in position during driving, leading to "spit-out" of rollers	Possible loss of engine torque	II or III
Rollers	As required by design	Transmits torque between input and output member; allows overrunning of output	Brinelling	None	Eventual progressing to point of roller spit-out	Possible loss of engine torque	II
			Excessive wear	None	Eventual progression to point of roller spit-out	Possible loss of engine torque	II or III
			Roller Fracture	Chip detector light activation	Leads to cage fracture and secondary damage to other clutch components	Loss of engine torque	II
Housing	1	Acts as output or input member depending on design by transmitting torque from or to rollers.	Fretting of spline	None	Possible progression to spline shear failure	Complete failure of spline leads to loss of engine torque	II or III
			Excessive wear of bore	None	Eventual failure to maintain rollers in position during driving leading to "spit out" of rollers	Possible loss of engine torque	II or III
			Cracking	Chip detector light activation	Loss of torque-carrying capability	Loss of engine torque	II
Pin	2	Used in conjunction with spring to hold rollers in contact with both cam and outer housing	Fracture	Chip detector light activation	Cage fracture or failure of clutch to engage	Loss of engine torque	II
			Excessive Wear	None	Failure of clutch to engage or late engagement, leading to shock loading and failure of clutch	Loss of engine torque	II

TABLE 16 - Continued

Part Name	Quantity Per Clutch	Function	Failure Mode	Failure Detection Method	Effect of Failure Mode on Clutch	Effect of Failure Mode on Aircraft	Failure Mode
Spring	2	Used in conjunction with pin to hold rollers in contact with both cam and outer housing	Fracture	Chip detector light activation	Failure of clutch to engage or late engagement, leading to shock loading and failure of clutch	Loss of engine torque	II
Cage	1	Retain clutch rollers in proper axial and circumferential position	Excessive wear	None	Causes rollers to skew and jam, leading to excessive roller wear and eventual loss of torque-carrying capability	Loss of engine torque	II
			Fracture	Chip detector light activation	Roller skew and jam, leading to excessive wear and loss of torque-carrying capability. Secondary damage to other clutch components.	Loss of engine torque	II
Bushings	Number depends on design	Provides axial positioning of cage relative to cam	Excessive Wear	None	Sloppiness in position of cage and rollers could lead to roller skewing and excessive roller wear. Eventual loss of torque-carrying capability	Eventual loss of engine torque	II
Ball Bearing	2	Maintain relative position of housing and cam; permit overrunning of output member	Cage fracture	Chip detector light activation	Bearing seizure and secondary damage to other clutch components	Loss of overrunning capability	II
			Spalling	Eventual chip detector light activation	Debris generation during overrunning, possibly causing secondary damage to other clutch components	Possible loss of overrunning capability	II
			False brinnelling	None	Lack of bearing rotation because of low overrunning time causes bearing balls to wear slight pockets in races. Usually does not affect clutch performance.	None	III

DESIGN EXAMPLE, SPRING CLUTCH

The spring clutch assembly used in contract DAAJ02-74-C-0028 is depicted in Figure 66.

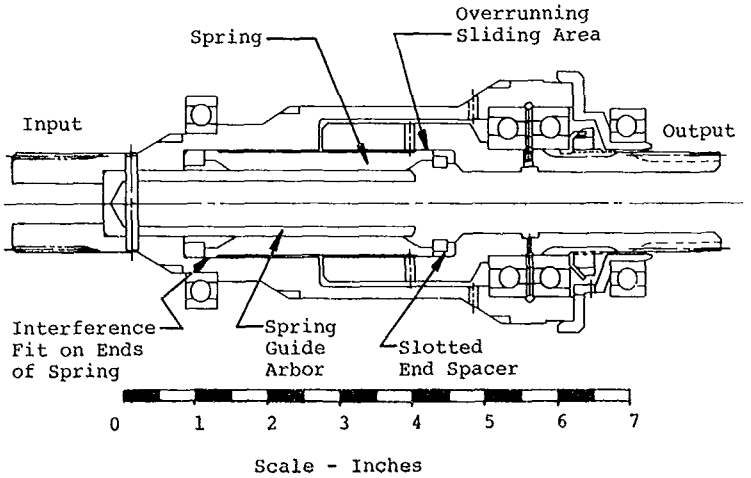

Figure 66. Spring Clutch Assembly.

Calculation of Spring Stress

The spring clutch has been designed to operate at 1500 hp and 20,000 rpm.

rpm = 20,000
hp = 1500

$$T = \frac{63{,}025 \text{ hp}}{\text{rpm}} = \frac{63{,}025\ (1500)}{20{,}000} = 4730 \text{ in.-lb} = \text{clutch design torque}$$

A cross section of the spring is shown in Figure 67.

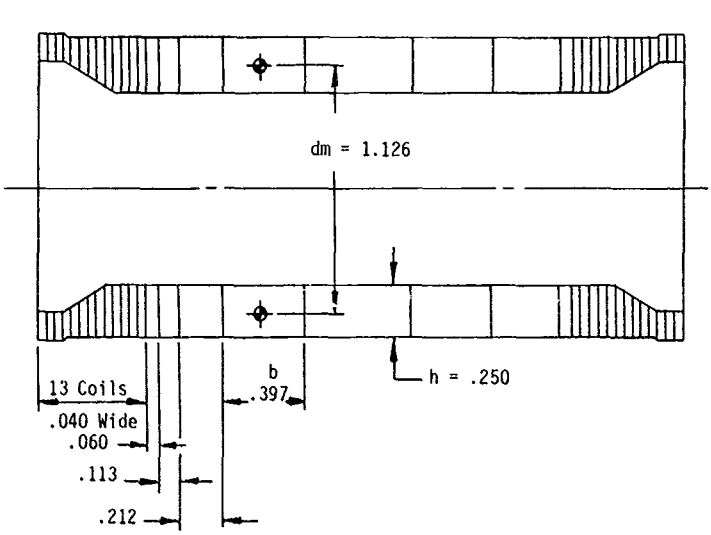

Figure 67. Spring Cross Section.

The axial compressive spring stress, from Equation 10, is

$$f_a = - \frac{2\,T}{d_m\,b\,h}$$

$$f_a = - \frac{2\,(4730)}{(1.126)(.397)(.250)}$$

$$f_a = -84{,}650 \text{ psi @ center coil}$$

The bending stress is found using curvature correction factor's calculated with Equation 14 and using the spring geometry shown in Figure 67.

$$\frac{i}{c} = \frac{d_m}{h} - \frac{2}{\ln\left(\frac{d_m/h+1}{d_m/h-1}\right)}$$

$$\frac{j}{c} = \frac{1.126}{.250} - \frac{2}{\ln \frac{1.126/.250+1}{1.126/.250-1}}$$

$$\frac{j}{c} = .075$$

Next, the curvature correction factor for inside stress is found with Equation 15.

$$Ki = \frac{1}{3j/c} \quad \frac{1 - j/c}{d_m/h - 1}$$

$$Ki = \frac{1}{3(.075)} \quad \frac{1 - .075}{4.504 - 1}$$

$$Ki = 1.173$$

The curvature correction factor for outside stress is found with Equation 16.

$$Ko = - \frac{1}{3j/c} \quad \frac{1 + j/c}{d_m/h + 1}$$

$$Ko = - \frac{1}{3(.075)} \quad \frac{1 + .075}{4.504 + 1}$$

$$Ko = - .868$$

The bending stress on the inside fiber is found with Equation 13 and using an "a" of .010 inch (diametral clearance between spring and housing.

$$fb_i = Ki \frac{E\ a\ h}{d_m^2}$$

$$fb_i = 1.173 \frac{30x10^6(.010)(.25)}{1.126^2}$$

$$fb_i = 69,390 \text{ psi}$$

The bending stress on the outside fiber is found with Equation 13 using Ko for the curvature correction factor.

$$fb_o = Ko \frac{E\ a\ h}{d_m^2}$$

$$fb_o = -.868 \frac{30x10^6(.010)(.25)}{1.126^2}$$

$$fb_o = -51,350 \text{ psi}$$

The total stress on outside fiber is found with Equation 17.

$$f_o = fa + fb_o = -84,650 - 51,350$$

f_o = -136,000 psi = total stress on outside of spring

The total stress on the inside fiber is found from Equation 18,

$$f_i = f_a + f_{bi} = -84,650 + 69,390$$

f_i = -15,260 psi = total stress on inside of spring

The low cycle fatigue GAG stress steady component is found from Equation 19.

$$f_s = \frac{f_{bi} + f_i}{2} = \frac{69,390 - 15,260}{2}$$

The steady low cycle stress is

f_s = 27,070 psi

The low cycle fatigue GAG stress vibratory component is found from Equation 20.

$$f_v = \pm \frac{f_{bi} - f_i}{2} = \pm \frac{69,390 + 15,260}{2}$$

The vibratory low cycle GAG stress is

$f_v = \pm$ 42,330 psi

The spring is manufactured from H-11 tool steel, (CPS 4907, AMS 6487) heat-treated to Rc 54-56. For this material the properties are,

Ftu = 275,000 psi
Fty = 242,000 psi
Fen = 56,000 psi @ 10^7 cycles and 3σ (R=.7)

Under normal load, the margin of safety is found with,

$$M.S. = \frac{Fty}{1.15\, f_o} - 1 = \frac{242,000}{1.15(136,000)} - 1$$

M.S. = + .55 (normal)

For GAG cycles, the margin of safety is found using a combined stress formula given by,

$$M.S. = \frac{1}{\sqrt{\left[\frac{f_s}{Fty}\right]^2 + \left[\frac{f_v}{Fen}\right]^2}} - 1 = \frac{1}{\sqrt{\left[\frac{27,070}{242,000}\right]^2 + \left[\frac{42,330}{56,000}\right]^2}} - 1$$

M.S. = +.31 (GAG)

Calculation of Spring Shape

The torque in any coil is found with Equation 12.

$$T_i = \frac{T}{e^{2\pi\mu(N-i)}}$$

Assuming $\mu = .1$ = coefficient of friction for steel on steel lubricated

$$T_i = \frac{4730}{e^{2\pi(.1)(N-i)}} = \frac{4730}{e^{.6283(N-i)}}$$

The stress at any coil is found with Equation 11.

$$f_{ai} = - \frac{2T_i}{d_m\, b_i\, h_i}$$

Table 17 lists the stress and torque for each coil of the spring using N = 17 for the total number of coils from teaser to center.

TABLE 17. SPRING STRESS DATA BY COIL.

i	Spring Geometry d_m	b	h	T_i in.-lb	f_{ai} psi
1	1.254	.040	.122	.20	- 65
2	1.254	.040	.122	.38	-120
3	1.254	.040	.122	.71	-230
4	1.241	.040	.135	1.3	-390
5	1.222	.040	.154	2.5	-660
6	1.190	.040	.186	4.7	-1060
7	1.164	.040	.212	8.8	-1780
8	1.139	.040	.237	16	-2960
9	1.126	.040	.250	31	-5510
10	1.126	.040	.250	58	-10300
11	1.126	.040	.250	109	-19400
12	1.126	.040	.250	204	-36200
13	1.126	.040	.250	380	-67500
14	1.126	.060	.250	720	-84600
15	1.126	.113	.250	1350	-84600
16	1.126	.212	.250	2520	-84600
17	1.126	.397	.250	4730	-84600

Calculation of Input Housing Stress

To determine the stresses in the spring clutch input housing, the dimensions indicated in Figure 68 are required.

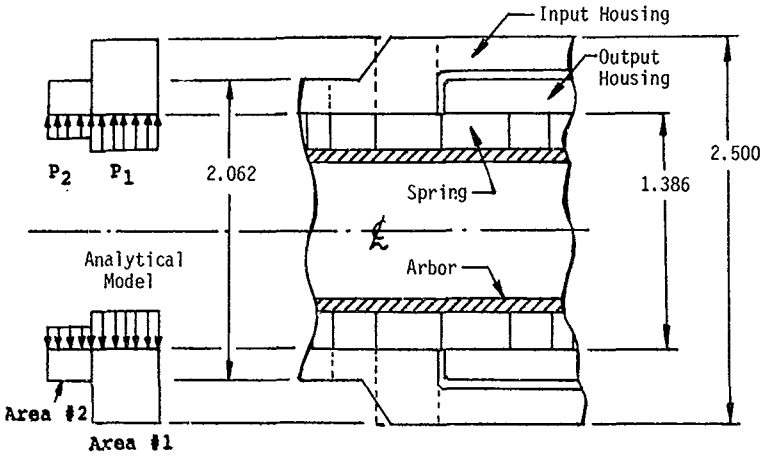

Figure 68. Outer Housing Analytical Model and Basic Dimensions.

From Figure 68, the basic inside radii, a, of the areas and the basic outside radii, b, of the area are found by

$$a_1 = 1.386/2 = .693$$

$$b_1 = 2.500/2 = 1.250$$

$$a_2 = 1.386/2 = .693$$

$$b_2 = 2.062/2 = 1.031$$

From Equation 24, the geometry cylinder parameter for area #1 is

$$n_1 = \frac{b_1^2+a_1^2}{b_1^2-a_1^2} = \frac{1.250^2+.693^2}{1.250^2-.693^2}$$

$$n_1 = 1.888$$

From Equation 25, the geometry cylinder parameter for area #2 is,

$$\eta_2 = \frac{b_2^2+a_2^2}{b_2^2-a_2^2} = \frac{1.031^2+.693^2}{1.031^2-.693^2}$$

$$\eta_2 = 2.648$$

At 1500 hp and 20,000 rpm and using Equation 21 with i=1, the pressure on area #1 from the spring is,

$$p_1 = \frac{4\ T_1}{b_1 d_m^2} = \frac{4(4730)}{.397(1.126)^2} = 37{,}500 \text{ psi}$$

The pressure on area #2 from the spring is also calculated from Equation 21 with i=2,

$$p_2 = \frac{4\ T_2}{b_2 d_m^2} = \frac{4(2520)}{.212(1.126)^2} = 37{,}500 \text{ psi}$$

Since the pressures are equal (constant stress spring) and the inside radii of the areas are equal ($a_1 = a_2$), the geometry constant is calculated from Equation 28 as,

$$\zeta = \frac{\eta_1+\nu}{\eta_2+\nu} = \frac{1.888+.3}{2.648+.3} = .742$$

The percent pressure relief is found from Equation 30 as,

$$X = \frac{1-\zeta}{1+\zeta} = \frac{1-.742}{1+.742} = .148$$

from which the load is found from Equation 29

$$W = pX = 37{,}500\ (.148) = 5550$$

The stresses are found from Equations 31 and 32,

$$ft_1 = (p_1+W)\eta_1 = (37{,}500 + 5550)(1.888) = 81{,}300 \text{ psi}$$

$$ft_2 = (p_1-W)\eta_2 = (37{,}500 - 5550)(2.648) = 84{,}600 \text{ psi}$$

The housing is manufactured from H-11 tool steel heat-treated to Rc 54-56. The material properties are

Ftu = 275,000 psi
Fty = 242,000 psi
Fen = 96,000 psi @ 10,000 cycles, 3σ Rel (GAG design)

The margin of safety is calculated at both 1500 hp and 20,000 rpm, and low cycle fatigue (GAG). The GAG life cycles are assumed to be 10,000 cycles. The vibratory GAG stress is one-half of the maximum tensile hoop stress.

$$M.S. = \frac{Fty}{1.15\ ft} - 1 = \frac{242,000}{1.15\ (84,600)} - 1$$

M.S. = +1.49 (normal operation @ 1500 hp, 20,000 rpm)

When checking the margin of safety in fatigue, the vibratory stress is one-half of the maximum stress.

$$M.S._{GAG} = \frac{2Fen}{ft} - 1 = \frac{2(96,000)}{84,600} - 1$$

$$M.S._{GAG} = +1.27$$

Calculation of Output Housing Stress

The output housing is analyzed as a thick ring subjected to internal pressure. The housing is uniform in thickness with the diameters as follows:

$d_o = 2.062$
$d_i = 1.386$

The stresses are calculated by Equation 22.

$$ft = \frac{4\ T}{b\ d_m^2} \frac{d_o^2+d_i^2}{d_o^2-d_i^2}$$

The torque corresponds to 1500 hp and 20,000 rpm.

$$ft = \frac{4\ (4730)}{.397(1.126)^2} \frac{2.062^2+1.386^2}{2.062^2-1.386^2}$$

ft = 99,500 psi

The housing material is H-11 tool steel heat-treated to Rc 54-56. The material properties are

Ftu = 275,000 psi
Fty = 242,000 psi
Fen = 96,000 psi @ 10,000 cycles, 3σ Rel (GAG design)

$$M.S. = \frac{Fty}{1.15\ ft} - 1 = \frac{242,000}{1.15\ (99,500)} - 1$$

$$M.S. = +1.11 \text{ (normal operation @ 1500 hp, 20,000 rpm)}$$

$$M.S._{GAG} = \frac{Fen}{f_v} - 1 = \frac{2Fen}{ft} - 1 = \frac{2(96,000)}{99,500} - 1$$

$$M.S._{GAG} = +.93 \text{ (fatigue from GAG cycles)}$$

Calculation of Spring Centrifugal Effects

During differential speed overrun, the spring will expand from centrifugal force. The expansion is calculated by Equation 39 as

$$\delta = 2.01 \times 10^{-13} \frac{d_m^5 \, rpm^2}{h^2}$$

$$\delta = 2.01 \times 10^{-13} \frac{1.126^5 \, 20,000^2}{(.250)^2}$$

$$\delta = .0023 \text{ in.}$$

The spring interference fit on the spring guide arbor is .0025 to .005 inch; hence, the spring will not leave the arbor, which is the design objective.

Calculation of Spring Teaser Coil Geometry

The torque required to energize the clutch is given by Equation 40 as

$$T_{energ} = \frac{T}{e^{2\pi\mu N}}$$

assuming the coefficient of friction, μ, is 0.1

$$T_{energ} = \frac{4730}{e^{2\pi(.1)(16)}}$$

$$T_{energ} = .204 \text{ in.-lb}$$

The teaser-coil interference fit is calculated by Equation 41.

$$T_{int} = \frac{E \, b \, h^3 \, a}{6 \, d_m^2}$$

where

a = .0085 inch = average diametral interference between teaser coils and housing.

Coil dimensions, b, h, and d_m, are taken at the teaser coils (N = 17, and i = 1, in Table 17).

$$T_{int} = \frac{30x10^6(.040)(.122)^3(.0085)}{6\ (1.254)^2}$$

$$T_{int} = 1.96 \text{ in.-lb}$$

Hence, the interference torque is well above the energizing torque, and the clutch will drive.

$$M.S._{energ} = \frac{T_{int}}{T_{energ}} - 1 = \frac{1.96}{.204} - 1 = +8.61$$

The allowable wear is found from Equation 42.

$$\Delta wear = \left(a - \frac{6T_c d_m^2}{E\ b\ h^3\ e^{2\pi\mu N}}\right) \times \frac{1}{F.S.}$$

Assuming a factor of safety of 2.0

$$\Delta wear = \left(.0085 - \frac{6(4730)(1.254)^2}{30x10^6(.040)(.122)^3 e^{2\pi}(.1)(16)}\right) \times \frac{1}{2}$$

$\Delta wear$ = .0038 = allowable spring teaser coil wear.

Calculation of Flow Requirements

νo = 3.0 centistokes for MIL-L-7808 @ 210°F
rpm = 20,000

Duplex bearings: MRC7107 KRD

$$d_m \approx \frac{d_o + d_i}{2} = \frac{2.441+1.378}{2} = 1.91$$

The friction loss from load is zero while the viscous drag is found using Equation 171.

$$M\nu = 1.42x10^{-5}\ f_o\ (\nu o\ rpm)^{2/3}\ d_m^3$$

f_o = 8 for angular contact double row (from Table 13)

$$M\nu = 1.42x10^{-5}\ (8)\ (3x20,000)^{2/3}\ (1.91)^3$$

$M\nu$ = 1.21 in.-lb = drag torque on clutch bearings.

For the spring's teaser coils

b	=	.040	= width of teaser coils
h	=	.122	= height of teaser coils
d_m	=	1.254	= mean diameter of teaser coils
a	=	.0085	= diametral interference between spring and bore
n	=	3	= number of teaser coils
μ	=	.1	= coefficient of friction
E	=	30×10^6 psi	= Young's modulus

The spring's teaser coil drag is calculated from Equation 176.

$$MSP = \frac{E\, b\, h^3\, a}{6\, d_m^2} \left(1 - \frac{1}{e^{2\pi\mu n}}\right)$$

$$MSP = \frac{30\times10^6 (.04)(.122)^3 (.0085)}{6\,(1.254)^2} \left(1 - \frac{1}{e^{2\pi(.1)(3)}}\right)$$

$$MSP = 1.66 \text{ in.-lb}$$

Total drag torque is the sum of bearing and clutch torques from Equation 177.

$$Mt = MSP + M\nu$$

$$Mt = 1.66 + 1.21$$

$$Mt = 2.87 \text{ in.-lb}$$

The heat loss is calculated by Equation 174 as

$$H = \frac{Mt \times rpm}{1486} = \frac{2.87\ (20{,}000)}{1486}$$

$$H = 38.6 \text{ btu/min}$$

Assuming a Δt of $40^{\circ}F$ across the clutch, the oil flow is found from Equation 175.

$$Q = \frac{.13H}{Cp\Delta t}$$

$$Q = \frac{.13(38.6)}{.51\ (40)}$$

$$Q = .25 \text{ gpm}$$

From test data, the 100% flow condition was established at 0.8 gpm

DESIGN EXAMPLE, SPRAG CLUTCH

The sprag clutch assembly used in contract DAAJ02-74-C-0028, is depicted in Figure 69.

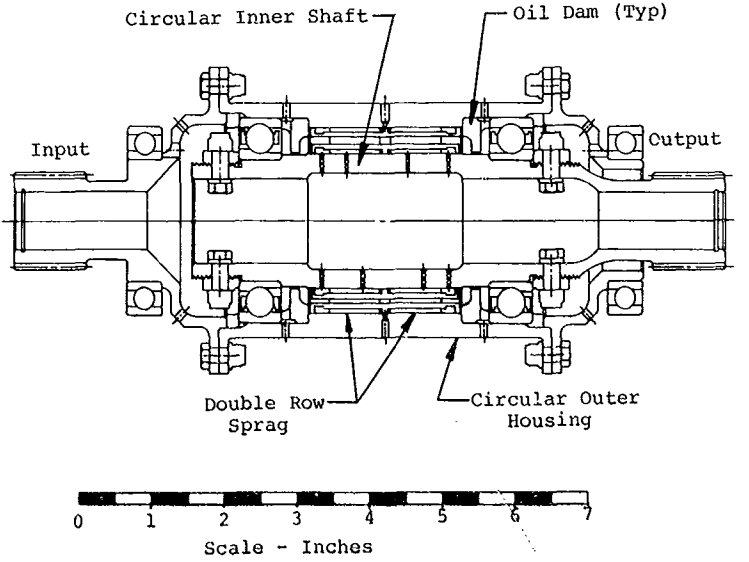

Figure 69. Sprag Clutch Assembly.

Calculation of Gripping Angles

The sprag clutch has been designed to operate at 1500 hp and 20,000 rpm.

rpm = 20,000
hp = 1500

$$T = \frac{63{,}025\ hp}{rpm} = \frac{63{,}025(1500)}{20{,}000} = 4730\ \text{in. lb} = \text{clutch design torque}$$

The initial step in the calculation of sprag gripping angles is the calculation of the influence coefficients for deflections. The data required is

Ro	= 1.203	Rod	= 1.525
Ri	= .875	Rid	= .625

Sprag X 138272-S - double row

The sprag section J is .328 and the basic data is found from Table 8.

N	=	18 sprags/row
T	=	4730/2 = 2360 in. lb per row
ℓ	=	.665 = sprag length/row
b	=	.194 = sprag width
ro	=	.178
ri	=	.177
Z	=	.0294
α	=	49.821°

The centrifugal deflection of the outer shaft is found from Equation 54.

$$\Delta cent = \frac{Ro}{E}\frac{(3+\nu)}{4}\frac{\rho}{g}\left(\frac{\pi rpm}{30}\right)^2\left\{Rod^2 + Ro^2\left(\frac{1-\nu}{3+\nu}\right)\right\}$$

$$\Delta cent = \frac{1.203}{30x10^6}\quad\frac{3+.3}{4}\quad\frac{(.283)}{386}\quad\left(\frac{\pi x20,000}{30}\right)^2$$

$$\left\{1.525^2 + 1.203^2\left(\frac{1-.3}{3+.3}\right)\right\}$$

$$\Delta cent = .000280 \text{ in.}$$

The influence coefficient for outer shaft is found from Equation 60.

$$Co = \frac{N}{2\pi\ell E}\left(\frac{Rod^2 + Ro^2}{Rod^2 - Ro^2} + \nu\right)$$

$$Co = \frac{36}{2\pi(.665)(30x10^6)}\left(\frac{1.525^2 + 1.203^2}{1.525^2 - 1.203^2} + .3\right)$$

$$Co = 1.381 \times 10^{-6} \text{ in./lb}$$

The influence coefficient for the inner shaft is found from Equation 61.

$$Ci = \frac{N}{2\pi\ell E}\left(\frac{Ri^2 + Rid^2}{Ri^2 - Rid^2} - \nu\right)$$

$$Ci = \frac{36}{2\pi(.665)(30\times10^6)} \left(\frac{.875^2 + .625^2}{.875^2 - .625^2} - .3\right)$$

$$Ci = 0.979 \times 10^{-6} \text{ in./lb}$$

The influence coefficient for the sprag is calculated by Equation 62.

$$Cs = \frac{Ro - Ri}{b\ \ell\ E}$$

$$Cs = \frac{1.203 - .875}{.194(.665)(30\times10^6)}$$

$$Cs = .0847 \times 10^{-6} \text{ in./lb}$$

The influence coefficient for Hertz is given by Equation 63.

$$C_1 = \frac{2(1-\nu^2)}{\pi\ \ell\ E}$$

$$C_1 = \frac{2(1-.3^2)}{\pi(.665)(30\times10^6)}$$

$$C_1 = .0290 \times 10^{-6} \text{ in./lb}$$

The influence coefficient for Hertz between the sprag and the outer shaft is found from Equation 64 as

$$C_2 = C_1\left[\frac{2}{3} + \ln\frac{\pi\ \ell\ E\ (Ro-ro)}{2(1-\nu^2)}\right]$$

$$C_2 = .0290 \times 10^{-6}\left[\frac{2}{3} + \ln\frac{\pi(.665)(30\times10^6)(1.203-.178)}{2\ (1-.3^2)}\right]$$

$$C_2 = 0.5233 \times 10^{-6} \text{ in./lb}$$

The influence coefficient for Hertz between the sprag and the inner shaft is found from Equation 65 as,

$$C_3 = C_1\left[\frac{2}{3} + \ln\frac{\pi\ \ell\ E\ (Ri+ri)}{2\ (1-\nu^2)}\right]$$

$$C_3 = .0290 \times 10^{-6}\left[\frac{2}{3} + \ln\frac{\pi(.665)(30\times10^6)(.875+.177)}{2\ (1-.3^2)}\right]$$

$$C_3 = 0.5241 \times 10^{-6} \text{ in./lb}$$

The gripping angles are then calculated using the iterative procedure as outlined in Steps 1 through 10 (Equations 66 through 75).

FIRST ITERATION

Step 1 from Equation 66 gives the first guess for Ω. Note: Ro, ro, Ri and ri have been used for $\bar{R}o$, $\bar{r}o$, $\bar{R}i$ and $\bar{r}i$ respectively for the first guess.

$$\Omega_1 = \arcsin \frac{(\bar{R}i+\bar{r}i)^2-(Z)^2(\bar{R}o-\bar{r}o)^2}{2\ Z\ (\bar{R}o-\bar{r}o)} - \alpha$$

$$\Omega_1 = \arcsin \frac{(.875+.177)^2-(.0294)^2-(1.203-.178)^2}{2\ (.0294)\ (1.203-.178)} - 49.821$$

$$\Omega_1 = 16.5445^{\circ}$$

Step 2 from Equation 67 gives the first guess for ψ. Note: again on the first guess, the undeflected values of Ri and ri have been used for the deflected values.

$$\psi_1 = \arcsin \frac{Z \cos(\alpha+\Omega_1)}{\bar{R}i + \bar{r}i}$$

$$\psi_1 = \arcsin \frac{.0294 \cos(49.821+16.5445)}{(.875+.177)}$$

$$\psi_1 = .6419^{\circ}$$

The first guess for outer gripping angle is found from Equation 68, Step 3, as

$$W_1 = \arctan \frac{\bar{R}i \sin \psi_1}{\bar{R}o-\bar{R}i \cos \psi_1}$$

$$W_1 = \arctan \frac{.875 \sin .6419}{1.203-.875 \cos .6419}$$

$$W_1 = 1.7116^{\circ}$$

The first guess for inner gripping angle is found from Equation 69, Step 4, as

$$V_1 = W_1 + \psi_1 = 1.7116 + .6419$$

$$V_1 = 2.3535^{\circ}$$

The angles Ω_1, ψ_1, W_1, and V_1, as calculated above, represent the no-load or overrunning values of the sprag geometry. The procedure is then continued as follows:

The first guess of the inner normal sprag load is found from Equation 70, Step 5, as

$$Ni = \frac{T \text{ ctn } V_1}{\bar{R}i \ N} = \frac{2360 \text{ ctn } 2.3535}{.875 \ (18)} = 3650 \text{ lbs}$$

The first guess of the outer normal sprag load is found from Equation 71, Step 6, as

$$No = \frac{T \text{ ctn } W_1}{\bar{R}o \ N} = \frac{2360 \text{ ctn } 1.7116}{1.203 \ (18)} = 3650 \text{ lbs}$$

The first guess of the deflected inner shaft radius is found from Equation 72, Step 7, as

$$\bar{R}i = Ri - CiNi - \frac{Ni}{2}(C_3 - C_1 \ln Ni)$$

$$\bar{R}i = .875 - .979 \times 10^{-6}(3650) - \frac{3650}{2} \times 10^{-6} \qquad (.5241 - .029 \ln 3650)$$

$$\bar{R}i = .875 - .003573 - .000522 = .870905$$

The first guess of the deflected inner cam sprag radius is found from Equation 73, Step 8, as

$$\bar{r}i = ri - \frac{CsNi}{2} - \frac{Ni}{2}(C_3 - C_1 \ln Ni)$$

$$\bar{r}i = .177 - \frac{.0847 \times 10^{-6}(3650)}{2} - \frac{3650}{2} \times 10^{-6} \qquad (.5241 - .029 \ln 3650)$$

$$\bar{r}i = .177 - .000154 - .000522 = .176324$$

The first guess of the deflected outer housing radius is found from Equation 74, Step 9, as

$$\bar{R}o = Ro + \Delta cent + CoNo + \frac{No}{2}(C_2 - C_1 \ln No)$$

$$\bar{R}o = 1.203 + .000280 + 1.381x10^{-6}(3650) + \frac{3650}{2} x10^{-6}$$

$$(.5233-.029\ln 3650)$$

$$\bar{R}o = 1.203 + .000280 + .005041 + .000521 = 1.208842$$

The first guess of the deflected outer cam sprag radius is found from Equation 75, Step 10, as

$$\bar{r}o = ro - \frac{CsNo}{2} - \frac{No}{2} (C_2-C_1 \ln No)$$

$$\bar{r}o = .178 - \frac{.0847x10^{-6}(3650)}{2} - \frac{3650}{2} (10^{-6})$$

$$(.5233-.029 \ln 3650)$$

$$\bar{r}o = .178 - .000155 - .000521 = .177324$$

This procedure is now repeated using the values of $\bar{R}i$, $\bar{r}i$, $\bar{R}o$, and $\bar{r}o$ that have just been calculated. Table 18 summarizes the results of this procedure for seven trials.

From Table 18, it is seen that the gripping angles V and W (Figure 40) are quite close to their final values after the fourth iteration and do not change (to three decimals) after the seventh iteration. Thus, the full load (1500 hp, 20,000 rpm) gripping angles are

V = 4.200 = gripping angle on inner race
W = 3.037 = gripping angle on outer race

Solving Equation 49 for Fi and Fo, and using deflected values in place of undeflected radii,

$$Fi = \frac{T}{\bar{R}i\ N} = \frac{2360}{.8727(18)} = 150 \text{ lb} = \text{tangential load on inner race}$$

$$Fo = \frac{T}{\bar{R}o\ N} = \frac{2360}{1.2064(18)} = 109 \text{ lb} = \text{tangential load on outer race}$$

TABLE 18. SUMMARY OF ITERATIONS TO OBTAIN SPRAG CLUTCH GRIPPING ANGLES AND LOADS.

		First	Second	Third	Fourth	Fifth	Sixth	Seventh
Ω	(deg)	16.5445	-18.2062	-3.8276	-6.9136	-6.0611	-6.2617	-6.2398
ψ	(deg)	.6419	1.3699	1.1150	1.1761	1.1595	1.1634	1.1630
W	(deg)	1.7116	3.5231	2.9192	3.0682	3.0281	3.0376	3.0366
V	(deg)	2.3535	4.8930	4.0342	4.2443	4.1876	4.2010	4.1996
Ni	(lb)	3650	1760	2130	2020	2050	2045	2046
No	(lb)	3650	1760	2130	2020	2050	2048	2049
$\bar{R}i$	(in.)	.87091	.87301	.87260	.87272	.87269	.87270	.87270
$\bar{r}i$	(in.)	.17632	.17666	.17659	.17661	.17660	.17660	.17660
$\bar{R}o$	(in.)	1.20884	1.20598	1.20654	1.20639	1.20642	1.20642	1.20642
$\bar{r}o$	(in.)	.17732	.17766	.17759	.17761	.17760	.17760	.17760

Examining Figure 40, the normal forces are found as

$Ni = Fi \text{ ctn } V = 150 \text{ ctn } 4.200 = 2050 \text{ lb} =$ normal load on inner race

$No = Fo \text{ ctn } W = 109 \text{ ctn } 3.037 = 2050 \text{ lb} =$ normal load on outer race

These load values are used for the remainder of the analysis.

Calculation of Hertz Stress

The Hertz stress between the sprag and the outer shaft are calculated from Equation 79.

$$f_{co} = \sqrt{\frac{No\ E}{2\pi\ell(1-\nu^2)}\left[\frac{Ro-ro}{Roro}\right]}$$

$$f_{co} = \sqrt{\frac{2050(30\times10^6)}{2\pi(.665)(1-.3^2)}\left[\frac{1.203-.178}{(1.203)(.178)}\right]}$$

$$f_{co} = 278{,}300 \text{ psi}$$

The Hertz stress between the sprag and the inner shaft are calculated from Equation 80.

$$f_{ci} = \sqrt{\frac{Ni\ E}{2\pi\ell(1-\nu^2)}\left[\frac{Ri+ri}{Riri}\right]}$$

$$f_{ci} = \sqrt{\frac{2050(30\times10^6)}{2\pi(.665)(1-.3^2)}\left[\frac{.875+.177}{(.875)(.177)}\right]}$$

$$f_{ci} = 331{,}500 \text{ psi}$$

The allowable Hertz stress for carburized materials is 450,000 psi for the sprag clutch.

$$M.S. = \frac{f_{c\ allow}}{f_{ci}} - 1 = \frac{450{,}000}{331{,}500} - 1$$

$$M.S. = +.36$$

Calculation of Inner-Shaft Hoop Stress

The pressure on the inner shaft from the sprag's normal load is calculated from Equation 83.

$$p_i = \frac{-T \cot V}{2\pi \ell \ Ri^2} = \frac{2360 \cot 4.200}{2\pi(.665)(.875)^2}$$

$$p_i = -10{,}050 \text{ psi}$$

The hoop stress (compression) of the inner shaft is found from Equation 84.

$$f_i = p_i \left[\frac{2Ri^2}{Ri^2-Rid^2}\right] = -10{,}050 \left[\frac{2(.875)^2}{.875^2-.625^2}\right]$$

$$f_i = -41{,}040 \text{ psi}$$

The inner shaft is manufactured from AISI 9310 steel, case-carburized, and heat-treated to 136,000-psi minimum tensile strength, Rc 30, core hardness. For this steel,

$$F_{tu} = 136{,}000 \text{ psi}$$
$$F_{ty} = 115{,}000 \text{ psi}$$

$$M.S. = \frac{F_{ty}}{1.15 f_i} - 1$$

$$M.S. = \frac{115{,}000}{1.15(41{,}040)} - 1 = 1.44$$

Calculation of Outer-Race Hoop Stress

The pressure on the outer shaft from the sprag normal loads is found from Equation 88.

$$p_o = \frac{T \cot W}{2\pi \ell \ Ro^2} = \frac{2360 \cot 3.037}{2\pi(.665)(1.203)^2}$$

$$p_o = 7360 \text{ psi}$$

The hoop stress (tension) of the outer shaft is found from Equation 89.

$$f_o = p_o \left[\frac{Rod^2+Ro^2}{Rod^2-Ro^2}\right]$$

$$f_o = 7360\left[\frac{1.525^2+1.203^2}{1.525^2-1.203^2}\right]$$

$$f_o = 31{,}600 \text{ psi}$$

The outer shaft is manufactured from AISI 9310 steel, case-carburized, and heat-treated to 136,000-psi minimum tensile strength, Rc 30, core hardness. For this steel,

$$Ftu = 136{,}000 \text{ psi}$$
$$Fty = 115{,}000 \text{ psi}$$

$$M.S. = \frac{Fty}{1.15\, f_o} - 1$$

$$M.S. = \frac{115{,}000}{1.15(31{,}600)} - 1$$

$$M.S. = + 2.16$$

Calculation of Sprag Rise

The deflections of the sprags and the races are calculated from the normal loads and deflection influence coefficients as

$\Delta cent = .000280$ in. = radial growth of outer housing from centrifugal force

The radial growth of the outer shaft is found from Equation 55 as

$$\Delta_o = CoNo = 1.381 \times 10^{-6}(2050) = .002831 \text{ in.}$$

The radial deflection of the inner shaft is found from Equation 56 as

$$\Delta i = CiNi = 0.979 \times 10^{6}(2050) = .002007 \text{ in.}$$

The compression of the sprag is calculated using Equation 57.

$$\Delta sprag = CsNi = .0847 \times 10^{-6}(2050) = .000174 \text{ in.}$$

The Hertzian deflection of the sprag to outer shaft contact point is found from Equation 58.

$$\Delta Ho = No(C_2 - C_1 \ln No) = 2050(10^{-6})(.5233 - .029 \ln 2050)$$

$$\Delta Ho = .000619 \text{ in.}$$

The Hertzian deflection of the sprag to inner shaft contact point is found from Equation 59.

$$\Delta Hi = Ni(C_3 - C_1 \ln Ni) = 2050(10^{-6})(.5241 - .029 \ln 2050)$$

$$\Delta Hi = .000621 \text{ in.}$$

The total deflection is found from Equation 76 as

$$\Delta total = \Delta cent + \Delta o + \Delta i + \Delta sprag + \Delta Ho + \Delta Hi$$

$$\Delta total = .00028 + .00283 + .00201 + .00017 + .00062 + .00062$$

$$\Delta total = .00653$$

The sprag rise is .013 (Table 8)

$$\% \text{ of sprag rise} = \frac{\Delta total}{S.R.} = \frac{.00653}{.013}$$

$$\% \text{ of sprag rise} = 50.2\%$$

which is the design objective

DESIGN EXAMPLE, RAMP ROLLER CLUTCH

The ramp roller clutch assembly used in Contract DAAJ02-74-C-0028 is depicted in Figure 70.

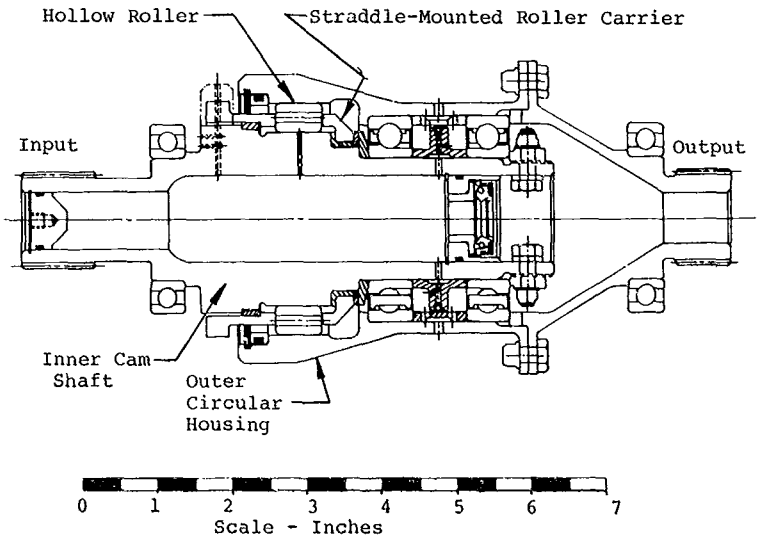

Figure 70. Ramp Roller Clutch Assembly.

Calculation of Roller Contact Angle

The first step in the calculation of roller contact angle is to calculate the section properties and influence coefficients for the outer housing. Refer to Figure 71 for the basic dimensions.

The housing cross sectional area is

$$Ah = (.372)(.397)+(.314)(.448) = .2884 \text{ in.}^2$$

The centroid is calculated as

$$\bar{X} = \frac{\Sigma Ai Xi}{\Sigma Ai} = \frac{(.372)(.397)(.372/2)+(.314)(.448)(.314/2)}{.2884}$$

$$\bar{X} = .172$$

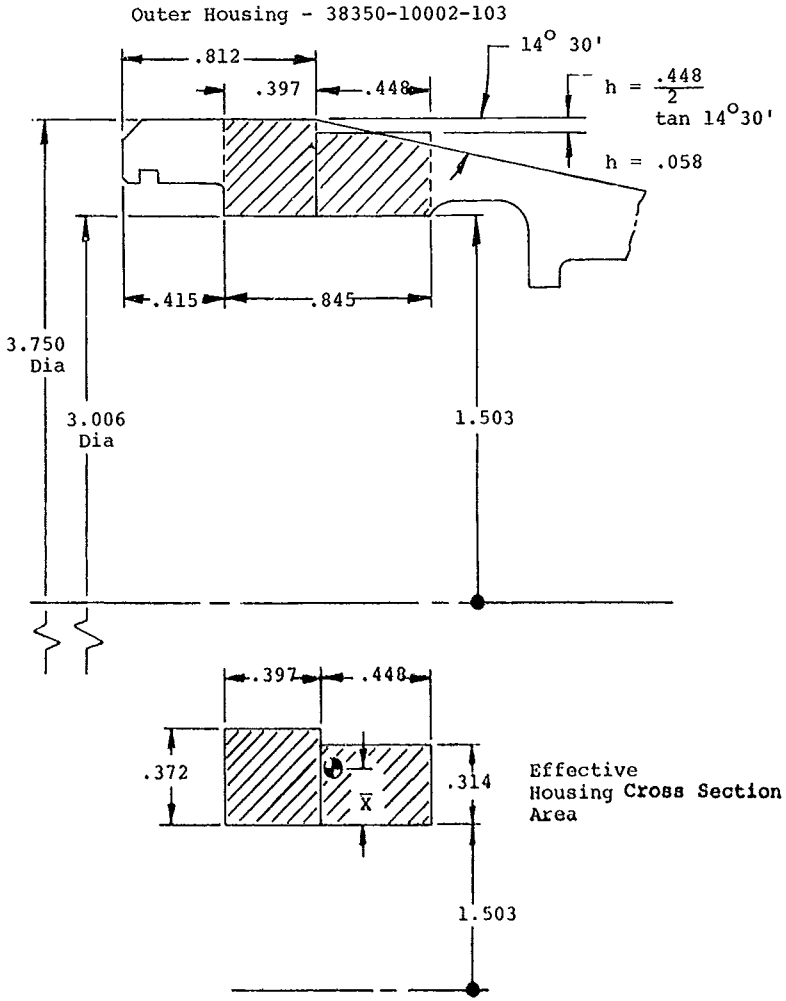

Figure 71. Ramp Roller Clutch Outer Housing Dimensions.

The housing centroidal radius is

$$\bar{R} = 1.503 + X = 1.503 + .172 = 1.675 \text{ in.}$$

The housing moment of inertia about the center of gravity is

$$Ih = \frac{(.397)(.372)^3}{12} + (.397)(.372)(.014)^2 + \frac{(.448)(.314)^3}{12} + (.448)(.314)(.015)^2$$

$$Ih = .00292 \text{ in.}^4$$

$$\theta = \frac{\pi}{n} = \frac{\pi}{14}$$

The constant, A, is calculated from Equation 101 as

$$A = \frac{\theta}{\sin^2\theta} + \cot\theta - \frac{2}{\theta} = \frac{\pi}{14\sin^2(\pi/14)} + \cot\frac{\pi}{14} - \frac{2x14}{\pi}$$

$$A = .000507$$

The constant, B, is calculated from Equation 102 as

$$B = \frac{\theta}{\sin^2\theta} + \cot\theta = \frac{\pi}{14\sin^2(\pi/14)} + \cot\frac{\pi}{14}$$

$$B = 8.91318$$

The constant, C, is calculated from Equation 103 as

$$C = \frac{\theta}{\sin^2\theta} - \cot\theta = \frac{\pi}{14\sin^2(\pi/14)} - \cot\frac{\pi}{14}$$

$$C = .15061$$

Next, the influence coefficient for the outer housing is found using Equation 99.

$$CR = \frac{A\,\bar{R}^3}{4\,E\,Ih} + \frac{B\,\bar{R}}{4\,E\,Ah} + \frac{3\,C\,\bar{R}}{10\,G\,Ah}$$

for steel,

$E = 29x10^6$ psi = Young's modulus
$G = 11x10^6$ = shear modulus

$$CR = \frac{.000507(1.675)^3}{4(29x10^6(.00292)} + \frac{8.91318(1.675)}{4(29x10^6(.2884)} +$$

$$\frac{3(.15061)(1.675)}{10(11x10^6)(.2884)}$$

$$CR = .477 \times 10^{-6}$$

The next step is to calculate the section properties and influence coefficients for the cam. Refer to Figure 72 for basic dimensions.

The cam cross section area is

$$Ak = (.092)(.500) + (.908)(.563) + (.18)(.375) =$$

$$.6247 \text{ in.}^2$$

The centroid is calculated by

$$\bar{X} = \frac{\Sigma AiXi}{\Sigma Ai}$$

$$\bar{X} = \frac{.092(.500)(.500/2) + .908(.536)(.563/2) +}{.6247}$$

$$\frac{.18(.375)(.375/2)}{.6247}$$

$$\bar{X} = .269$$

The cam centroidal radius is

$$\bar{R} = .562 + X = .562 + .269 = .831 \text{ in.}$$

The cam moment of inertia about the center of gravity is found by

$$Ik = \frac{.092(.500)^3}{12} + (.092)(.500)(.019)^2 + \frac{.908(.563)^3}{12} +$$

$$(.908)(.563)(.012)^2 + \frac{.18(.375)^3}{12} + (.18)(.375)(.0815)^2$$

$$Ik = .01579 \text{ in.}^4$$

Cam Shaft - 38350-10001-042

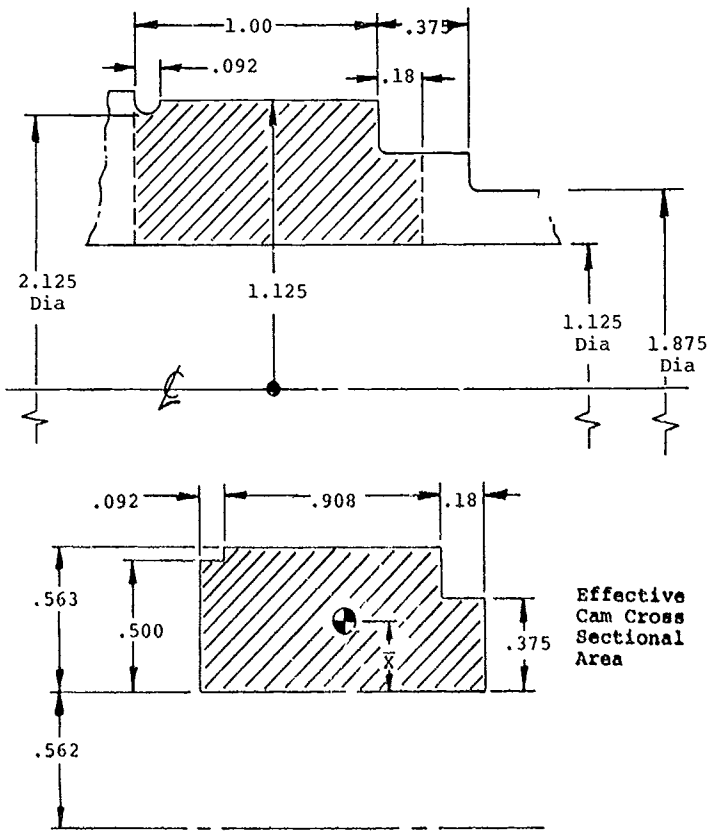

Figure 72. Ramp Roller Clutch Cam Shaft Dimensions.

The cam influence coefficient is calculated using Equation 100.

$$Ck = \frac{A\,\bar{K}^3}{4\,E\,Ik} + \frac{B\,\bar{K}}{4\,E\,Ak} + \frac{C\,\bar{K}}{10\,G\,Ak}$$

$$Ck = \frac{.000507\ (.831)^3}{4(29\times10^6)(.01579)} + \frac{8.91318\ (.831)}{4(29\times10^6)(.6247)} + \frac{3(.15061)(.831)}{10(11\times10^6)(.6247)}$$

$$Ck = .108 \times 10^{-6}$$

Next, the roller influence coefficient is found using the roller dimensions shown in Figure 73.

Roller 2439-03750-06245-701-10

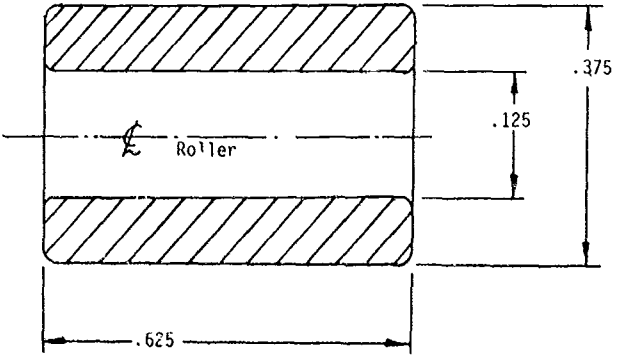

Figure 73. Ramp Roller Clutch Roller Dimensions.

The ratio of inside to outside roller diameter is

$$h = \frac{ID}{OD} = \frac{.125}{.375} = \frac{1}{3}$$

ρ = .1875 in. = roller radius

L = .625 in. = roller length

The constant, rm, is defined as

$$rm = \rho(1+H)/2 = .1875(1.33333)/2 = .125$$

The constant, er, is defined as

$$er = \rho \left[\frac{(1+H)}{2} - \frac{(1-H)}{\ln(1/H)} \right]$$

$$er = .1875 \left[\frac{1.33333}{2} - \frac{.66667}{\ln 3} \right] = .0112$$

The roller influence coefficient is calculated by Equation 104 as

$$C\rho = \frac{rm^2}{\rho(1-H)\ L\ E\ er} \left\{ \frac{\pi}{4} - \frac{2}{\pi} \left[1 - \left[\frac{er}{rm} \right]^2 \right] + \right.$$

$$\left. \frac{2er}{rm} \left[\frac{2}{\pi} \left[1 - \frac{er}{rm} \right] - \frac{\pi}{8} \right] + \frac{15\pi er}{16\ rm} \right\}$$

$$C\rho \quad \frac{(.125)^2}{.1875(.6667)(.625)(29x10^6)(.0112)}$$

$$\left\{ \frac{\pi}{4} - \frac{2}{\pi} \left[1 - \left[\frac{.0112}{.125} \right]^2 \right] + \quad \frac{2x.0112}{.125} \right.$$

$$\left. \left[\frac{2}{\pi} \left[1 - \frac{.0112}{.125} \right] - \frac{\pi}{8} \right] + \frac{15\pi.0112}{16\ x\ .125} \right\}$$

$$C\rho = .2778 \times 10^{-6}$$

n = 14 rollers
rpm = 20,000
hp = 1500

$$T = \frac{63{,}025\ hp}{rpm} = \frac{63{,}025(1500)}{20{,}000} = 4730\ in.\text{-}lb =$$

clutch design torque

Summarizing the basic data required to calculate load

$$R = 1.503 \qquad CR = .477 \times 10^{-6}$$
$$K = 1.125 \qquad Ck = .108 \times 10^{-6}$$
$$\rho = .1875 \qquad C\rho = .278 \times 10^{-6}$$

$$(-R+K+2\rho) = -.003$$

$$(CR+Ck+2C\rho) = 1.141 \times 10^{-6}$$

From Equation 107, the function of Pi is

$$f(Pi) = \frac{T^2(R+K)}{n^2 R^2} + Pi^2 (-R+K+2\rho) - Pi^3 (CR+Ck+2C\rho)$$

$$f(Pi) = \frac{(4730)^2(2.628)}{(14)^2 (1.503)^2} + Pi^2(-.003) - Pi^3(1.141 \times 10^{-6})$$

$$f(Pi) = 132{,}792 - .003Pi^2 - 1.141 \times 10^{-6} Pi^3$$

From Equation 108, the derivative of the function is

$$f'(Pi) = 2Pi\ (-R+K+2\rho) - 3Pi^2\ (CR+Ck+2C\rho)$$

$$f'(Pi) = -.006\ Pi - 3.423 \times 10^{-6} Pi^2$$

An iterative procedure is now used to calculate the roller, normal load P. The procedure is summarized by Equation 109 with i varying as 1, 2, 3, etc., until successive values of the load, P, are within the desired accuracy.

Trial #1, i = 1

The first guess for roller load is

$$\text{Assume } P_1 = \frac{T}{.05nR} = \frac{4730}{.05(14)(1.503)} = 4490 \text{ lb}$$

The function of P_1 is found from Equation 107 as

$$f(P_1) = 132{,}792 - .003(4490)^2 - 1.141 \times 10^{-6}(4490)^3 = -30{,}970$$

The derivative of the function is found from Equation 108 as

$$f'(P_1) = -.006(4490) - 3.423 \times 10^{-6}(4490)^2 = -95.9$$

The second guess (i+1=2) is found from Equation 109 as

$$P_2 = P_1 - \frac{f(P_1)}{f'(P_1)} = 4490 - \frac{(-30{,}970)}{(-95.9)}$$

$$P_2 = 4167 \text{ lb}$$

Trial #2, i=2

The procedure is repeated for i=2.

$$f(P_2) = 132{,}792 - .003\,(4167)^2 - 1.141\text{x}10^{-6}\,(4167)^3 = -1857$$

$$f'(P_2) = -.006(4167) - 3.423\text{x}10^{-6}\,(4167)^2 = -84.4$$

The third guess of the roller load is

$$P_3 = P_2 - \frac{f(P_2)}{f'(P_2)} = 4167 - \frac{(-1857)}{(-84.4)}$$

$$P_3 = 4145 \text{ lb}$$

Trial #3, i=3

$$f(P_3) = 132{,}792 - .003(4145)^2 - 1.141\text{x}10^{-6}\,(4145)^3 = -8.$$

$$f'(P_3) = -.006(4145) - 3.423\text{x}10^{-6}(4145)^2 = -83.7$$

The fourth guess for the roller load is

$$P_4 = P_3 - \frac{f(P_3)}{f'(P_3)} = 4145 - \frac{(-8)}{(-83.7)}$$

$$P_4 = 4145 \text{ lb}$$

Hence, the roller load is 4162 lb since the third and fourth answer were the same (within 1-lb error)

$$P = 4162 \text{ lb} = \text{roller normal load}$$

From Equation 95, F is found by

$$F = \frac{T}{nR} = \frac{4730}{14(1.503)} = 225 \text{ lb} = \text{roller tangential load}$$

and finally the full load nip angle is calculated from Equation 105.

$$\tan \frac{\psi f}{2} = \frac{F}{P} = \frac{225}{4145} = .05428$$

$$\psi f = 6^{o}13' = \text{roller contact angle at 1500 hp}$$

Calculation of Outer Housing Hoop Stress

n	=	14 rollers
P	=	4145 lb = normal roller load @ 1500 hp
F	=	225 lb = tangential roller load @ 1500 hp
$\bar{R}$	=	1.675 in. = housing radial c.g.
RS	=	1.62 in. = assumed shear radius
T	=	4730 in.-lb = torque @ 1500 hp and 20,000 rpm
Ah	=	.2884 $in.^2$ = effective housing area
Ih	=	.00292 $in.^4$ = effective housing moment of inertia
$\bar{y}o$	=	.200 in. = distance from c.g. to outer fiber
$\bar{y}i$	=	.172 in. = distance from c.g. to inner fiber

The internal bending moment is found from Equation 111.

$$MB = -\frac{P\bar{R}}{2}\left[\frac{1}{\theta} - \frac{\cos\beta}{\sin\theta}\right] - \frac{F\bar{R}}{2}\frac{\sin\beta}{\sin\theta} + \frac{T\beta}{2\pi}$$

The internal axial force is found from Equation 112 as

$$PA = +\frac{P}{2}\frac{\cos\beta}{\sin\theta} - \frac{F}{2}\frac{\sin\beta}{\sin\theta}$$

The internal shear force is calculated from Equation 113 as

$$Vs = -\frac{P}{2}\frac{\sin\beta}{\sin\theta} - \frac{F}{2}\frac{\cos\beta}{\sin\theta} + \frac{T}{2\pi RS}$$

$$\theta = \pi/14$$

The internal loads are evaluated within the range from

$$\beta = +\frac{\pi}{n} \text{ to } \beta = -\frac{\pi}{n}$$

Figure 74 shows the results. The highest load condition occurs at $\beta = -\pi/14$. At this point

MB	=	-241 in.-lb (compression on outer fiber)
PA	=	9190 lb
Vs	=	2040 lb

The critical stress is on the inside of the housing, where the bending adds to the tension. The section modulus at this point is

$$Zhi = \frac{I_H}{\bar{y}i} = \frac{.00292}{.172} = .0170 \text{ in.}^3$$

The bending stress is found from Equation 114 as

$$f_{bi} = \frac{MB}{Zhi} = \frac{241}{.0170} = +14{,}180 \text{ psi}$$

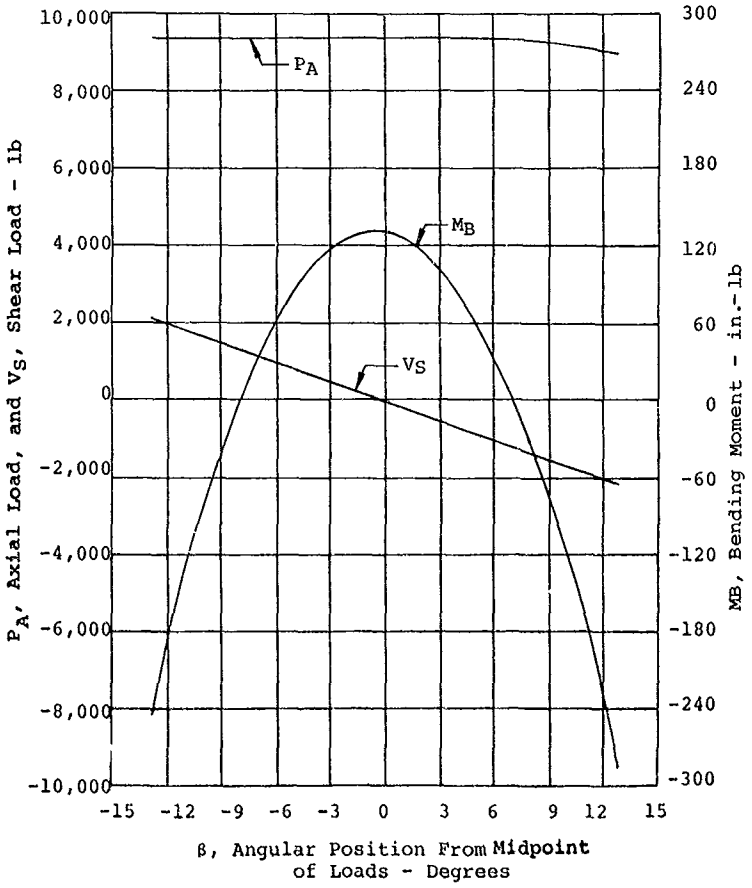

Figure 74. Outer Housing Internal Loads.

The axial stress is found from Equation 115 as

$$fa = \frac{PA}{Ah} = \frac{9190}{.2884} = 31{,}800 \text{ psi}$$

The shear stress is found from Equation 116 as

$$fs = \frac{Vs}{Ah} = \frac{2040}{.2884} = 7070 \text{ psi}$$

The housing is manufactured from AISI 9310 steel, case-carburized and heat-treated to 136,000-psi minimum tensile strength (Rc 30) core hardness. For this steel,

Ftu = 136,000 psi
Fty = 115,000 psi

$$M.S. = \frac{Fty}{1.15\sqrt{(fa+fb)^2+(2\ fs)^2}} - 1$$

$$M.S. = \frac{115{,}000}{1.15\sqrt{(31{,}800+14{,}180)^2+(2x7070)^2}} - 1$$

M.S. = +1.08

Calculation of Cam Compressive Stress

Basic Data

n	=	14 rollers
K	=	1.125 in. = cam flat dimension
R	=	1.503 in. = outer housing bore radius
ρ	=	.1875 in. = roller radius
ψf	=	$6^{o}13'$ = full load roller contact angle
P	=	4145 lb = normal roller load @ 1500 hp
F	=	225 lb = tangential roller load @ 1500 hp
$\bar{R}$	=	.831 in. = cam radial c.g.
RS	=	.80 in. = assumed shear radius
T	=	4730 in.-lb = torque @ 1500 hp and 20,000 rpm
Ak	=	.6247 $in.^2$ = effective cam area
Ik	=	.0158 $in.^4$ = effective cam moment of inertia
$\overline{yo}$	=	.294 in. = distance from c.g. to outer fiber
$\overline{yI}$	=	.269 in. = distance from c.g. to inner fiber

Next, the cam applied loads are found from Equation 115.

$$d = (R-\rho) \sin \psi f = (1.503 - .1875) \sin 6^{o}13'$$

d = .1425

From Equation 116,

$$\tan \gamma = \frac{d}{\bar{K}} = \frac{.1425}{1.125} = .12667$$

$$\sin \gamma = .12566$$

$$\cos \gamma = .99207$$

The cam applied normal load is found from Equation 120.

$$Pc = P \cos \gamma + F \sin \gamma$$

$$Pc = 4145\ (.99207) + 225\ (.12566)$$

$$Pc = 4140 \text{ lb}$$

The cam applied tangential load is found from Equation 121.

$$Fc = P \sin \gamma - F \cos \gamma$$

$$Fc = 4145\ (.12566) - 225\ (.99207)$$

$$Fc = 296 \text{ lb}$$

The cam applied moment is found from Equation 122.

$$Mc = Fc \left[\frac{K}{\cos \gamma} - \bar{K} \right]$$

$$Mc = 296 \left[\frac{1.125}{.99207} - .831 \right]$$

$$Mc = 90.3 \text{ in.-lb}$$

The next step is to calculate the internal cam loads, which must be evaluated in the range from $\beta = +\pi/N$ to $\beta = -\pi/N$. The equations used are 123, 124 and 125 and are summarized below.

$$MB = + \frac{Pc\ \bar{K}}{2} \left[\frac{1}{\theta} - \frac{\cos\beta}{\sin\theta} \right] + \frac{Fc\ \bar{K}}{2} \frac{\sin\beta}{\sin\theta} - \frac{T\ \beta}{2\pi} =$$

internal bending moment

$$PA = - \frac{Pc}{2} \frac{\cos\beta}{\sin\theta} + \frac{Fc}{2} \frac{\sin\beta}{\sin\theta} = \text{internal axial force}$$

$$Vs = + \frac{Pc}{2} \frac{\sin\beta}{\sin\theta} + \frac{Fc}{2} \frac{\cos\beta}{\sin\theta} - \frac{T}{2\pi RS} =$$

internal shear force

$$\theta = \pi/14$$

Substituting in the values of applied loads K and θ for various values of β leads to a series of moments, forces, and shears that are plotted in Figure 75. Figure 75 shows that the highest internal loads are found at $\beta = \pi/14$. At this point

MB = +84 in.-lb = tension on outer fiber
PA = -8920 lb
Vs = +1780 lb

The critical stress is on the inside of the cam, where the bending moment is negative. The section modulus is

$$Zki = \frac{Ik}{\overline{yi}} = \frac{.0158}{.269} = .0587 \text{ in.}^3$$

The bending compression stress on the inner fiber is found from Equation 126.

$$fbi = \frac{MB}{ZKi} = \frac{-84}{.0587} = -1430 \text{ psi}$$

The axial compression stress is found from Equation 127.

$$fa = \frac{PA}{Ak} = \frac{-8920}{.6247} = -14{,}280 \text{ psi}$$

The shear stress is calculated from Equation 128 as

$$fs = \frac{Vs}{Ak} = \frac{+1780}{.6247} = +2850 \text{ psi shear}$$

The cam is manufactured from AISI 9310 steel, case-carburized and heat-treated to 136,000-psi minimum tensile strength (Rc 30) core hardness. For this steel,

Ftu = 136,000 psi
Fty = 115,000 psi

$$M.S. = \frac{Fty}{1.15\sqrt{(fa+fb)^2 + (2fs)^2}} - 1$$

$$M.S. = \frac{115{,}000}{1.15\sqrt{(-14{,}280-1430)^2 + (2x+2850)^2}} - 1$$

M.S. = +5.88

Calculation of Roller Hoop and Hertz Stress

P = 4145 lb = normal roller load @ 1500 hp
L = .625 in. = roller length
ρ = .1875 in. = roller outer radius
ρi = .0625 in. = roller inner radius

The roller hollowness ratio is

$$H = \frac{\rho i}{\rho} = \frac{.0625}{.1875} = .3333$$

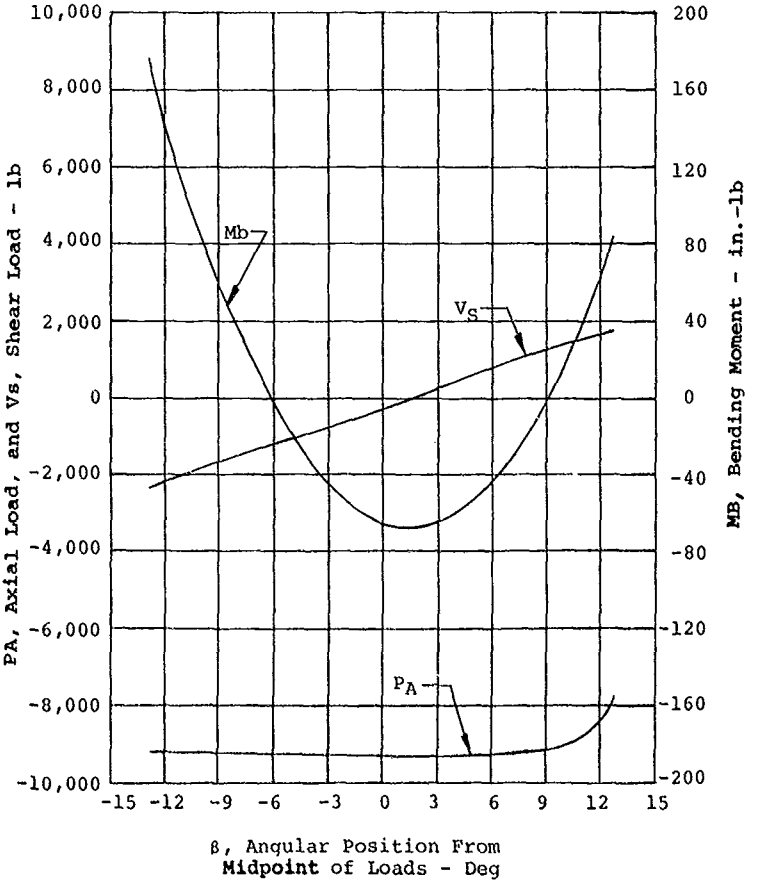

Figure 75. Cam Internal Loads.

The constant, Z, is defined as

$$Z = -1 + \left[\frac{(1+H)}{2(1-H)}\right] \ln \frac{1}{H}$$

$$Z = -1 + \left[\frac{(1+.3333)}{2\ (1-.3333)}\right] \ln 3$$

$$Z = .09861$$

The maximum roller stress from bending is on the inside diameter of the roller, below the load point. At this point, the stress is found from Equation 131 as

$$f = \frac{P}{\pi \rho L}\left[\frac{1}{2\ Z\ H} - \frac{1}{(1-H)}\right]$$

$$f = \frac{4145}{\pi(.1875)(.625)}\left[\frac{1}{2(.09861)(.3333)} - \frac{1}{(1-.3333)}\right]$$

f = 154,000 psi = roller bending stress from 1500 hp load

The roller is manufactured from case-carburizing steel with a case hardness of Rc59 minimum. For this hardness

$$Ftu = 325{,}000$$

$$M.S. = \frac{Ftu}{1.5\ f} - 1 = \frac{325{,}000}{1.5(154{,}000)} - 1$$

$$M.S. = +.41$$

The roller to cam Hertz stress is calculated from Equation 133.

$$fc_{K-\rho} = \sqrt{\frac{P\ E}{2\ \pi\ L\ \rho(1-\nu^2)}}$$

where

E = 30×10^6 psi

ν = .30 = Poisson's ratio

$$fc_{K-\rho} = \sqrt{\frac{4145\ (30 \times 10^6)}{2\pi\ (.625)(.1875)(1-.3^2)}}$$

$fc_{K-\rho}$ = 431,000 psi

The allowable Hertz stress for case-carburized materials is 550,000 psi.

$$M.S. = \frac{fc\ allow}{fc_{K-\rho}} - 1 = \frac{550,000}{431,000} - 1$$

$$M.S. = +.28$$

Calculation of Carrier Resistance Torque

Q	=	carrier torque = rolling resistance torque + viscous friction torque = Qℓ+Qv
do	=	2ρ = .375 = roller O.D.
di	=	2ρi = .125 = roller I.D.
R	=	1.503 in.
d_m	=	(2R-do) = 2(1.503) -.375 = 2.631 = clutch mean diameter
L	=	.625 in. = roller length
ρr	=	.283 lb/in.^{3} = density of steel roller
g	=	386 in./sec^2 = gravitational constant

The centrifugal force per roller is found from Equation 138 as

$$Fc = \rho r \frac{\pi}{4} \frac{(do^2-di^2)}{g} L \left[\frac{d_m}{2}\right] \left[\frac{\pi}{30} \text{ rpm cam}\right]^2$$

$$Fc = .283 \frac{\pi}{4} \frac{(.375^2-.125^2)}{386} (.625) \left[\frac{2.631}{2}\right] \left[\frac{\pi}{30}\right]^2 \text{ rpm cam}^2$$

$$Fc = 6.49 \times 10^{-7} \text{ rpm}_{cam}^2$$

The drag torque from rolling resistance is found from Equation 136 as

$$Q\ell = \mu_1 Fc\ R\ n$$

where

$$\mu_1 = .0003$$
$$Q\ell = (.0003)(6.49\times10^{-7} \text{ rpm}_{cam}^2)(1.503)(14)$$
$$Q\ell = 4.097\times10^{-9} \text{ rpm}_{cam}^2$$

The drag torque from viscous friction is found from Equation 139 as

$$Qv = 1.42\times10^{-5}\ fo\ d_m^3 \left[\nu_o\ \Delta_{rpm}\right]^{2/3}$$

where

$$fo = 6$$
$$\nu_o = 3.0 \text{ centistokes for MIL-L-7808 @ } 210^oF$$
$$Qv = 1.42\times10^{-5}\ (6)\ (2.631)^3\ (3.0)^{2/3}\ (\Delta rpm)^{2/3}$$
$$Qv = .00323\ (\Delta rpm)^{2/3}$$

Assuming the housing is rotating at 20,000 rpm, the cam/housing differential speed is given by

$$\Delta rpm = 20{,}000 - rpm_{cam}$$

Figure 76 shows Qℓ, Qv, and Q versus cam rpm with the outer housing at 20,000 rpm. As shown, the highest total cage torque occurs when the cam is at rest. At this point, the total torque is 2.38 inch-pounds. The pin and spring assembly is then designed to exceed this torque.

Calculation of the Pin and Spring Loads

The geometry of the pin and spring mechanism is shown in Figure 77. From the figure

T	=	.812 in.
fs	=	1.25 in.
S	=	.563 in.
Ks	=	3.2 lb/in. spring rate
L	=	.625 in.
hs	=	.478 in. = spring solid height
ℓ	=	.625 in. (through hole)
do	=	.120 in. = spring O.D.
D	=	.125 in.
dw	=	.016 in. = spring wire diameter
d	=	.0625 in.
ρs	=	.283 lb/in.^{3}
Rp	=	1.252 in.
n	=	2 pin/spring assemblies

The weight of the spring is estimated from Equation 140 as

$$Ws = \rho s \frac{\pi}{4} (do-dw)\, dw\, hs$$

$$Ws = .283 \frac{\pi}{4} (.120-.016)(.016)(.478)$$

$$Ws = .000555 \text{ lb}$$

The spring center of gravity is located by Equation 141 as

$$\overline{Xs} = \frac{T-S+L}{2} = \frac{.812-.563+.625}{2}$$

$$\overline{Xs} = .437$$

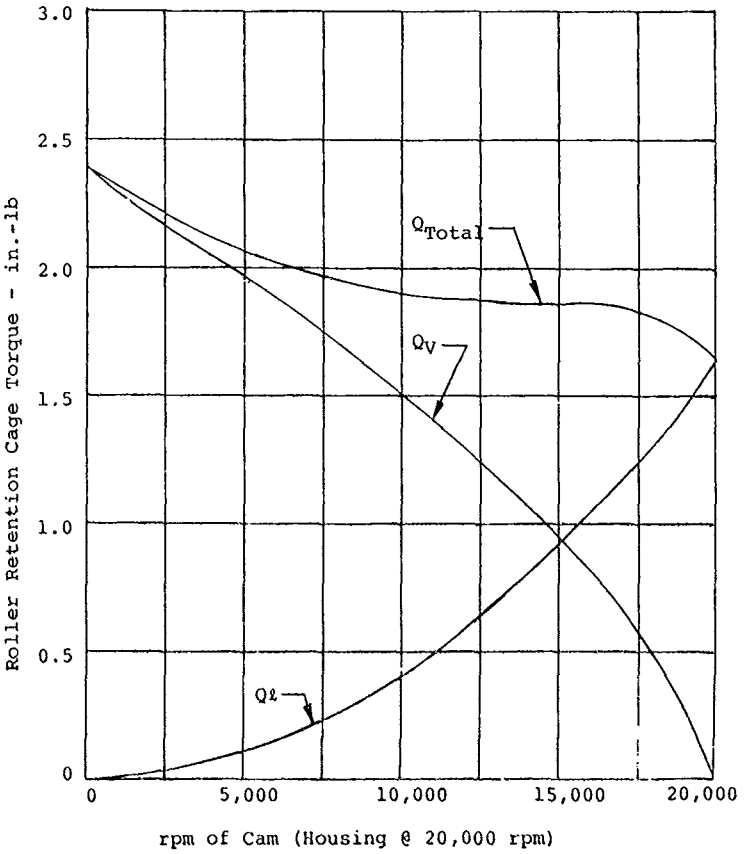

Figure 76. Viscous and Rolling Resistance Torques on Ramp Roller Clutch.

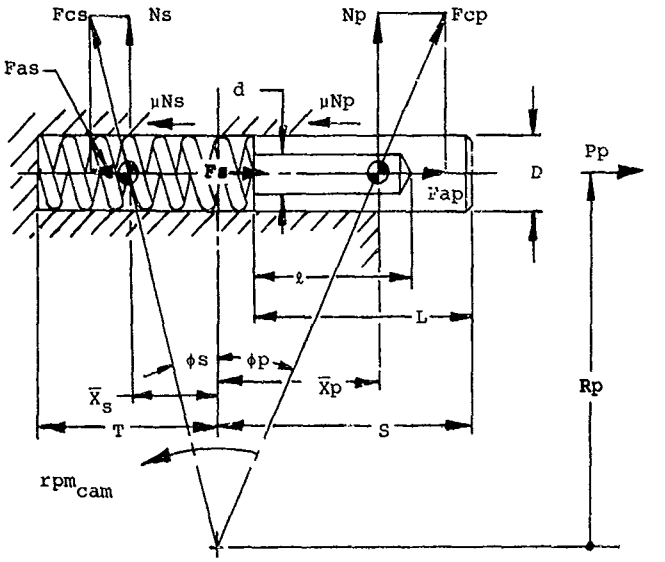

Figure 77. Ramp Roller Clutch Pin and Spring Dimensions.

The centrifugal force acting on the spring is found from Equation 142

$$Fcs = \frac{\pi^2 \, Ws \, rpm^2}{900 \, g} \sqrt{Rp^2 + \bar{X}s^2}$$

$$Fcs = \frac{\pi^2 \, (.00055) \, rpm^2}{900 \, (386)} \sqrt{1.252^2 + .437^2}$$

$$Fcs = 2.091 \times 10^{-8} \, rpm^2$$

The normal spring force is found from Equation 143

$$Ns = Fcs \frac{Rp}{\sqrt{Rp^2 + \bar{X}s^2}}$$

$$Ns = 2.091 \times 10^{-8} \, rpm^2 \frac{1.252}{\sqrt{1.252^2 + .437^2}}$$

$$Ns = 1.974 \times 10^{-8} \, rpm^2$$

The axial spring force is found from Equation 144 as

$$Fas = Ns \frac{\overline{Xs}}{Rp}$$

$$Fas = 1.974x10^{-8} \; rpm^2 \; \frac{.437}{1.252}$$

$$Fas = .689x10^{-8} \; rpm^2$$

Equation 145 is used to calculate the spring force at the installed position.

$$Fs = Ks \; (fs - T - S + L) = 3.2 \; (1.25 - .812 - .563 + .625)$$

$$Fs = 1.600 \text{ lb}$$

The resultant spring force acting on the pin is given by Equation 146.

$$Ps = Fs - (Fas + \mu \, Ns)$$

$$Ps = 1.600 - rpm^2x10^{-8} \; (.689 + 1.974\mu)$$

Note: Ps can never be negative. The speed at which Ps will be zero is found from Equation 147 as

$$rpm_x = \sqrt{\frac{1.6 \times 10^8}{(.689 + 1.974\mu)}}$$

Figure 78 shows a curve of rpm_x versus μ, the coefficient of friction. Generally, .075 will be the value obtained for μ in practice, which corresponds to a speed of 13,830 rpm. Thus, if $\mu = .075$, the spring will be inoperative above cam speeds of 13,830 rpm.

The weight of the pin is found from Equation 148 as

$$Wp = \rho p \; \frac{\pi}{4} \; (D^2L - d^2\ell)$$

$$Wp = .283 \; \frac{\pi}{4} \; (.125^2x.625 - .0625^2x.625)$$

$$Wp = .00163 \text{ lb} = \text{weight of pin}$$

The pin center of gravity is located by Equation 149 as

$$\overline{Xp} = \frac{DL^2 - d\ell^2}{2 \; (DL - d\ell)} + S - L$$

$$\overline{Xp} = \frac{.125x.625^2 - .0625x.625^2}{2 \; (.125x.625 - .0625x.625)} + .563 - .625$$

$$\overline{Xp} = .2505 \text{ in.}$$

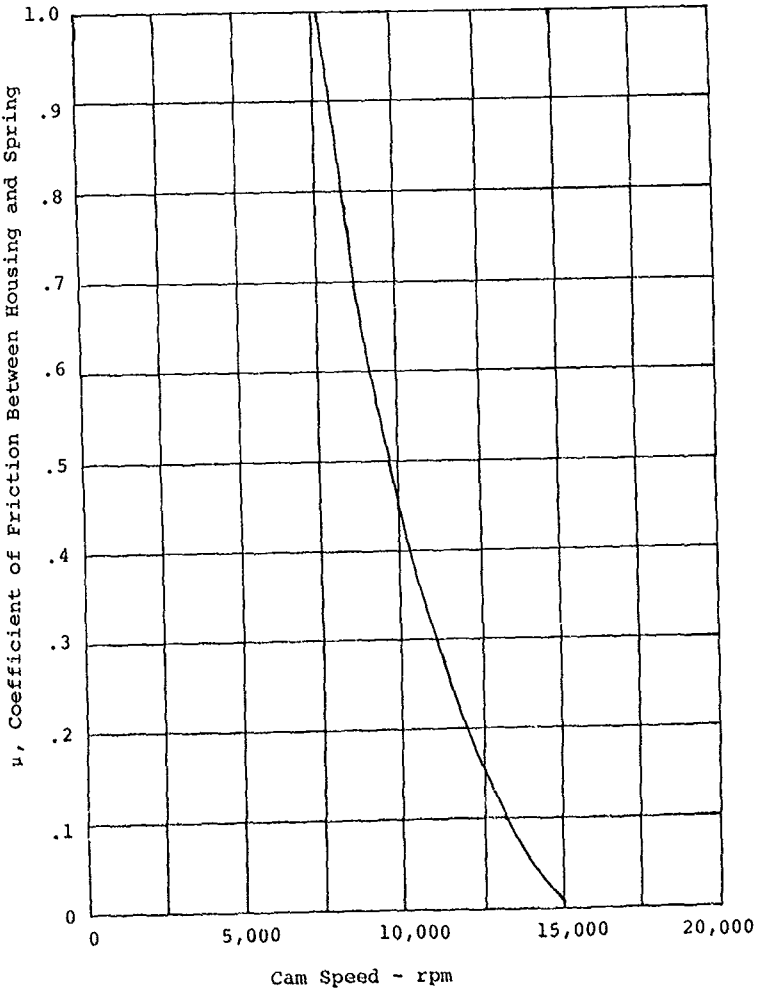

Figure 78. Speed at Which Spring Becomes Inoperative for Various Values of the Coefficient of Friction.

The centrifugal force on the pin is found from Equation 150 as

$$Fcp = \frac{\pi^2 \, Wp \, rpm^2}{900 \, g} \sqrt{Rp^2 + \overline{Xp}^2}$$

$$Fcp = \frac{\pi^2 (.00163) rpm^2}{900 \, (386)} \sqrt{1.252^2 + .2505^2}$$

$$Fcp = 5.913 \times 10^{-8} rpm^2$$

The pin normal force on the housing is found from Equation 151 as

$$Np = Fcp \frac{Rp}{\sqrt{Rp^2 + \overline{Xp}^2}}$$

$$Np = 5.913 \times 10^{-8} rpm^2 \frac{1.252}{\sqrt{1.252^2 + .2505^2}}$$

$$Np = 5.798 \times 10^{-8} rpm^2$$

The pin axial load is determined by Equation 152.

$$Fap = Np \frac{\overline{Xp}}{Rp}$$

$$Fap = 5.798 \times 10^{-8} rpm^2 \frac{.2505}{1.252}$$

$$Fap = 1.160 \times 10^{-8} rpm^2$$

The total load that the pin exerts on the roller carrier is the sum of the total spring load and the total pin load and is found from Equation 153.

$$Pp = Ps + Fap - \mu Np$$

$$Pp = 1.600 - rpm^2 \times 10^{-8} \, (.689 + 1.974\mu) + rpm^2 \times 10^{-8} \, (1.16 - 5.798\mu)$$

The total torque on the carrier is calculated from Equation 154.

$$Tc = n\ Rp\ Pp = 2\ (1.252)\ Pp$$

$$Tc = 2.504\ Pp$$

$$Tc = \underbrace{4.006\text{-}rpm^2x10^{-8}(1.725+4.943\mu)}_{\text{spring contribution}} + \underbrace{rpm^2x10^{-8}(2.905-14.518\mu)}_{\text{pin contribution}}$$

In the above equation, the rpm^2x10^{-8} terms cannot be combined because the spring contribution can reach zero but can never be negative; thus, the form of the equation must remain as is. Substituting various values of the coefficient of friction, μ, and of the rpm of the cam from 0 to 20,000, one obtains a series of curves of carrier torque versus rpm, as depicted in Figure 81. The components of the torque (i.e., the contribution of the spring and the contribution of the pin) are shown in Figures 79 and 80. Figure 82 is a plot of total carrier torque for $\mu = .075$ and resistance torque from viscous drag and rolling friction. Note that the applied cage torque is always greater than the resistance torque, which is the design objective.

Calculation of Flow Requirements

νo = 3.0 centistokes for MIL-L-7808 @ 210°F
rpm = 20,000

Duplex bearings 2MM 9108 WO-CR-DU-E-7236

$$d_m = \frac{do + di}{2} = \frac{2.677 + 1.575}{2} = 2.126$$

The rolling resistance is zero since the loads are zero while the viscous friction is calculated using Equation 171.

$$M\nu = 1.42x10^{-5}\ f_o\ (\nu o\ rpm)^{2/3}\ d_m^3$$

where

f_o = 8 for angular-contact double-row from Table 13
$M\nu = 1.42x10^{-5}\ (8)\ (3x20,000)^{2/3}\ (2.126)^3$
$M\nu$ = 1.67 in.-lb = bearing viscous drag

For the ramp roller clutch rollers

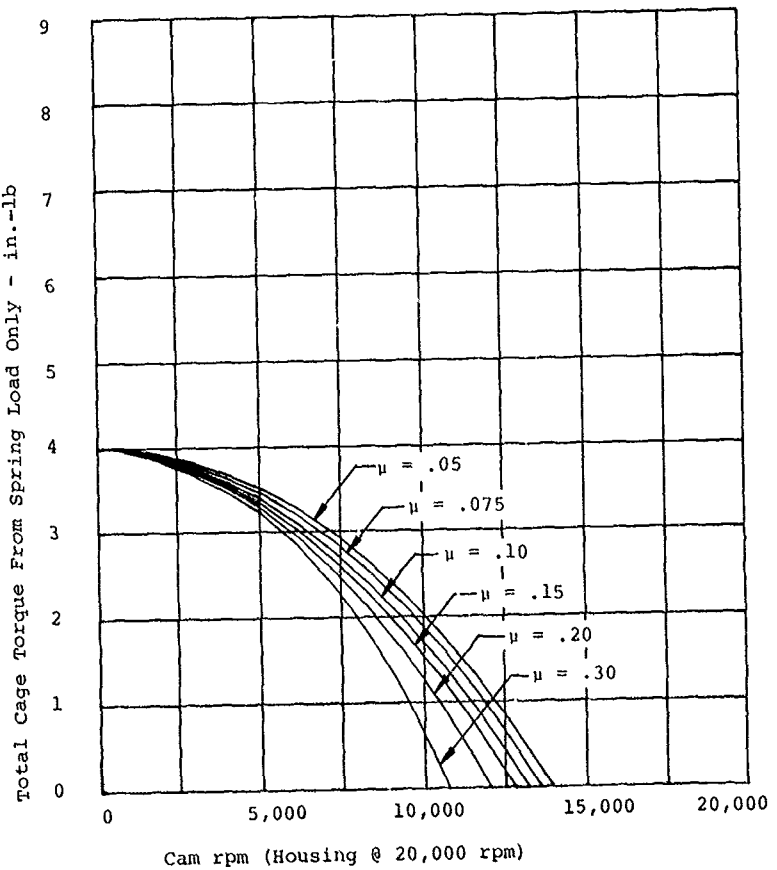

Figure 79. Cage Torque From Spring Load Versus Cam Speed for Ramp Roller Clutch.

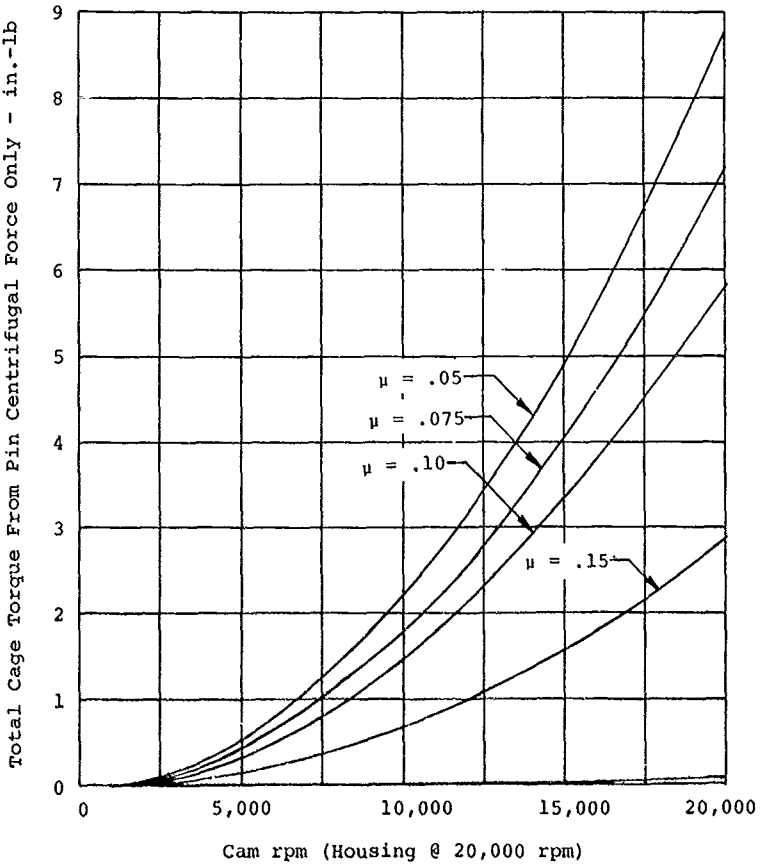

Figure 80. Cage Torque From Pin Centrifugal Force Versus Cam Speed for Ramp Roller Clutch.

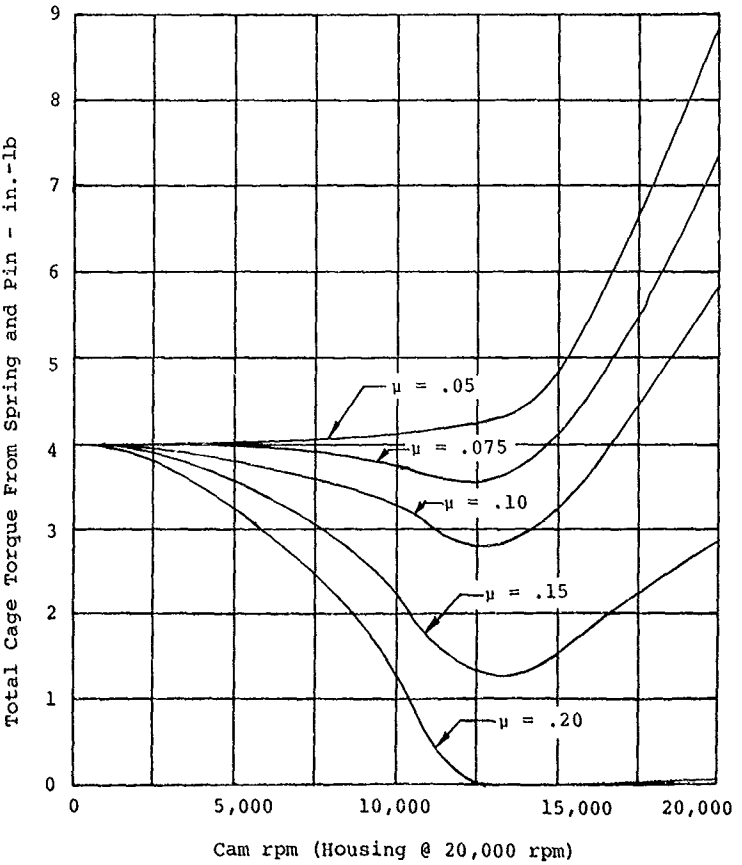

Figure 81. Total Cage Torque From Spring and Pin Versus Cam Speed for Ramp Roller Clutch.

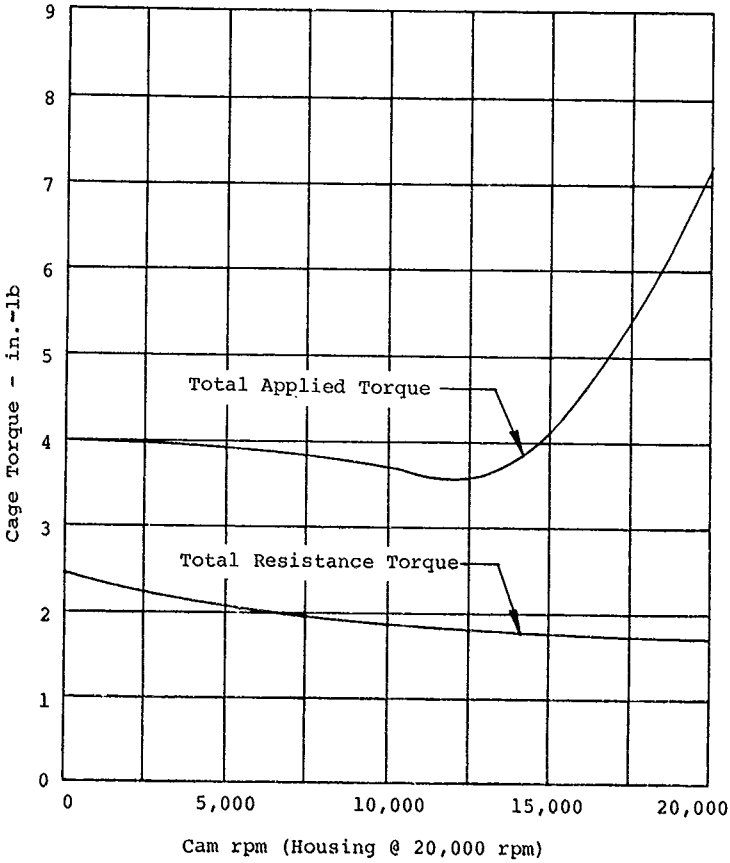

Figure 82. Cage Applied and Resistance Torques Versus Cam Speed for Ramp Roller Clutch.

$$d_m = 2\ (R-\rho) = 2\ (1.503-.1875) = 2.631$$

where

f_o = 20 for rollers of the clutch

The clutch roller drag torque is given by Equation 179 as

$$MRR = 1.42\text{x}10^{-5}\ f_o\ (\nu o\ rpm)^{2/3}\ d_m^{3}$$

$$MRR = 1.42\text{x}10^{-5}\ (20)\ (3\text{x}20{,}000)^{2/3}\ (2.631)^{3}$$

$$MRR = 7.92\ \text{in.-lb}$$

Total drag torque is the sum of bearing torque and clutch torque and is given by Equation 181 as

$$Mt = M\nu + MRR$$

$$Mt = 1.67 + 7.92$$

$$Mt = 9.59\ \text{in.-lb}$$

The heat generated is given by Equation 174 as

$$H = \frac{Mt\ rpm}{1486} = \frac{9.59\ (20{,}000)}{1486}$$

$$H = 129\ \text{btu/min}$$

Assuming a Δt of $40^{\circ}F$ across clutch, the required flow is found from Equation 175 as

$$Q = \frac{.13\ H}{Cp\ \Delta t}$$

$$Cp = .51\ \text{btu/lb}\ ^{\circ}F \text{ for MIL-L-7808}$$

$$Q = \frac{.13(129)}{.51\ (40)}$$

$$Q = 0.82\ \text{gpm}$$

From test data, the 100% flow condition was established at 0.80 gpm, which is in good agreement with the calculated flow.

LITERATURE CITED

1. Kish, Jules G., ADVANCED OVERRUNNING CLUTCH TECHNOLOGY, Sikorsky Aircraft, USAAMRDL Technical Report 77-16, Eustis Directorate, U. S. Army R & D Laboratory, Fort Eustis, Virginia (to be published).

2. Lynwander, P., Meyer, A. G., Chachakis, S., SPRING OVERRIDING AIRCRAFT CLUTCH, Avco Lycoming Division, USAAMRDL Technical Report 73-17, Eustis Directorate, U. S. Army R & D Laboratory, Fort Eustis, Virginia, May 1973, AD 769064.

3. Roark, Raymond J., and Young, Warren C., FORMULAS FOR STRESS AND STRAIN, McGraw Hill Book Co., New York, Fifth Edition, 1975.

4. Herger, O. J., FATIGUE TESTS OF SOME MANUFACTURED PARTS, Proceeding of the Society for Experimental Stress Analysis, Vol III, No. II, 1946.

5. Seeley, Fred B., and Smith, James O., ADVANCED MECHANICS OF MATERIALS, Second Edition, New York, John Wiley and Sons, Inc., 1966, pp 177-182.

6. SKF Computer Program AE66Y004, ANALYSIS OF DYNAMIC PERFORMANCE CHARACTERISTICS OF CYLINDRICAL ROLLER BEARING UNDER RADIAL LOAD, King of Prussia, Pennsylvania, SKF Industries, Inc.

7. Harris, T. A., and Aaronson, S. F., AN ANALYTICAL INVESTIGATION OF CYLINDRICAL ROLLER BEARINGS HAVING ANNULAR ROLLERS, ASLE Transactions 10, 1967.

8. Battelle Memorial Institute, ANALYSIS OF A ROLLER BEARING ASSEMBLY WITH HOLLOW ROLLERS, Columbus, Ohio, Battelle Memorial Institute.

9. Harris, T. A., ROLLING BEARING ANALYSIS, John Wiley and Sons, Inc., New York, 1966.

LIST OF SYMBOLS

a	Nominal radial dimension between races of sprag - in./Spring interference between teaser coil and bore - in./Spring diametral clearance - in./Inside radius of ring/Spring diametral interference between inside diameter and arbor - in.
a_1	Inside radius of cylinder #1 - in.
a_2	Inside radius of cylinder #2 - in.
A	Center of sprag outer cam radius - in./Area - $in.^2$ or Area - ft^2/Coefficient for roller clutch deflection
$\bar{A}$	Roller parameter for crown drop
Ah	Effective cross section area of outer housing - $in.^2$
Ak	Effective cross section area of cam - $in.^2$
b	Maximum dimension across sprag - in./Spring center coil width - in./Outside radius of ring - in./ Width of sprag - in.
b_1	Outside radius of cylinder #1 - in., Width of spring coil #1
b_2	Outside radius of cylinder #2 - in., Width of spring coil #2
b_{base}	Baseline spring coil width at crossover - in.
b_i	Width of spring coil at ith turn - in.
B	Center of sprag inner cam radius/Coefficient for roller clutch deflection
c	Minimum dimension across sprag - in./one-half of spring thickness (h/2) - in.
C	Contact point between sprag and outer race/ Coefficient for roller clutch deflection
C_1	Influence coefficient for sprag Hertzian deflection
C_2	Influence coefficient for sprag Hertzian deflection
C_3	Influence coefficient for sprag Hertzian deflection

LIST OF SYMBOLS (Cont'd)

C_c	Contraction coefficient for flow through orifice
Ci	Influence coefficient for deflection of inner shaft of sprag
CK	Influence coefficient for deflection of cam
Co	Influence coefficient for deflection of outer housing of sprag
Cp	Specific heat of lubricant - btu/lb ^{o}F
CR	Influence coefficient for deflection of outer housing of ramp roller
Cs	Influence coefficient of deflection of sprag/ Basic static capacity for bearing - lb
C_v	Velocity coefficient for flow through orifice
Cp	Influence coefficient for hollow roller deflection
$\mathcal{L}$	Centerline
d	Inside diameter of hole in pin in ramp roller clutch - in.
d_i	Housing inside diameter - in./2 times sprag inner cam radius - in./roller inside diameter - in.
d_m	Spring mean diameter - in.
$d_{m\ base}$	Baseline spring mean diameter - in.
d_o	Housing outside diameter - in./roller outside diameter - in.
dw	Spring wire diameter - in.
D	Outside diameter of pin in ramp roller clutch - in.
Di	Inner shaft outside diameter sprag clutch - in.
Do	Outer shaft inside diameter sprag clutch - in.
D_x	Diameter which establishes oil level - in.

e_i	Sprag inner radius of compound sprag - in.
er	Hollow roller geometry factor
E	Young's modulus - psi
f_a	Axial stress - psi
f_{ai}	Axial stress in ith coil - psi
f_b	Bending stress - psi
f_{bi}	Bending stress on inside fiber - psi
f_{bo}	Bending stress on outside fiber - psi
f_c	Hertz stress - psi
f_{ci}	Hertz stress on inside - psi
f_{co}	Hertz stress on outside - psi
f_i	Total stress on inside fiber - psi
fl	Factor for coefficient in bearings
f_o	Total stress on outside fiber - psi/Bearing factor
f_s	Steady stress - psi/Shear stress - psi/Free length of spring - in.
f_t	Combined stress - psi/Hoop stress - psi
f_{t1}	Tensile stress in ring #1 - psi
f_{t2}	Tensile stress in ring #2 - psi
f_v	Vibratory stress - psi
F	Roller tangential load - lb/Frictional force
Fa	Axial load - lb
Fap	Axial load on pin - lb
Fas	Axial load on spring - lb
Fc	Roller tangential load on cam - lb/Centrifugal force - lb

Fcp	Centrifugal load on pin - lb
Fcs	Centrifugal load on spring - lb
Fen	Endurance limit - psi
Fi	Tangential sprag load on inner race - lb
Fo	Tangential sprag load on outer race - lb
Fr	Radial load - lb
Fs	Static equivalent load - lb
F.S.	Factor of safety
Ftu	Ultimate tensile strength - psi
Fty	Tensile yield strength - psi
Fβ	Bearing load factor - lb
g	Gravitational constant - $in./sec^2$
G	Shear modulus of elasticity - psi
h	Spring center coil height - in.
h_{base}	Baseline spring center coil height - in.
h_i	Thickness of spring at ith turn - in.
hs	Spring solid height - in.
H	I.D./O.D. of hollow roller
i	Coil number
I	Moment of inertia - $in.^4$
Ih	Moment of inertia of housing - $in.^4$
Ik	Moment of inertia of cam - $in.^4$
j	Distance from neutral axis to spring c.g. - in.
J	Sprag nominal section - in.

LIST OF SYMBOLS (Cont'd)

K	Curvature correction factor/Distance from cam flat to centerline - in.
$\bar{K}$	Distance from cam centerline to c.g. of effective cam area - in.
Ki	Curvature correction factor for inside stress
Ko	Curvature correction factor for outside stress
Ks	Spring rate - lb/in.
ℓ	Sprag length - in./Depth of hole in pin - in./ Roller length - in.
L	Spring length - in./Sprag length including cages - in./Overall length of pin - in.
L_{base}	Baseline spring length - in.
Lc	Crown length - in.
Lf	Flat length of roller - in.
Lg	Gage length of roller - in.
m	Sprag contact line with outer housing
M	Bending moment - in. lb/Total friction torque - in. lb
MB	Internal bending moment - in. lb
Mc	Moment at cam c.g. - in. lb
M_ℓ	Bearing friction torque - in. lb
MRR	Ramp roller clutch viscous friction torque - in. lb
M.S.	Margin of safety
M.S. ult	Ultimate margin of safety
M.S. yield	Yield margin of safety
M_{spring}	Sprag clutch spring induced moment

LIST OF SYMBOLS (Cont'd)

MSP	Spring clutch drag torque from spring - in. lb
Mt	Total spring clutch drag torque - in. lb
Mv	Viscous friction torque of bearings - in. lb
n	Number of roller clutch rollers
N	Number of spring coils in 1/2 spring/Number of sprags per row/Normal force - lb
Ni	Sprag normal load on inner shaft - lb
No	Sprag normal load on outer housing - lb
Np	Normal load on pin - lb
Ns	Normal load on spring - lb
O	Center of rotation
p	Pressure - psi
p_1	Pressure on cylinder #1 - psi
p_2	Pressure on cylinder #2 - psi
p_i	Pressure on housing ith coil - psi/Pressure on inner shaft - psi
p_o	Pressure on output shaft - psi
P	Roller normal load - lb/Spring center coil load - lb
PA	Internal axial force - lb
Pc	Minimum sprag circumferential pitch - in./Roller load through cam center of rotation - lb
P_i	Roller load ith guess - lb
Po	Roller load - lb
Pp	Total load on pin - lb
Ps	Total load on spring - lb

q	Linear pressure - lb/in.
q_h	Shear linear pressure - lb/in.
Q	Flow - ft^3/sec/Imaginary load - lb/Contact point between sprag and inner race/Total drag torque on cage - in. lb
Qbrg	Flow to bearings - gpm
Ql	Drag torque from rolling resistance - in. lb
Q_m	Theoretical flow - lb/sec
QS	Total flow to sprag clutch - gpm
Qsp	Flow to sprag area only - gpm
Qv	Drag torque from viscous friction - in. lb
$\bar{r}$	Radius to centroid of rotating oil dam - in.
ri	Inner cam radius - in.
$\bar{r}i$	Deflected value of ri - in.
rm	Hollow roller geometry factor
ro	Outer cam radius - in.
$\bar{r}o$	Deflected value of ro
rpm	Revolutions per minute
rpm_x	Speed at which spring is ineffective
R	Outer housing bore radius - in.
$\bar{R}$	Radius to spring c.g. - in./Housing centroidal radius - in.
Rc	Crown radius of roller - in./Rockwell "C"
Ri	Outside radius of inner shaft - in.
$\bar{R}i$	Deflected value of Ri - in.
Rid	Inside radius of inner shaft - in.

Ro	Inside radius of outer shaft - in.
$\bar{R}o$	Deflected value of Ro - in.
Rod	Outside radius of outer shaft - in.
Rp	Radius to c.g. of pin - in.
RS	Radius to shear load - in.
S	Distance from pin end to centerline - in.
S.F.	Spring selection size factor
t	Oil height in dam - in.
T	Clutch design torque - in. lb/Distance from bottom of spring hole to centerline - in.
Tc	Torque on carrier - in. lb
TDC	Drag clip torque, sprag clutch - in. lb
TDS	Drag strip torque, sprag clutch - in. lb
Te	Energizing torque - in. lb
T_{ENERG}	Torque required on 1st coil to energize spring - in. lb
T_i	Torque on ith coil - in. lb
T_{int}	Interference torque between teaser coils and bore - in. lb
To	Output torque - in. lb
U	Strain energy - in. lb
V	Sprag inner gripping angle - deg/Velocity - ft/sec
Vs	Internal shear force - lb
W	Sprag outer gripping angle - deg/Load relief on multiple rings - lb
Ws	Weight of sprag - lb/Weight of spring - lb
Wp	Weight of pin - lb

X	Percent pressure relief for multiple rings
$\bar{X}p$	Distance from pin c.g. to centerline - in.
$\bar{X}s$	Distance from spring c.g. to centerline - in.
y	Distance from inner or outer fiber to c.g. - in.
Z	Distance between sprag centers of radii of curvature - in./Section modulus - $in.^3$/Roller geometry factor
α	Angle defining pressure at any point - deg
β	Angle to load positions - deg
γ	Angle between cam and roller contact point and perpendicular centerline of cam flat - deg/Lubricant density $lb/in.^3$
δ	Spring centrifugal diametral growth - in.
Δ	Deflection - in.
Δcam	Radial deflection of cam - in.
Δcent	Centrifugal deflection of outer housing - in.
Δhsg	Radial deflection of outer housing - in.
ΔHo	Hertzian deflection between sprag and outer housing - in.
ΔHi	Hertzian deflection between sprag and inner shaft - in.
Δi	Deflection of inner housing from normal sprag load - in.
Δo	Deflection of outer housing from normal sprag load - in.
Δroller	Radial deflection of roller - in.
Δsprag	Deflection of sprag as a column or compression member - in.
Δt	Temperature difference - ^{o}F

LIST OF SYMBOLS (Cont'd)

Δtotal	Summation of total radial deflections - in.
Δwear	Allowable wear - in.
ζ	Multiple cylinder geometry constant
η	Geometric cylinder parameter
η_1	Geometric cylinder parameter for ring #1
η_2	Geometric cylinder parameter for ring #2
θ	Angle defining spring centrifugal growth - deg
μ	Coefficient of friction
ν	Poisson's ratio
ν_o	Oil viscosity - centistokes
ρ	Roller radius - in./Material density lb/in.^{3}
ρ_r	Material density of roller lb/in.^{3}
ρ_s	Spring wire density lb/in.^{3}
ϕ_p	Angle defining pin c.g. - deg
ϕ_s	Angle defining spring c.g. - deg
ψ	Nip angle - deg
ψ_o	No load nip angle - deg
ψ_f	Full load nip angle - deg
ω	Angular velocity - rad/sec
Ω	Sprag rotational angle